Spring 3-28-2022

A Comparison of Natural, Living, and Hardened Shorelines Ability to Prevent Coastal Erosion and Maintain a Healthy Ecosystem

Gabrielle Spellmann

A COMPARISON OF NATURAL, LIVING, AND HARDENED SHORELINES ABILITY TO PREVENT COASTAL EROSION AND MAINTAIN A HEALTHY ECOSYSTEM

by

Gabrielle Spellmann

A Thesis
Submitted to the Graduate School,
the College of Arts and Sciences
and the School of Ocean Science and Engineering
at The University of Southern Mississippi
in Partial Fulfillment of the Requirements
for the Degree of Master of Science

Approved by:

Dr. Patrick Biber, Committee Chair
Dr. Eric Sparks
Dr. Chet Rakocinski

May 2022

Published by the Graduate School

ABSTRACT

It is important to find a suitable method to protect the U.S. Gulf Coast shoreline, since its' low elevation and the Loop current make it vulnerable to sea level rise. I focused on two manmade methods, hardened, and living shorelines, of coastal protection for when the natural marsh suffers excess erosion rates. Living shorelines are a suite of shoreline conservation and restoration techniques that usually involve some sort of hardened structure that dampens wave energy so that the native vegetation behind it can take root and stabilize the shoreline. This study looked at six different sites, all containing a natural, living, and hardened shoreline across two different energy groups (low and high) to see how hydrographic, geomorphic, and vegetative parameters are affected. The erosion rate of the coastline and its geographic shape were influenced by the two energy groups, with the high energy coastlines eroding quicker. Hardened shorelines were found to have little to no erosion, while natural shorelines had the greatest amount of erosion. Living shorelines lessened the rate of erosion. However, the natural and living shorelines were similar in slope and sediment parameters, while hardened shorelines had steep slopes and higher sand content. I found that coastlines with high turbidity, erosion rates, wave power and relative exposure had steeper slopes and a higher percent of sand in the sediment, but lower percent cover and percent of marsh dominant vegetation species. This research is important because it will increase our knowledge on what environmental conditions may be most suitable for living shorelines to decrease erosion rates.

ACKNOWLEDGMENTS

I would like to thank my everyone that has physically and mentally helped me to complete this project. To Dr. Patrick Biber, my major advisor, thank you for guiding me in my ability as a researcher and the development of my project. To the rest of my committee, Dr. Eric Sparks and Dr. Chet Rakocinski, thank you for helping to add depth and another point of view to the development of my project.

I would like to thank John D. Caldwell and James P. Kelly for assistance in the field and with species identification. I would like to thank Brittany Juneau for helping to further the depth of my research by providing erosion and slope data for the same sites. Finally, I would like to thank my friends and family for supporting and guiding me through life.

TABLE OF CONTENTS

ABSTRACT ii

ACKNOWLEDGMENTS iii

LIST OF TABLES vii

LIST OF ILLUSTRATIONS xii

LIST OF ABBREVIATIONS xix

CHAPTER 1- INTRODUCTION 1

1.1 Problem Statement 1

1.2 Background 2

1.2.1 Natural Shorelines 2

1.2.2 Hardened Shorelines 3

1.2.3 Living Shorelines 5

1.2.4 Geomorphic Processes 6

1.2.5 Vegetation Processes 7

1.3 Objectives and Hypothesis 9

CHAPTER 2 - METHODS 11

2.1 Sites 11

2.2 Tasks 18

2.2.1 Hydrographic Features 18

2.2.2 Geomorphic Features 18

2.2.2.1 Relative Exposure 18
2.2.2.2 Erosion Rates and Shoreline Slope 22
2.2.2.3 Sediment composition 24
2.2.3 Vegetation 26
2.3 Data Analysis 27
2.3.1 Hydrographic Features 27
2.3.2 Geomorphic Features 28
2.3.3 Vegetation 28
2.3.4 Data Interactions 28
CHAPTER 3 - RESULTS 29
3.1 Hydrographic Features 29
3.1.1 Wave Gauge Data 29
3.1.2 YSI Data 31
3.2. Geomorphic Features 33
3.2.1 Relative Exposure 33
3.2.2 Erosion Rates and Shoreline Slope 37
3.2.3 Sediment Bulk Density and Organic Matter Content 44
3.2.4 Sediment Grain Size 52
3.3 Vegetation 60
3.3.1 Species Richness 60

3.3.2 Percent Cover 67

3.3.3 Diversity 68

3.4 Data Interactions 70

CHAPTER 4 - DISCUSSION 78

4.1 Summary 78

4.2 Hydrographic Features 79

4.3 Geomorphic Features 80

4.4 Vegetation 83

4.5 Data Interactions and Conceptual Model 85

CHAPTER 5 - CONCLUSION 87

APPENDIX A – Wave gauge Kruskal-Wallis rank sums test table. Turbidity, relative exposure, shoreline slope, bulk density, organic matter, sediment grain size, species richness, total average percent cover, percent cover of dominant marsh species summary and ANOVA tables 90

APPENDIX B – Data analysis for the other data calculated from the wave gauges: average wave power, significant wave period, average wave height, maximum wave height, significant wave height, and wave percentiles 96

APPENDIX C - More detailed tables and figures for the results. 104

REFERENCES 116

LIST OF TABLES

Table 1. Average wave power (kW/m) at each site and YSI data for both seasons include mean (±SE) turbidity (NTU), temperature (^{o}C), salinity (ppt), and dissolved oxygen concentration (mg/L). 30

Table 2. Relative Exposure for natural, living, and hardened shorelines at each site and the average (±SE). Significant differences in means are indicated by superscript letter groups in the average column. 34

Table 3. Average (±SE) Relative Exposure for natural, living, and hardened shorelines for each wave power group and the average (±SE) for each wave energy group. Significant differences in means are indicated by superscript letter groups in the average column..... 36

Table 4. Average erosion rates (m/yr ± SE) for the three different shorelines at each site, as well as the average (±SE) for each site and each type of shoreline. All Sites excludes the living shoreline and hardened shoreline at Hancock County. Significant letters are from the two-way ANOVA with the parameters being site and shoreline with all shorelines included..... 38

Table 5. Average erosion rates (m/yr ± SE) for the three different shorelines for the two energy groupings, as well as the average (±SE) for each energy group. Significant letters are from the two-way ANOVA with the parameters being energy and shoreline with all shorelines included..... 38

Table 6. The average slope (±SE) for the natural, living, and hardened shorelines at all six sites. Significant letters are between the six sites within each of the three treatment types. 41

Table 7. Average (±SE) of the sediment composition (BD, OM) collected at six sites, with three shoreline types at each site. Significant differences in means are indicated by superscript letter groups in each column for the different types of shorelines. 46
Table 8. Average (±SE) of the three sediment size fractions collected for high and low energy groups, with three shoreline types at each group. Significant differences in means are indicated by superscript letter groups in each column. 47
Table 9. Average (±SE) of the three sediment size fractions collected at six sites, with three shoreline types at each site. Significant differences in means are indicated by superscript letter groups in each column for the different types of shorelines. 57
Table 10. Mean (±SE) of three sediment size fractions collected for high and low energy groups, with three shoreline types for each group. Significant differences in averages are indicated by superscript letter groups in each column. 58
Table 11. List of all the species found at the six different sites. 61
Table 12. Vegetation data by site and shoreline for the average species richness, total percent cover (±SE), dominant marsh species cover, the Shannon H index, and the Simpson's D index. Significant differences in means are indicated by superscript letter groups in the average percent cover column..... 63
Table 13 Vegetation data by energy groups and shoreline for the average species richness, total percent cover (±SE), dominant marsh species cover, the Shannon H index, and the Simpson's D index. Significant differences in means are indicated by superscript letter groups in the average percent cover and in dominant marsh species cover column. 64
Figure 28. Scree plot for the principal component analysis (PCA). 73

Table 14. Principle component analysis contributions (eigenvectors) for each factor used for the first three dimensions (PC1, PC2, and PC3). The factors include percent of dominant marsh species, percent cover for all species, average slope, percent of sand in the sediment, average wave power, turbidity, relative exposure, percent organic matter, species richness, and erosion rates. 74
Table.A.1 Kruskal-Wallis rank sums test for the average wave power by energy. 90
Table.A.2 Kruskal-Wallis rank sums test for the average wave power by site 90
Table.A.3 ANOVA of turbidity by site and season 90
Table.A.4 One-way ANOVA of Relative Exposure by Site 90
Table.A.5 ANOVA of erosion by site and shoreline 90
Table.A.6 One-way ANOVA of slope by shoreline. 91
Table.A.7 One-way ANOVA of bulk density by shoreline. 91
Table.A.8 ANOVA bulk density by site and shoreline. 91
Table.A.9 ANOVA of bulk density by energy and shoreline. 91
Table.A.10 One-way ANOVA of organic matter by shoreline. 91
Table.A.11 One-way ANOVA of organic matter by site. 91
Table.A.12 ANOVA of organic matter by site and shoreline 92
Table.A.13 ANOVA of organic matter by energy and shoreline. 92
Table.A.14 One-way ANOVA of depth by percent sand. 92
Table.A.15 One-way ANOVA of depth by percent silt and clay. 92
Table.A.16 One-way ANOVA of coarse sand and pebbles by site. 92
Table.A.17 One-way ANOVA of percent sand by site. 92
Table.A.18 One-way ANOVA of percent silt and clay by site. 93

Table.A.19 One-way ANOVA of species richness by site. 93
Table.A.20 One-way ANOVA of species richness by shoreline. 93
Table.A.21 One-way ANOVA of species richness by energy. 93
Table.A.22 One-way ANOVA of percent cover by shoreline. 93
Table.A.23 One-way ANOVA of percent cover by site. 93
Table.A.24 One-way ANOVA of percent cover by energy. 94
Table.A.25 One-way ANOVA of percent of dominant marsh species by shoreline. 94
Table.A.26 ANOVA of percent of dominant marsh species by energy and shoreline. 94
Table.A.27 Kruskal-Wallis rank sums test for the significant wave period by site. 94
Table.A.28 Kruskal-Wallis rank sums test for the significant wave period by energy. ... 94
Table.A.29 Kruskal-Wallis rank sums test for the average wave height by sites. 94
Table.A.30 Kruskal-Wallis rank sums test for the average wave height by energy. 95
Table.A.31 Kruskal-Wallis rank sums test for the maximum wave height by site. 95
Table.A.32 Kruskal-Wallis rank sums test for the maximum wave height by energy. 95
Table.A.33 Kruskal-Wallis rank sums test for the significant wave height by site. 95
Table.A.34 Kruskal-Wallis rank sums test for the significant wave height by energy. ... 95
Table.A.35 One-way ANOVA of bulk density by depth. 95
Table.A.36 One-way ANOVA of organic matter by depth. 95
Table.B.1 Average wave power, signficant wave period, average wave height, maximum wave height, and signficant wave height for the six sites. Significant differences by site are indicated by Wilcoxon Rank Test letter groups. 96
Table.B.2 Average wave power, signficant wave period, average wave height, maximum wave height, and signficant wave height for the high and low wave power groups. 96

Figure.B.1 99

Table.B.3. Wave Height Percentiles for the three different types of shorelines (NS, LS, and HS) for all six sites during winter and summer of 2020. 101

Table.C.1 Wave gauge data results, heights are in cm, and wave period is in seconds. Hours of collection were calculated at timeanddate.com, which rounds down. 104

Table.C.2 Maximum fetch distance (m) for natural, living, and hardened shorelines at each and the average maximum fetch for each site. Fetch average is the mean of all the fetch transects at the site that did not equal zero (n=19). 105

Table.C.3 Average fetch distance (m) for natural, living, and hardened shorelines at each and the average fetch for each site. The avg fetch distance is the mean of all the fetch transects at the site that did not equal zero. 106

Table.C.4 Mean Relative Exposure (±SE) for natural, living, and hardened shorelines for each season and wave power group (n=3). 106

Table.C.5 Relative Exposure for natural, living, and hardened shorelines at each site for each season..... 106

Table.C.6 Mean (± SE) of the percent coarse sand and pebbles, percent sand, percent silt/clay, bulk density, and organic matter (OM) for the different depths for the shorelines at all six sites. n=5..... 107

Table.C.7 Vegetation data by site and shoreline for the average total percent cover, species richness, species found, average percent cover (±SE) for each of the species, the maximum and minimum percent cover each for each of the species, the Shannon H index, and the Simpson D index. 113

LIST OF ILLUSTRATIONS

Figure 1. Map of six study site sites in Mississippi and Alabama – each site has three shoreline types (natural, living, and a hardened shoreline). 12

Figure 2. The natural shoreline (blue arrow), living shoreline (yellow arrow) and hardened shoreline (red arrow) for the six study sites. The high wave energy sites are Hancock County Marsh (A), Swift Tract (B) and Alonzo Landing (C). The low wave energy sites are Camp Wilkes (D), Ocean Springs Inner Harbor (E) and Grand Bay NERR (F). 13

Figure 3. Images of the Natural Shorelines (NS) were taken on fieldwork days. Panels are A.) Hancock County Marsh, B.) Swift Tract, C.) Alonzo Landing, D.) Camp Wilkes, E.) Ocean Springs Inner Harbor, F.) Grand Bay NERR. 14

Figure 4. Images of the Living Shorelines (LS) were taken either on the day of elevation surveying or on previous fieldwork days. Panels are A.) Hancock County Marsh, B.) Swift Tract, C.) Alonzo Landing, D.) Camp Wilkes, E.) Ocean Springs Inner Harbor, F.) Grand Bay NERR. 15

Figure 5. Images of the Hardened Shorelines (HS) were taken either on the day of elevation surveying or on previous fieldwork days. Panels are A.) Hancock County Marsh, B.) Swift Tract (picture is of a similar shoreline to the site studied), C.) Alonzo Landing, D.) Camp Wilkes, E.) Ocean Springs Inner Harbor, F.) Grand Bay NERR. 16

Figure 6. Schematic showing the spatial layout of sampling methods in the field. Wave gauges and YSI were deployed in the winter and summer. One wave gauge was deployed in front of each shoreline, hardened shoreline (HS), living shoreline (LS), and natural shoreline (NS). Five sediment cores from each shoreline type were collected in the

winter. Ten vegetation quadrats were collected in the summer for the hardened, living, and natural shoreline. 17
Figure 7. Wind rose diagram showing wind speed (m/s) and compass direction for Bay Saint Louis (A), Pascagoula (B), and Fairhope (C). 19
Figure 8. Images of the 16 bearing lines used to measure the fetch for the Natural Shorelines (NS) on Google Earth. Panels are A.) Hancock County Marsh, B.) Swift, C.) Alonzo Landing, D.) Camp Wilkes, E.) Ocean Springs Inner Harbor, F.) Grand Bay NERR. 20
Figure 9. Images of the 16 bearing lines used to measure the fetch for the Living Shorelines (LS) on Google Earth. Panels are A.) Hancock County Marsh, B.) Swift, C.) Alonzo Landing, D.) Camp Wilkes, E.) Ocean Springs Inner Harbor, F.) Grand Bay NERR. 21
Figure 10. Images of the 16 bearing lines used to measure the fetch for the Hardened Shorelines (HS) on Google Earth. Panels are A.) Hancock County Marsh, B.) Swift, C.) Alonzo Landing, D.) Camp Wilkes, E.) Ocean Springs Inner Harbor, F.) Grand Bay NERR. 22
Figure 11. Example erosion rate data from the Camp Wilkes natural shoreline (left) and living shoreline (right) traced in 2011 and 2019, and an overlap of each year with the corresponding background for 2011 and 2019, the background for the combined tracings are from 2019. 23
Figure 12. Average wave power (kW/m), and turbidity (NTU) for the six sites. Significant differences by site are indicated by Wilcoxon Rank Test letter groups. 31

Figure 13. Boxplot of turbidity (NTU) separated by season and wave power group. Significant differences by season and wave power group are indicated by Tukey's HSD post-hoc letter groups. 32

Figure 14. Wind rose diagram for Hancock County (HC), Swift Tract (ST), Alonzo Landing (AL), Camp Wilkes (CW), Ocean Springs (OS) for each season. Each image has the three different shorelines; natural (blue), living (yellow), and hardened (red) with the shorelines oriented by compass bearings. The shaded section of each color represents the land. 36

Figure 15. Erosion rates (m/yr) for the different six sites and three shoreline types with natural shorelines (blue), living shorelines (yellow), and hardened shorelines (red). The LS and HS for HC were zeroed. Tukey's HSD post-hoc letter groups show the significant differences for the three shorelines and sites. 40

Figure 16. Erosion rates (m/yr) for the different two energy groups and three shoreline types with natural shorelines (blue), living shorelines (yellow), and hardened shorelines (red). This excludes the living shoreline for HC because it had a high rate of accretion. Tukey's HSD post-hoc letter groups show the significant differences for the three shorelines and energy groups. 40

Figure 17. A graph of the average elevation change (cm/m) for natural (blue), living (yellow), and hardened (red) shorelines. The coordinate (0,0) represents the mean water level at the shoreline at the time of sampling. Negative elevation point distances are seaward, while positive transect point distances are landward. 42

Figure 18. A graph of the average elevation change (cm/m) for the six different sites, separated by (A) natural, (B) living, and (C) hardened shorelines. The coordinate (0,0)

represents the mean water level at the shoreline at the time of sampling. Negative elevation points are seaward, while positive transect points are landward..... 43
Figure 19. Bulk density (g/cm^3) and organic matter (%) for the different two energy groups and three shoreline types with natural shorelines (blue), living shorelines (yellow), and hardened shorelines (red). 50
Figure 20. Scatterplot of OM to BD for the two energy groups and three shoreline types. Symbols and colors indicate sample origin, filled symbols indicate high energy sites and hollow symbols indicate low energy..... 51
Figure 21. Boxplot of the different depth fractions (cm) for the different sediment features grouped across all six sites: percent of coarse sand and pebbles, percent of sand, and percent of silt and clay. Significant differences by depth are indicated by Tukey's HSD post-hoc letter groups..... 54
Figure 22. Sediment grain size composition at three shoreline types (NS, LS, HS) collected from the high and low energy groups. Tukey's HSD post-hoc letter groups show the significant differences for the three shorelines and energy groups by the different sediment fractions (pebbles, sand, and silt). 59
Figure 23. Species richness, average percent cover (%, ± SE), average dominant marsh species cover (%, ± SE), Simpson's Index of Diversity (D), and the Shannon Weiner Index (H) for the natural (blue), living (yellow), and hardened (red) shorelines at each site. Tukey's HSD post-hoc letter groups show the significant differences for the three shorelines and sites for average percent cover and dominant marsh species cover..... 65
Figure 24. Species richness, average percent cover (%, ± SE), average dominant marsh species cover (%, ± SE), Simpson's Index of Diversity (D), and the Shannon Weiner

Index (H) for the natural (blue), living (yellow), and hardened (red) shorelines for the different energy groups. Tukey's HSD post-hoc letter groups show the significant differences for the three shorelines and energy groups for average percent cover and dominant marsh species cover. 66
Figure 25. Non-metric multidimensional scaling plot of the vegetation diversity found at the different shorelines per site. 69
Figure 26. Correlation matrices for high (A) and low (B) energy groups containing the different variables: erosion rate, percent silt, organic matter, average percent cover, average fetch distance, turbidity, relative exposure, Shannon-Weiner Index, species richness, Simpson's Index of Diversity, average wave power, bulk density, slope, percent sand, and percent of dominant species. 71
Figure 27. Non-metric multidimensional scaling plot representing relationship between for the different shorelines and sites, determined by the variables: average wave power, turbidity, relative exposure, average erosion rate, average slope, percent of sand, organic matter, species richness, percent of dominant species, and percent cover. 72
Figure 29. Principal Component Analysis for the three shoreline types at each site. High energy sites have solid shapes, while low energy sites are open symbols. PC1 represents the percent of dominant vegetative species, percent cover of vegetation, and the average slope of the shoreline. PC2 represents the turbidity, erosion rate, relative exposure, and average wave power. PC3 represents species richness. 75
Figure 30. A conceptual model representing the results found with the PCA. The ellipses are from the PCA and show the different types of shorelines: natural (blue), living (yellow), and hardened (red). Quadrant A represents high energy hitting a hardened

structure with sandy sediment at the base and has no native vegetation. Quadrant B represents high energy with the less sand but features a steeper slope with native vegetation. Quadrant C is a low energy shoreline but with a steep slope, moderate sand content and less native vegetation. Quadrant D represents a low energy shoreline, with mostly silt/clay sediments but little sand, and lots of native vegetation. 77

Figure.B.1 Average wave power (kW/m), significant wave period (s), average wave height (m), maximum wave height (m), significant wave height (m), and turbidity (NTU) for the six sites. Significant differences by site are indicated by Wilcoxon Rank Test letter groups. 99

Figure.B.2 Wave height percentiles from 50-100% showing the height (m) for the six sites: Hancock County (HC), Swift Tract (ST), Alonzo Landing (AL), Camp Wilkes (CW), Ocean Springs (OS), and Grand Bay (GB). 102

Figure.B.3 Wave height percentiles from 50-100% showing the height (m) for high and low wave power groups. 103

Figure.C.1 Boxplot of turbidity (NTU) separated by season and site. Significant differences by season and site are indicated by Tukey's HSD post-hoc letter groups. .. 105

Figure.C.2 Boxplot of the different depth fractions (cm) for the different sediment features grouped across all six sites: bulk density and organic matter. 109

Figure.C.3 Bulk density (g/cm^3) and organic matter (%) for the different six different sites and three shoreline types with natural shorelines (blue), living shorelines (yellow), and hardened shorelines (red). 110

Figure.C.4 Scatterplot of OM to BD for all six sites and three shoreline types. Symbols and colors indicate sample origin, filled symbols indicate high energy sites. 111

Figure.C.5 Sediment grain size composition at three shoreline types collected from six sites: Hancock County marsh (HC), Swift Tract (ST), Alonzo Landing (AL), Camp Wilkes (CW), Ocean Springs harbor (OS), and Grand Bay (GB). Significant differences by sediment fraction are indicated by Tukey's HSD post-hoc letter groups 112

LIST OF ABBREVIATIONS

AL	Alonzo Landing
BD	Bulk Density
CW	Camp Wilkes
GB	Grand Bay
HC	Hancock County
HS	Hardened Shoreline
LS	Living Shoreline
NS	Natural Shoreline
OM	Organic Matter
OS	Ocean Springs
ST	Swift Tract

CHAPTER 1- INTRODUCTION

1.1 Problem Statement

The world is currently populated with 7.8 billion people; 40% of the population lives within 100 km from the coast (US DoC & NOAA, 2013). Global sea level will continue to rise and endanger many large cities along the coast (US DoC & NOAA, 2008). This will cause many properties to be flooded, and people may lose their homes, businesses, and money (Temmerman et al., 2013). Property owners have been trying to prevent this from occurring by armoring the shoreline, this solution provides immediate protection of the shoreline. While stopping erosion, this destroys the natural ecosystem and a better solution may be to return the coast to its natural habitat.

There has been a decline in natural marshes because of sea level rise and other anthropogenic effects. Sea level has been rising at a faster rate because burning fossil fuels has increased the concentration of greenhouse gases, mainly carbon dioxide, resulting in the melting of glaciers and thermal expansion of water (US DoC & NOAA, 2008; IPCC, 2021). Humans have removed many marshes to create aesthetically pleasing sandy beaches or to make way for developments. The decrease in vegetation density in the sediment further exacerbates coastal erosion (Gedan et al., 2011). Marshes preserve coastal areas through increased sedimentation and storm protection, and removal of these habitats has diminished the ability of marshes to provide such ecosystem services (Arkema et al., 2013) leading to more frequent “sunny day” flooding of properties and roads (Sutton-Grier et al., 2015; Temmerman et al., 2013).

1.2 Background

1.2.1 Natural Shorelines

Natural marshes are nature's ability to prevent erosion, clean the water, and create habitat by acting as a buffer between the sea and land. Land protection is provided by wave breakage and storm dampening because vegetation helps to decrease the impact of waves and storms (Wu et al., 2012). Marsh ecosystems also provide benefits for coastal waterways as the vegetation filters runoff and increases sediment retention before it reaches the water. Another benefit of natural marsh is its ability to act as a repository of blue carbon, which is becoming increasingly important as fossil fuels are continuously burned and need to be sequestered. There are many factors that contribute to a healthy marsh ecosystem, which all play a vital role in the marsh ecosystem (Bilkovic & Mitchell, 2018; Craft et al., 2009).

Marshes are a great source of both primary and secondary production (Bilkovic & Roggero, 2008). Marshes host salt tolerant plant species that are an important source of organic matter (Craft et al., 2003; Currin et al., 2008; Matzke & Elsey-Quirk, 2018). They also act as a habitat for many organisms (Balouskus & Targett, 2016; Bilkovic & Roggero, 2008; Sutton-Grier et al., 2015). Marsh sediments are home to many benthic infauna species, and act as a nursery to nekton species and their prey (Bilkovic & Roggero, 2008). Many plant species and organisms are endemic to marshes (Bilkovic & Roggero, 2008; Crum et al., 2018; Drake, 1989; Greenberg et al., 2006; Greenberg & Maldonado, 2006).

Humans profit from the ecosystem services that are provided by marshes in many ways. Shoreline stabilization and protection is an ecosystem service because it protects human developments from flooding and destruction (Arkema et al., 2013; Augustin et al., 2009; Feagin et al., 2009; Silliman et al., 2019). The filtration of runoff provided by marshes makes the water aesthetically pleasing and protects organisms and vegetation from nutrient loads that could be detrimental (Álvarez-Rogel et al., 2016; Johnson et al., 2016; Valiela & Cole, 2002). Salt marshes are an important habitat because it provides both food and protection from predators (Cattrijsse et al., 1997; Green et al., 2012). Carbon sequestration is another ecosystem service provided by marshes, lessening the amount of carbon dioxide in the atmosphere (Chmura et al., 2003; Mitsch et al., 2014).

1.2.2 Hardened Shorelines

As natural marshes have decreased, property owners have taken action to prevent flooding by creating hardened shorelines (Erdle et al., 2006; Gittman et al., 2016; Swann, 2008). Hardened shorelines include sea walls, jetties, revetments, breakwaters, and bulkheads. Hardened shorelines' popularity has to do with the awareness and knowledge local communities have (Roberts, 2010), ease of permitting and construction, as well as perceived cost effectiveness at preventing erosion. After implementation, they provide immediate erosion protection; however, as time goes on, the negative benefits become apparent. Hardened shorelines can increase erosion of neighboring properties because the energy of the waves bouncing off the hardened structure (Bozek & Burdick, 2005; Gittman et al., 2015; Ruggiero, 2009). They do this by interrupting the natural water flow

and morphodynamic processes as well as sediment transportation between upland and intertidal zones (Bilkovic & Mitchell, 2018; Wu et al., 2012).

The interruption in water flow of the longshore current affects sedimentation, which causes an increase of erosion down the shoreline and scouring at the base of the hardened structure (Basco, 2006; Roberts, 2010), making hardened shorelines ecologically costly. Coarser sediment, such as sand or gravel, builds up around the base of the hardened structure and results in a spatial gradient towards fine sediment, silt or clay, with increased distance from the structure (Bozek & Burdick, 2005; Palinkas et al., 2018). The change in sediment size has led to a change in the ecosystem. This is apparent by a lack of vegetation, which helps promote sedimentation (Craft et al., 2003; Vargas-Luna et al., 2015). Sand is less compact, which makes it easier to be displaced by waves and currents (Bilkovic & Mitchell, 2013; Palinkas et al., 2018), however, due to the weight of sand it will quickly fall out of the water column (Molinaroli et al., 2009). Studies have conflicting results in the role that vegetation plays on sedimentation, one of which is that vegetation plays a role in enhancing sedimentation in low wave energy (Brueske & Barrett, 1994). Feagin et al., (2009) found that vegetation does not have a direct effect on erosion, but it does play a role in the sediment parameters.

Ecosystem services are interrupted through the loss of vegetation and organisms after implementation of a hardened structure (Roberts, 2010). The lack of intertidal vegetation at hardened shorelines has had negative effects on fish communities and densities (Balouskus & Targett, 2016; Bilkovic & Roggero, 2008; Crum et al., 2018). One common fish species of research is the mummichog (*Fundulus heteroclitus*);

research has shown that their productivity and population densities are lowest at hardened shorelines compared to natural shorelines (Balouskus & Targett, 2016; Crum et al., 2018; Partyka & Peterson 2008). These negative effects have led to the search for more self-sustaining and ecologically beneficial solutions to the coastal erosion problem.

1.2.3 Living Shorelines

Living shorelines are an alternative restoration method to combat the negative effect of erosion/hardened shorelines. Living shorelines are created from a natural marsh and commonly includes a hardened component, with the purpose of recreating ecosystem functioning like a natural marsh (Scyphers et al., 2011). One way living shorelines are created is by placing a hardened structure in front of planted native vegetation to act as a breakwater; but it can involve only planting, or addition of a hardened structure without vegetation. The vegetation can take root as the hardened structure provides erosion protection by dampening waves (Madsen et al., 2001; Swann, 2008). Some restoration sites use biodegradable material for a more sustainable hardened structure while allowing the vegetation to take root (O'Donnell, 2017). Living shorelines are a way of protecting the shoreline and maintaining the productivity of the ecosystem while meeting many desirable social priorities (Bilkovic & Mitchell, 2018; O'Donnell, 2017; Swann, 2008).

Living shorelines will not immediately function like their natural counterpart, because they must undergo vegetation and habitat succession (Bilkovic & Mitchell, 2018; Boerema et al., 2016). It takes time for primary producers to reach natural productivity and density; biogeochemical processes of the living shorelines take even

longer (Boerema et al., 2016; Craft et al., 2003). Scyphers et al. (2011) found that oyster reefs used as breakwaters help to increase the biodiversity of fish and invertebrates.

Living shorelines have been proven to prevent further coastline erosion and in some cases reversed its effects (Polk & Eulie, 2018; Swann, 2008). It is the vegetation that allows marshes and living shorelines to continuously fight sea level rise through the accretion of sediment (Mitchell & Bilkovic, 2019). Therefore, sediment at a living shoreline tends to be more like that of a natural marsh. One way in which living shorelines and natural marsh are similar is their ability to sequester carbon (Davis et al., 2015) and their ability to remove nitrogen (Onorevole et al., 2018). Unlike hardened shorelines, sediment accretion allows living shorelines and natural marshes to often maintain pace with sea level rise (Mitchell & Bilkovic, 2019). Bilkovic et al. (2016) stated that the common elements of living shorelines are erosion risk reduction, wave attenuation, habitat heterogeneity, and habitat migration allowance. Federal agencies have now recognized the importance of living shorelines for coastal protection (Bilkovic et al., 2016). According to Bayraktarov et al., (2015) marshes have the highest survival rate of marine restoration sites.

1.2.4 Geomorphic Processes

The majority of coastline erosion is caused by continuous wave and tidal current conditions, and only a small proportion (1%) is caused by hurricanes and other large storms (Leonardi et al., 2016). Although, hurricanes and other large storms can quickly cause drastic changes to the shorelines (Leonardi et al., 2016). Sediment grain size and composition inform us about sedimentation, organic matter, plant growth potential, and

benthic organism composition (Bilkovic & Mitchell, 2018). More exposed sites with high wave energy tend to have more coarse and more dense sediment particles, like sand, settle and contain less organic material (Bozek & Burdick, 2005). Sediment and vegetation at a living shoreline tend to be more like that of a natural marsh (Bilkovic & Mitchell, 2013). Feagin et al., (2009) found that restored sites had less cohesive coarser sediment (sand) while established marshes have fine organic detritus in the sediment, and Bilkovic and Mitchell (2013) found sills to have coarser sediment than the natural marsh but this could be due to their use of sand during construction. However, this can vary based on the erosion occurring. If heavy erosion is present, then the natural shoreline will tend to have coarser sediment (Palinkas et al., 2018).

Site selection for living shorelines is a crucial factor that relies on multiple elements (Bayraktarov et al., 2015). Living shorelines are not always able to stabilize, especially in high wave energy environments. Marshes and living shorelines are not only affected by wind waves, but also wake waves caused by boat traffic (Herbert et al., 2018). Wave energy is not the only key component of living shoreline stabilization; angel of the slope, sediment supply and space for the vegetation to retreat are also important (Doody, 2004; Mitchell & Bilkovic, 2019). Sedimentation increases in the presence of vegetation and the drag it creates in the water flow (Madsen et al., 2001; Vargas-Luna et al., 2015).

1.2.5 Vegetation Processes

The native vegetation of the U.S. Gulf Coast, more specifically for the Mississippi-Alabama coastal marshes, is dominated by *Juncus roemerianus* Scheele and

Spartina alterniflora Loisel. Other common species include *Spartina patens* (Aiton) Muhl, *Spartina cynosuroides* (L.) Roth, *Schoenoplectus americanus* (Pers.) Volkart ex Schinz & R. Keller, and *Distichlis spicata* (L.) Greene (Bilkovic & Mitchell, 2018; Eleuterius 1972). The dominant vegetation is determined by multiple factors including salinity and wave energy (Bozek & Burdick, 2005; Gedan et al., 2011; Pennings et al., 2005). *J. roemerianus* is controlled more by physical stress such as salinity and flooding while *S. alterniflora* is controlled through competition (Pennings et al., 2005). *S. alterniflora* is the species most affected by erosion, because it is closest to the water and receives the initial impact of wave energy (Eleuterius, 1972).

Many people have provided research on marsh plants' ability to dampen wave energy (Augustin et al., 2009; Fonseca & Cahalan, 1992; Gedan et al., 2011). Different vegetation will affect wave dampening differently depending on stem density and flexibility (Augustin et al., 2009). Wu et al. (2012) found that because *S. alterniflora* has more leaves and dormant plant material than *J. roemerianus,* it has a higher drag coefficient meaning that it has a greater impact on wave energy. Some research found that a plant's ability to prevent erosion is from its roots binding the sediments (Gedan et al., 2011). The roots binding the sediments is why living shoreline projects are often deemed successful, since vegetation present mimics sediment processes in that of a nearby natural marsh edge (Bilkovic & Mitchell, 2018). According to Howes et al., (2010) higher prevailing salinity often correlates with deeper rooted vegetation. Roots growing near the surface encourage the building up the marsh platform layer by layer and that root growth can be stimulated by tidal flooding (Nyman et al., 2006). However,

sediment supply also is very important and plays a major role in erosion prevention (Nyman et al., 2006).

1.3 Objectives and Hypothesis

The goal of this study was to investigate the effects of different shoreline types (natural marsh, living shoreline, and hardened shoreline) on the physical (wave energy), geological (landscape and sediment), and biological (vegetation) conditions based on a case study from six representative sites. The objectives were to (1) collect and compare data on hydrographic features, including wave power and turbidity, among the three different shoreline types at six sites along a fetch exposure gradient, (2) determine geomorphic features including fetch distance, edge erosion rate and the resulting slope, and sediment composition for the shorelines at each of the six sites, and (3) determine abundance and diversity of the vegetation for the three different shoreline types and two energy groupings. The specific hypotheses tested include:

$H1_0$: The hydrological, geomorphic and vegetative parameters (including exposure, wave energy, turbidity, sediment grain size, soil organic content, vegetation abundance and diversity) do not differ between natural marsh, living shorelines, and hardened structures at the six case study sites.

$H1_A$: The hydrological, geomorphic and vegetative parameters differ with an intermediate between natural marsh, living shorelines and hardened structures at the six case study sites.

$H2_0$: The erosion rates at sites with lower wave energy are not different than sites with higher wave energy.

$H2_A$: The erosion rates at sites with lower wave energy are lower than sites with higher wave energy.

$H3_0$: Erosion rates of the three different shoreline types (NS, LS, HS) are not different.

$H3_A$: Erosion rates of the three different shoreline types differ greatly, with living shorelines reducing erosion rate compared to adjacent natural shorelines.

CHAPTER 2 - METHODS

2.1 Sites

This study occurred at six different sites along the Mississippi and Alabama coastlines (Figure 1). Sites were sampled in the summer and winter of 2020. A-priori hypothesized site groupings had high, medium, and low wave exposure, however, after wave data obtained at the sites in the field was analyzed, the data supported only two energy groups based on the average wave power (kW/m) (Table 1). The three sites re-categorized as high energy sites are Alonzo Landing (AL) and the Swift Tract Project (ST) at Bon Secour Bay both in Alabama, and the Hancock County Marsh Project at Heron Bay (HC) in Mississippi (Rouge, 2000; Schmid, 2000; Swann, 2008)(Figure 1). The three sites re-categorized as low energy sites are Camp Wilkes (CW), Ocean Springs Inner Harbor (OS) and Bayou Heron, Grand Bay NERR (GB) all located in Mississippi (Sparks et al., 2013; NOAA, 2021)(Figure 1). The first of the LS implemented for these sites was at AL (2005), followed by HC (2015), ST (2016), OS (2006), CW (2018) and GB (2015). With the exception of AL and OS, all of these shorelines were created within five years of field sampling.

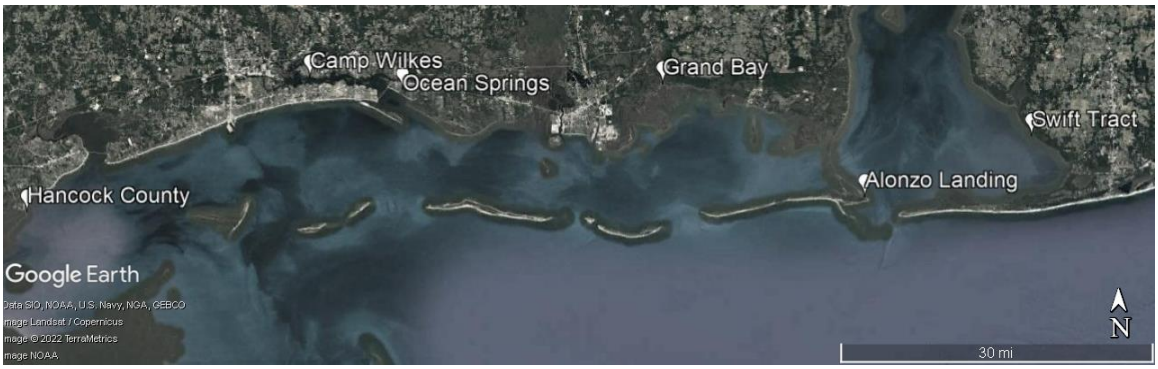

Figure 1. Map of six study site sites in Mississippi and Alabama – each site has three shoreline types (natural, living, and a hardened shoreline).

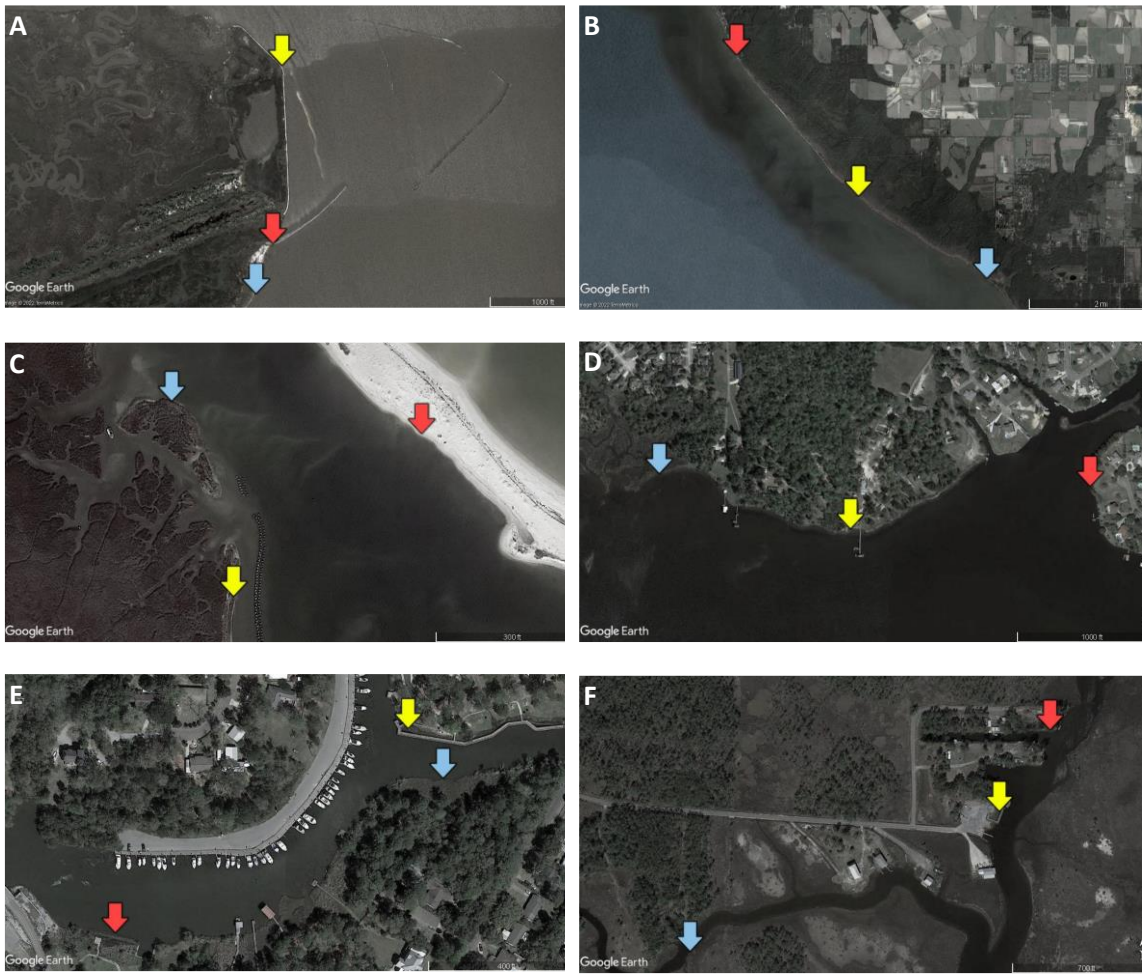

Figure 2. The natural shoreline (blue arrow), living shoreline (yellow arrow) and hardened shoreline (red arrow) for the six study sites. The high wave energy sites are Hancock County Marsh (A), Swift Tract (B) and Alonzo Landing (C). The low wave energy sites are Camp Wilkes (D), Ocean Springs Inner Harbor (E) and Grand Bay NERR (F).

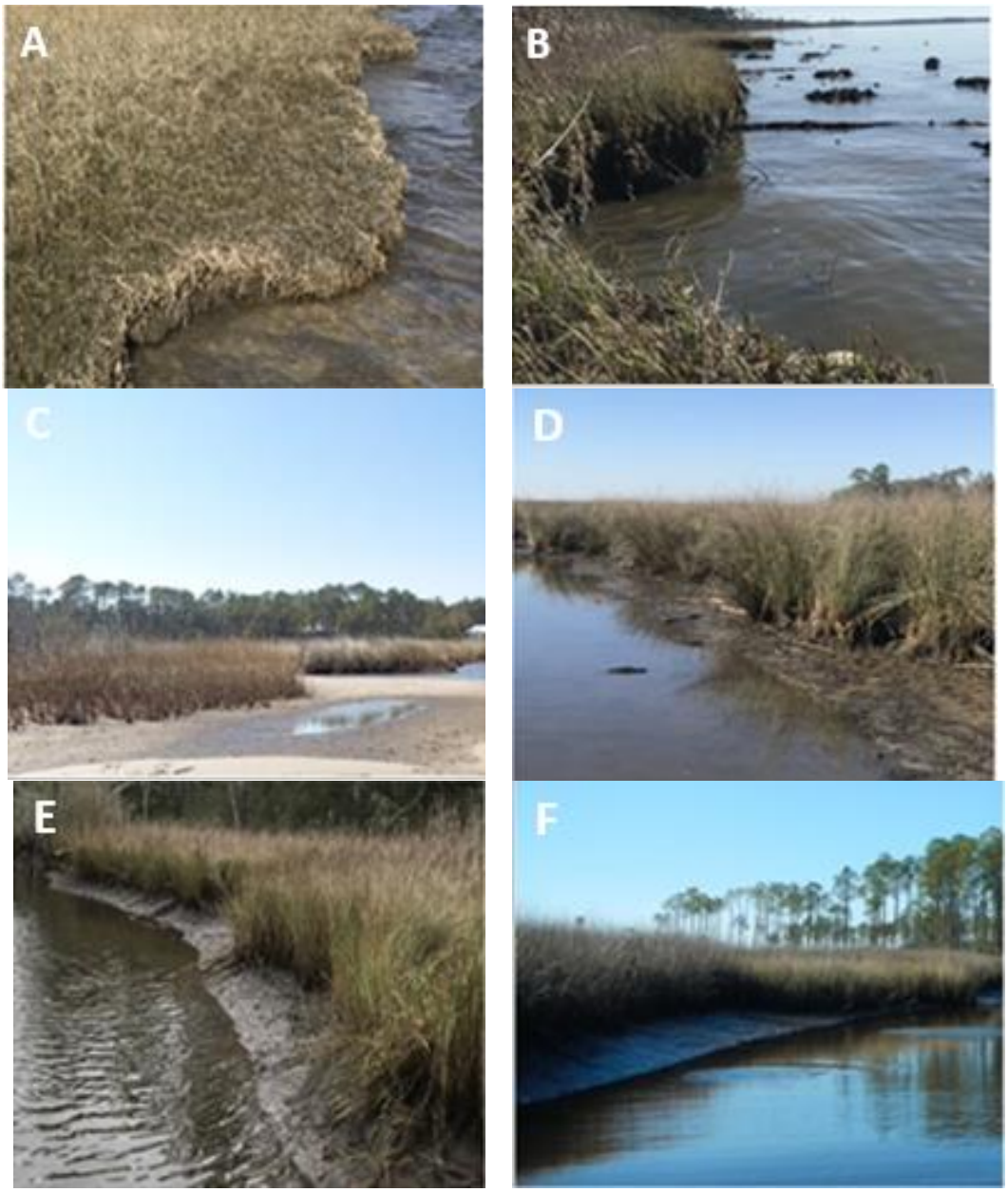

Figure 3. Images of the Natural Shorelines (NS) were taken on fieldwork days. Panels are A.) Hancock County Marsh, B.) Swift Tract, C.) Alonzo Landing, D.) Camp Wilkes, E.) Ocean Springs Inner Harbor, F.) Grand Bay NERR.

Figure 4. Images of the Living Shorelines (LS) were taken either on the day of elevation surveying or on previous fieldwork days. Panels are A.) Hancock County Marsh, B.) Swift Tract, C.) Alonzo Landing, D.) Camp Wilkes, E.) Ocean Springs Inner Harbor, F.) Grand Bay NERR.

Figure 5. Images of the Hardened Shorelines (HS) were taken either on the day of elevation surveying or on previous fieldwork days. Panels are A.) Hancock County Marsh, B.) Swift Tract (picture is of a similar shoreline to the site studied), C.) Alonzo Landing, D.) Camp Wilkes, E.) Ocean Springs Inner Harbor, F.) Grand Bay NERR.

At each of the six sites, I sampled three adjacent shoreline types: (1) natural marsh (NS), (2) living shoreline (LS), and (3) hardened shoreline (HS). Google Earth Pro and an initial field site visit were used to find each type of shoreline; these shorelines were marked using GPS coordinates. At each of the six sites and three shoreline types, I characterized: (1) hydrographic features, (2) geomorphic features, and (3) vegetation abundance (Figure 6).

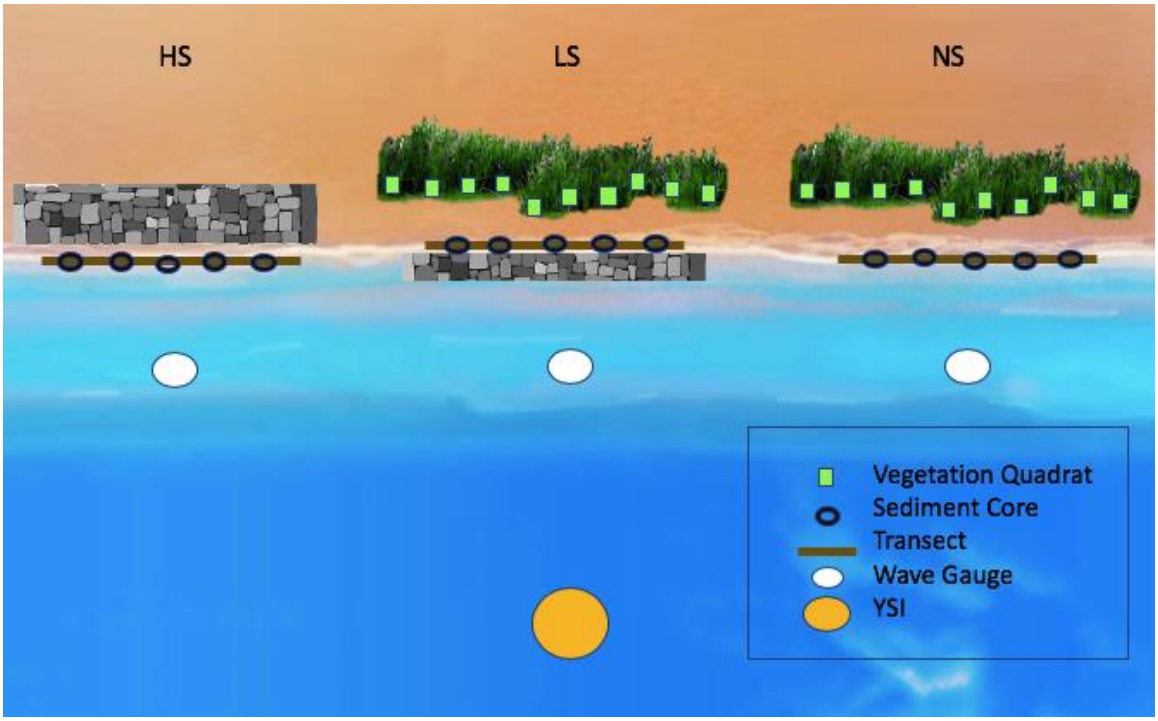

Figure 6. Schematic showing the spatial layout of sampling methods in the field. Wave gauges and YSI were deployed in the winter and summer. One wave gauge was deployed in front of each shoreline, hardened shoreline (HS), living shoreline (LS), and natural shoreline (NS). Five sediment cores from each shoreline type were collected in the winter. Ten vegetation quadrats were collected in the summer for the hardened, living, and natural shoreline.

2.2 Tasks

2.2.1 Hydrographic Features

The hydrographic factors I measured include wave pressure gauges to collect average wave power recorded at 1Hz Frequency (Temple et al. 2019), pre-calibrated YSI 6600 series sondes with turbidity, temperature, conductivity (salinity), and dissolved oxygen recorded at 15 min intervals during 5- to 10-day unattended logger deployments (Figure 3). At each site, a wave gauge was placed in front of each of the three shoreline types with a single YSI between them. However, at Ocean Springs the natural and living shorelines were right across from each other and shared a single wave gauge. Measurements were collected during two seasons (winter 2019 and summer 2020). To deploy the loggers, they were fastened to a cement block using plastic cable ties with a buoy tied to it. Loggers were placed between 5 and 30m offshore from each of the three shorelines.

2.2.2 Geomorphic Features

The geomorphic factors I measured included landscape derived attributes including relative exposure and sediment bulk density, organic content, and grain size distribution derived from cores.

2.2.2.1 Relative Exposure

Landscape derived fetch exposure was used as a proxy for wave energy exposure. Data from the Iowa Environmental Mesonet - ASOS Network was used in R studio to create three wind rose diagrams across the Mississippi/Alabama coast (Bay St Louis, MS

– HSA, Pascagoula, MS – PQL, and Fairhope, AL – CQF) (Figure 8). Relative exposure was calculated using fetch distance measured in Google Earth Pro integrated along 16 bearing lines following the method of La Peyre et al. (2014) (Figure 9, Eqn 2).

Relative exposure = *average speed* * *frequency* * *fetch* Eqn 2

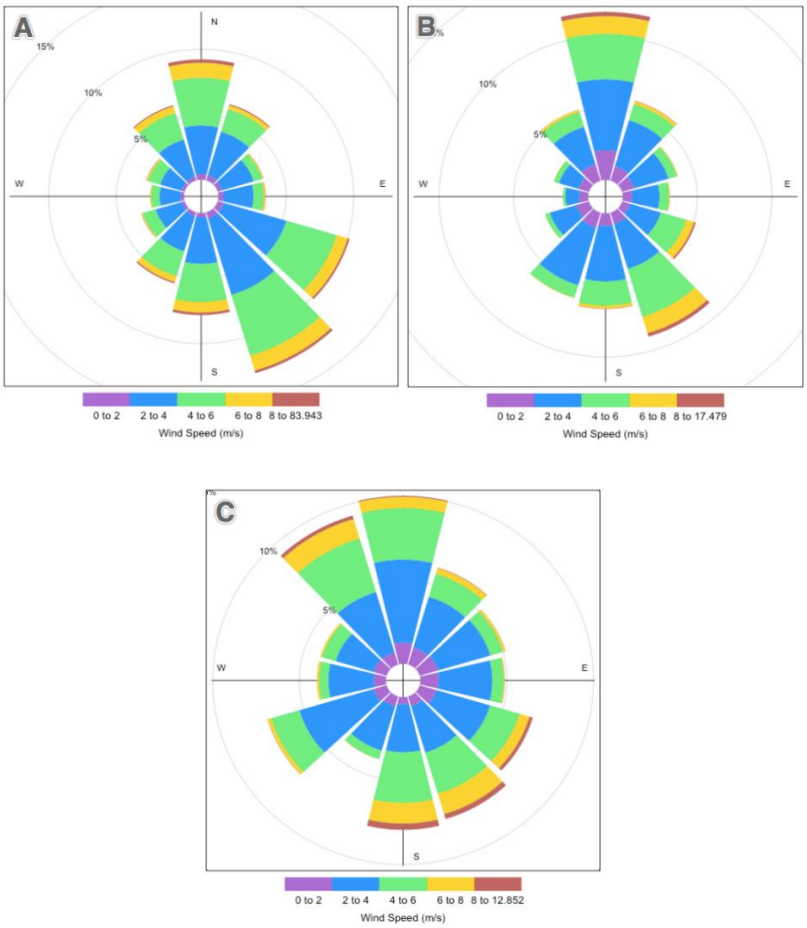

Figure 7. Wind rose diagram showing wind speed (m/s) and compass direction for Bay Saint Louis (A), Pascagoula (B), and Fairhope (C).

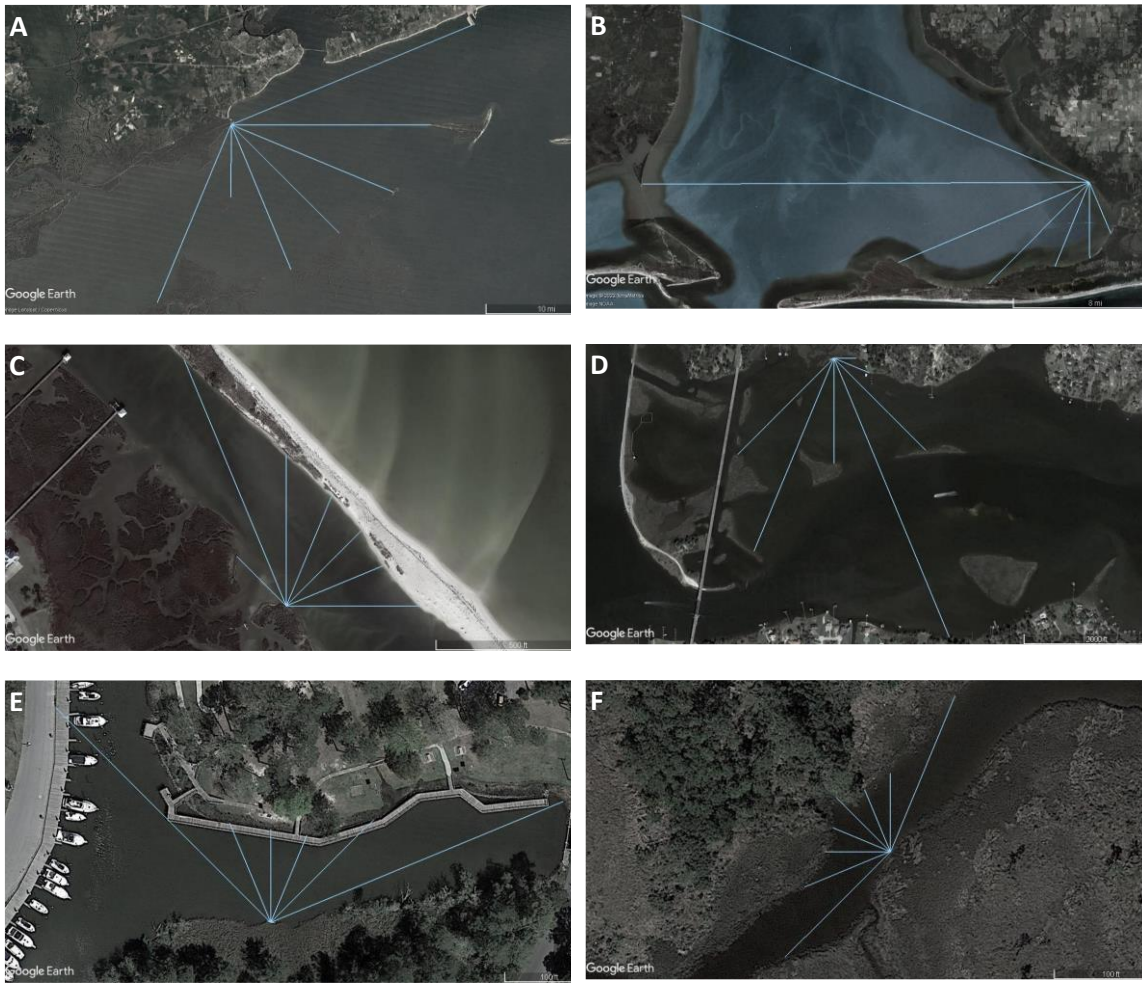

Figure 8. Images of the 16 bearing lines used to measure the fetch for the Natural Shorelines (NS) on Google Earth. Panels are A.) Hancock County Marsh, B.) Swift, C.) Alonzo Landing, D.) Camp Wilkes, E.) Ocean Springs Inner Harbor, F.) Grand Bay NERR.

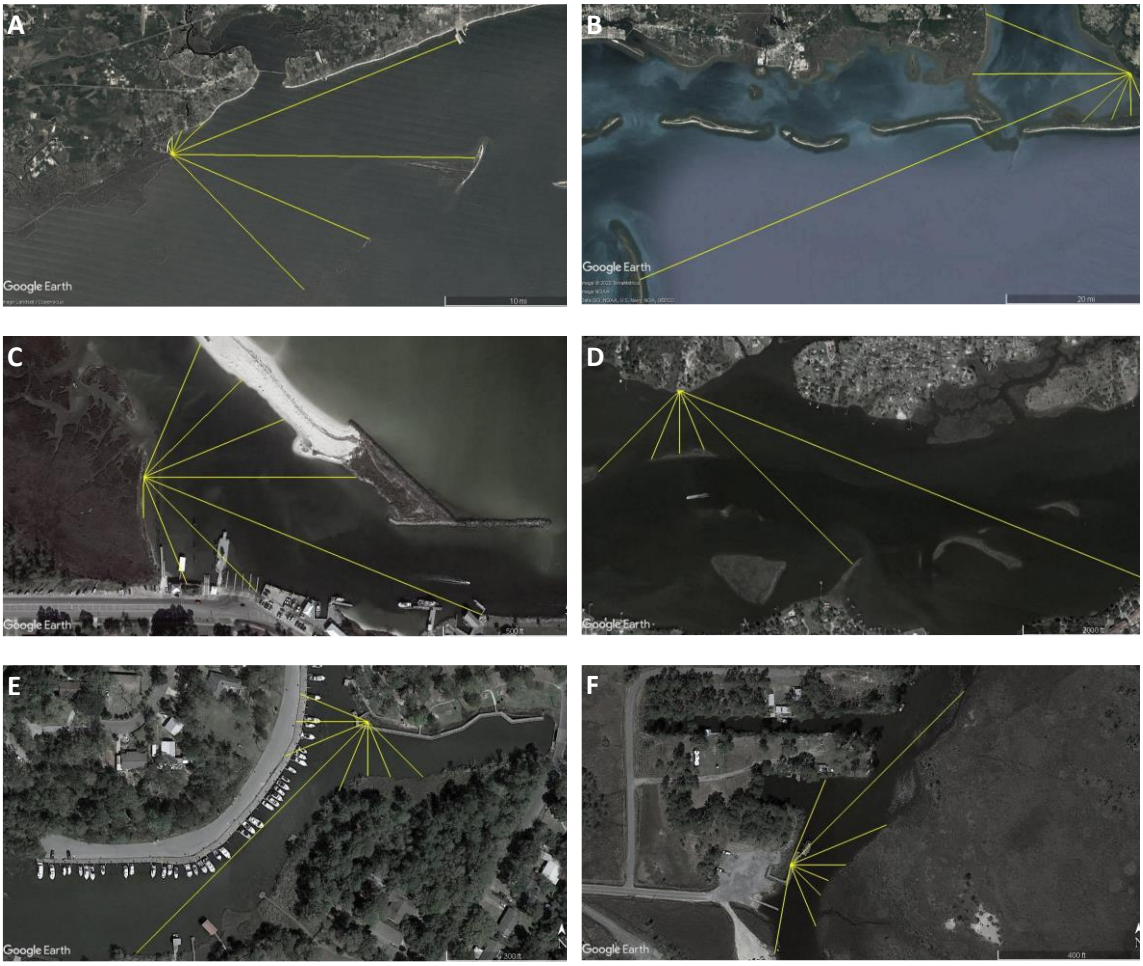

Figure 9. Images of the 16 bearing lines used to measure the fetch for the Living Shorelines (LS) on Google Earth. Panels are A.) Hancock County Marsh, B.) Swift, C.) Alonzo Landing, D.) Camp Wilkes, E.) Ocean Springs Inner Harbor, F.) Grand Bay NERR.

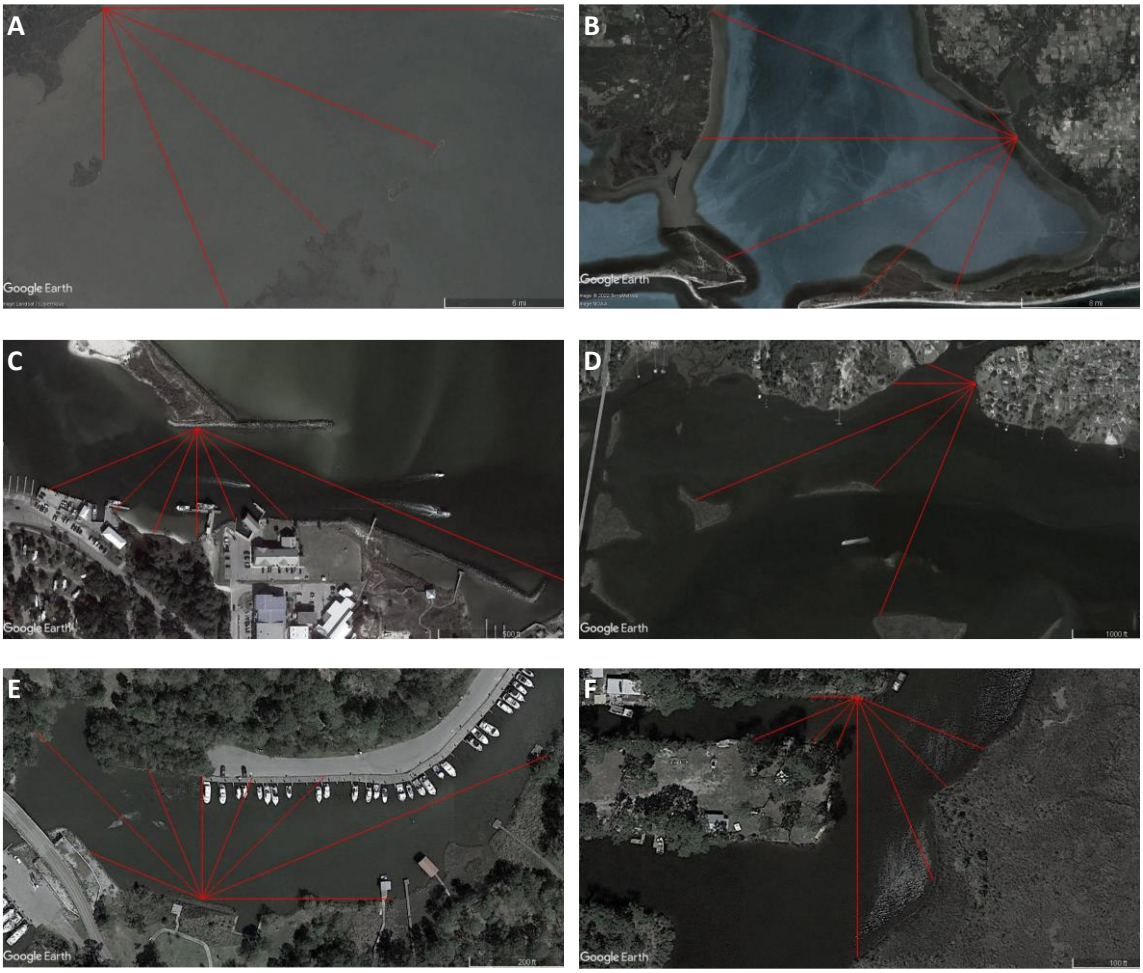

Figure 10. Images of the 16 bearing lines used to measure the fetch for the Hardened Shorelines (HS) on Google Earth. Panels are A.) Hancock County Marsh, B.) Swift, C.) Alonzo Landing, D.) Camp Wilkes, E.) Ocean Springs Inner Harbor, F.) Grand Bay NERR.

2.2.2.2 Erosion Rates and Shoreline Slope

I contributed to an honors project conducted during the same period by Brittany Juneau using the same sites and shorelines to measure coastal slope/elevation, and long-term shoreline erosion rates, which were used to further interpret the data (Juneau 2021). Long term (multi-annual) erosion rates were measured for all three shoreline types at each of the six sites by Juneau (2021). Google Earth Pro's timeline feature was used to

trace the shorelines in the years: 2011 and 2019. Not all sites had usable images from the same time so some of the years varied. Once the shorelines were traced, a baseline was created ~100 m inshore parallel to the shoreline using the ruler tool in Google Earth. Four transects perpendicular to the baseline were then drawn to the shorelines traced for each year and the distance to the baseline recorded (Figure 11). The distances were then used to determine the average rate of erosion per year 2011-2019.

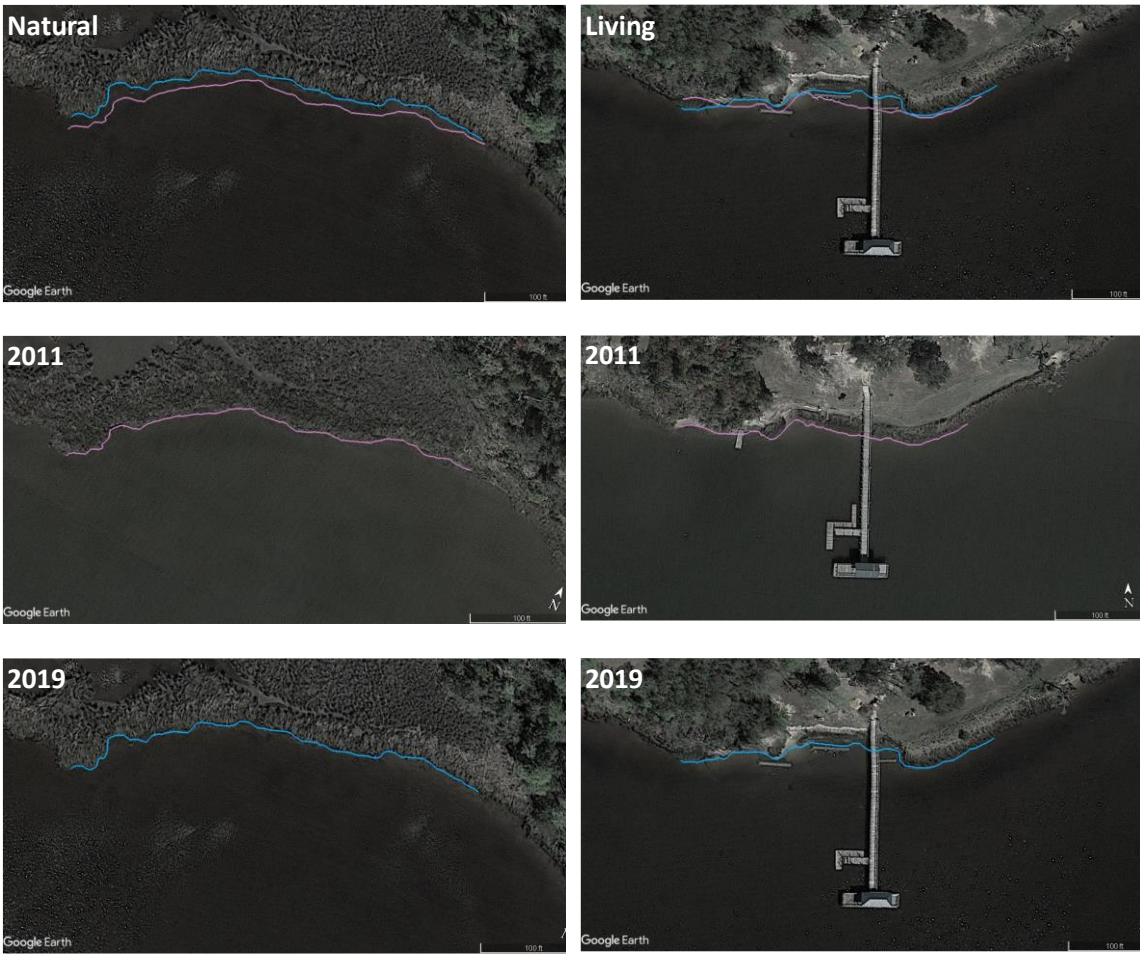

Figure 11. Example erosion rate data from the Camp Wilkes natural shoreline (left) and living shoreline (right) traced in 2011 and 2019, and an overlap of each year with the corresponding background for 2011 and 2019, the background for the combined tracings are from 2019.

It is also important to measure the slope of a shoreline to see how erosion has affected geomorphology; a steeper slope generally means more erosion, which can affect sediment grain size and organic content. Slope was measured using two elevation survey transects, where height above the water was recorded at every 1 m interval (Juneau 2021) for each of the 18 shorelines. These were used to create elevation profiles up to 10 m inland and 10 m offshore (when possible) from the water line.

2.2.2.3 Sediment composition

Sediment was collected in the subtidal flats immediately adjacent to the shoreline vegetation or hardened structure during the winter, when the tide was at its annual lowest. At each shoreline type within a site, I collected five sediment cores along a 50-100 m transect running parallel to and approximately two meters offshore from the marsh vegetation shoreline or bulkhead (Figure 3). A modification was required at Grand Bay's living shoreline, where a layer of oyster shells and rock would not allow us to sample, so the cores were taken approximately two meters into the vegetation. Each core was separated into three depths, 0-10 cm, 10-20 cm, and 20-30 cm. This gave us 45 core segments per site and a total of 270 sediment samples to process.

To collect the sediment samples, I used a PVC corer to get a soil depth of 30 cm and a diameter of 5.08 cm (2"). The corer had a beveled bottom edge to help break through roots and shells. The corer was pushed into the ground to 30 cm and a plug was placed in the vent hole as the corer was removed to preserve suction on the sediment sample inside the device. Once out of the ground, the corer handle was removed, and a plunger made of 3.81 cm (1.5") PVC pipe with an end cap was used to carefully extrude

the core onto a flat cutting board. Each core was cut into 10 cm segments and placed in separate labeled Ziploc® bags that were put on ice until they were returned to the lab where they were placed into the refrigerator and processed as soon as possible.

To process the sediment sample in each bag, it was homogenized by hand and then split into two subsamples to measure bulk density (BD), organic matter (OM) content, and grain size. Due to the shutdown and work from home initiatives caused by the coronavirus (COVID-19) most of the sediment samples were taken home where they were sieved using a garden hose and baked in an oven at the lowest possible temperature.

Subsample #1 – Bulk density and organic matter content: BD was calculated as mass/volume from an initial subsample of 1.5 tbs (22 ml) of the sediment. The subsample was placed in an oven to dry at 70-80 ^{o}C. Once a constant weight was achieved it was then combusted in a muffle furnace at 550 ^{o}C for four hours using the loss-on-ignition (LOI) method to determine OM content. I then record the ash free dry weight (AFDW) (Eqn 3). The equation

$$OM\% = (\text{dry weight} - AFDW)/\text{dry weight}*100 \qquad \text{Eqn 3}$$

was used to find the percent organic matter content of the original sample.

Subsample #2 – Sediment grain size: The sediment remaining in the bag was weighed and then wet sieved to separate the sand, fine sand, and silt-clay fractions using # 10 (2 mm), #18 (1 mm) and #230 (0.625 mm) sieves stacked on top of each other. The #10 sieve separated the large debris, #18 captured the coarse sand, and #230 captured the fine sand allowing the silt and clay to pass through. Water was run through the stacked

sieves to separate the sediment fractions until the water ran clear. The sample wet and dry weights were recorded for the sediment fraction remaining in each of the sieves. Silt/clay content was inferred from the difference in remaining sample weight (debris+sand) after sieving, subtracted from the initial total sample weight before sieving.

2.2.3 Vegetation

Vascular plant abundance was measured in ten replicate 1 m^2 quadrats spaced equidistant along a 50 m transect running parallel to shore and located three to five meters upslope from the vegetated marsh plant edge of the marsh (Figure 3). Since there were no plants downslope along hardened structures, vegetation for these shorelines was recorded on the landward side only when there was vegetation available. This encompassed 30 quadrats per site and a total of 180 quadrats documented in spring/summer 2020. The percent coverage for the full quadrat and each of the plant species within was estimated by visualization. Unknown plants were collected and brought back to the lab where they were then identified using taxonomic guides for the northern Gulf of Mexico (Correll and Johnston 1970; Radford et al. 1983; Clewell 1985). The average percent cover of dominant marsh species was also calculated based on the nine species that Eleuterius (1972) says are dominant marsh plant species in Mississippi, which include *Juncus roemerianus, Spartina alterniflora, Sagittaria lancifolia, Spartina patens, Spartina cynosuroides, Distichlis spicata, Fimbristylis castanea, Schoenoplectus americanus,* and *Schoenoplectus robustus.* This metric was calculated like average percent cover but only included those observed out of these nine species.

The percent cover of all species was used to find the alpha and beta diversity. Alpha diversity was calculated using Shannon's H and Simpson's D indices. Alpha diversity was used to calculate the diversity at an individual shoreline/site. Beta diversity was estimated between the different sites and types of shorelines using the Bray-Curtis dissimilarity matrix (Eqn 3). Bray Curtis dissimilarity is used to calculate the vegetative difference between sites.

$$BC_{ij} = 1 - \frac{2C_{ij}}{Si_i + S_j} \quad \text{Eqn 3}$$

Where i and j represent the two sites, C_{ij} is the sum of the counts for each species found in common at both sites, S_i and S_j is the total number of species counted at each site respectively.

2.3 Data Analysis

All data analysis was done in R using RStudio (ver. 1.9, Boston, MA).

2.3.1 Hydrographic Features

Turbidity data was analyzed by two-way ANOVAs using the factors: site & season and average wave power group & season. Data collected from the wave gauges were analyzed in MATLAB using code from Temple et al., (2021) to calculate the parameter average wave power (kW/m). The average wave power was compared using the Kruskal Wallis H Test since the code from MATLAB provided averages for the large amount of data, which meant it no longer met all the assumptions for ANOVA.

2.3.2 Geomorphic Features

Sediment data analysis included the calculations for bulk density, organic matter content, and sediment grain size composition. For each of these parameters a two-way ANOVA was performed using the factors: site & shoreline and average wave power group (high and low) & shoreline. Factors with a significant response (alpha ≤ 0.05) were followed by a Tukey's post hoc test to find groupings of statistically similar means.

2.3.3 Vegetation

Data analysis included two-way ANOVAs for species richness, average percent cover, and alpha diversity calculated using the Shannon H and Simpson D indices, and the Bray Curtis dissimilarity index for beta diversity. The three indices were calculated using the R package Vegan (Oksanen et al. 2020).

2.3.4 Data Interactions

A multivariate non-parametric ordination (nMDS) plot as well as a principal component analysis (PCA) were used for further data exploration. The data for both these tests were centered to mean zero and standardized to unit variance. Hydrographic data included were the average wave power and turbidity. Geomorphic data included were relative exposure, erosion rate, average slope, percent sand, and OM. I removed the factors BD and percent silt/clay because they were highly correlated with OM and percent sand. Vegetation factors that were included in the nMDS and PCA were species richness, percent cover and percent cover of dominant species. Not all response variables measured were included due to high correlation among some pairs of metrics.

CHAPTER 3 - RESULTS

3.1 Hydrographic Features

3.1.1 Wave Gauge Data

Wave gauge data was used to determine the energy exposure from the average wave power resulting in the high and low energy groupings (H (1) = 19.36, $p < 0.00$). Average wave power was significantly different among the six sites (H (5) = 21.49, $p < 0.00$). The average wave power indicated two significantly different groups: (1) the high energy sites at HC (M = 8.94 kW/m, SE = 1.78 kW/m), ST (M = 5.27 kW/m, SE = 1.09 kW/m) and AL (M = 7.35 kW/m, SE = 2.22 kW/m), and the low energy sites at CW (M = 1.98 kW/m, SE = 0.18 kW/m), OS (M = 0.53 kW/m, SE = 0.15 kW/m), and GB (M = 1.12 kW/m, SE = 0.46 kW/m) (Figure 10, Table 1). The average wave power for the high energy sites (M = 6.91 kW/m, SE = 0.95 kW/m) was over five times greater than the average at the low energy sites (M = 1.31 kW/m, SE = 0.23 kW/m). The different parameters recorded by the wave gauges all had similar trends, but the average wave power was used to divide the energy groups, as this was a more accurate reading of the amount of force that impacted the shorelines directly and contributes to wave erosion of sediments (Appendix B).

Table 1. Average wave power (kW/m) at each site and YSI data for both seasons include mean (±SE) turbidity (NTU), temperature (^oC), salinity (ppt), and dissolved oxygen concentration (mg/L).

Site	Avg Wave Power	Season	Turbidity	Temperature	Salinity	D.O. conc
Hancock County	8.94 ± 1.78^{d}	Winter	16.10 ± 0.68^{c}	13.93 ± 0.04	9.66 ± 0.00	6.29 ± 0.16
		Summer	30.43 ± 1.57^{e}	27.92 ± 0.01	3.25 ± 0.01	0.34 ± 0.01
Swift Tract	5.27 ± 1.09^{d}	Winter	20.49 ± 1.14^{d}	16.08 ± 0.07	9.36 ± 0.03	8.68 ± 0.09
		Summer	18.70 ± 1.15^{cd}	29.46 ± 0.07	8.95 ± 0.04	3.13 ± 0.13
Alonzo Landing	7.35 ± 2.22^{d}	Winter	19.13 ± 0.84^{cd}	9.49 ± 0.06	7.30 ± 0.13	10.34 ± 0.03
		Summer	3.89 ± 0.12^{ab}	28.73 ± 0.04	17.38 ± 0.06	2.03 ± 0.09
Camp Wilkes	1.98 ± 0.18^{bc}	Winter	5.22 ± 0.11^{b}	15.66 ± 0.03	10.50 ± 0.05	8.62 ± 0.06
		Summer	3.21 ± 0.08^{ab}	30.32 ± 0.10	6.75 ± 0.13	2.58 ± 0.24
Ocean Springs	0.53 ± 0.15^{ab}	Winter	1.92 ± 0.03^{a}	16.26 ± 0.03	19.02 ± 0.06	5.99 ± 0.07
		Summer	4.06 ± 0.07^{ab}	28.65 ± 0.05	10.80 ± 0.01	3.16 ± 0.07
Grand Bay	1.12 ± 0.46^{abc}	Winter	2.80 ± 0.10^{ab}	11.59 ± 0.07	14.26 ± 0.20	5.33 ± 0.08
		Summer	3.68 ± 0.05^{ab}	29.88 ± 0.05	7.61 ± 0.19	3.25 ± 0.09

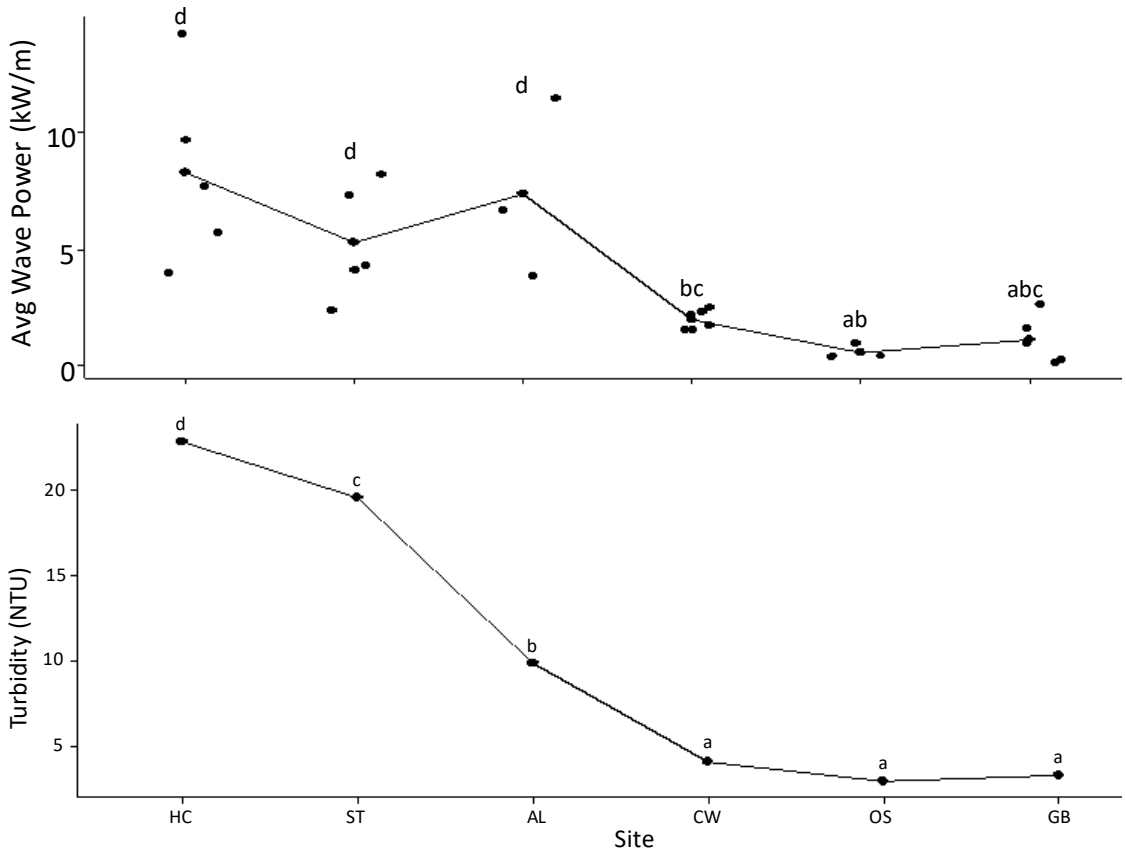

Figure 12. Average wave power (kW/m), and turbidity (NTU) for the six sites. Significant differences by site are indicated by Wilcoxon Rank Test letter groups.

3.1.2 YSI Data

Turbidity was significantly different between winter and summer among the six sites (F (1, 5) = 88.40, p < 0.00). The turbidity was significantly higher in the winter (M = 10.32 NTU, SE = 0.28 NTU) than the summer (M = 9.03 NTU, SE = 0.33 NTU) (Figure 10, Table 1). Turbidity in the winter at AL was 15.24 Nephelometric Turbidity Units (NTU) greater than in the summer, followed by CW (2.01 NTU), ST (1.79 NTU), GB (-0.88 NTU), OS (-2.14 NTU) and HC (-14.33 NTU). This shows that AL and HC varied the greatest between seasons, with AL having a higher turbidity in the winter and HC

having a higher turbidity in the summer. When comparing sites using the average of the two seasons sampled HC (*M* = 22.89 NTU, *SE* = 1.07 NTU) had the highest turbidity, followed by ST (*M* = 19.59 NTU, *SE* = 0.81 NTU), AL (*M* = 9.88 NTU, *SE* = 0.39 NTU), CW (*M* = 4.13 NTU, *SE* = 0.07 NTU), GB (*M* = 3.28 NTU, *SE* = 0.05 NTU), and OS (*M* = 2.99 NTU, *SE* = 0.05 NTU). The high energy sites' (*M* = 16.86 NTU, *SE* = 0.45 NTU) mean turbidity was almost five times greater than the mean turbidity of the low energy sites (*M* = 3.46 NTU, *SE* = 0.03 NTU) (Figure 11). These results for the turbidity data indicate that it is influenced by both site specific and energy group variables. Turbidity may also be influenced by relative exposure and wave power, as well as sediment grain size at the site, with finer-grained sediments resulting in more frequent and intense turbidity.

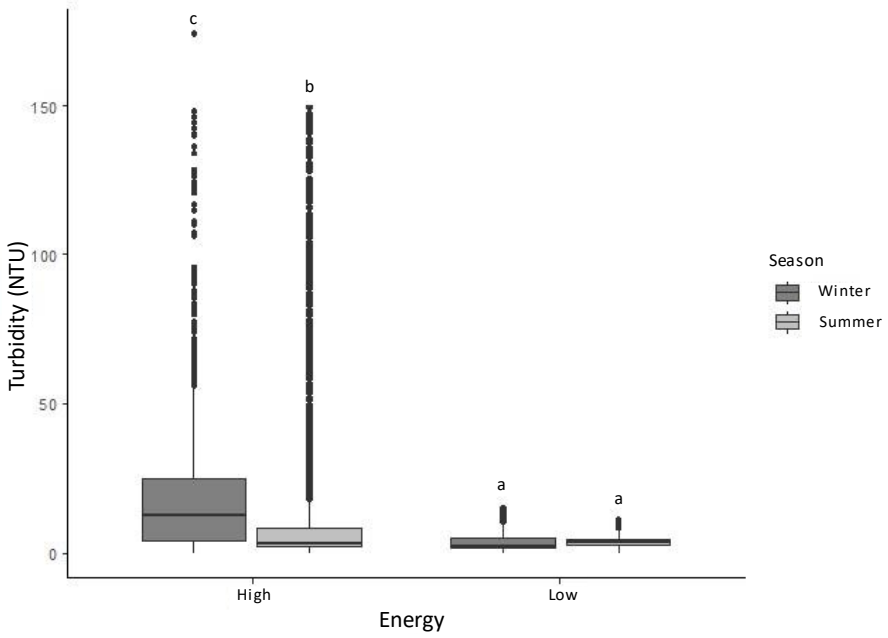

Figure 13. Boxplot of turbidity (NTU) separated by season and wave power group. Significant differences by season and wave power group are indicated by Tukey's HSD post-hoc letter groups.

3.2. Geomorphic Features

3.2.1 Relative Exposure

The relative exposure at each of the six sites was influenced by their orientation to the dominant seasonal wind direction. Relative exposure, therefore, differed by fetch distance and dominant wind direction, with sites exposed to the dominant seasonal winds across a long fetch experiencing the highest relative exposure (Figure 9, Table 2). There were significant differences due to site and energy groups, however, there was no significant effect of shoreline type or season on relative exposure, despite the different shoreline orientations and seasonal wind directions (Table.C.5).

The mean relative exposure was significantly different among the six sites (F (5, 1130) = 59.57, $p < 0.00$). The relative exposure at HC (M = 8458.55, SE = *604.99*) was significantly greater than at all other sites (Table 2). Swift Tract (M = 3285.29, SE = 484.21) had the next greatest relative exposure, while AL (M = 54.46, SE = 5.39), CW (M = 289.71, SE = 32.01), OS (M = 38.10, SE = 5.26), and GB (M = 17.61, SE = 2.19) were all similarly low. This finding suggests that relative exposure at a-shoreline may be strongly influenced by location and the cardinal direction of seasonally dominant winds.

Table 2. Relative Exposure for natural, living, and hardened shorelines at each site and the average (±SE). Significant differences in means are indicated by superscript letter groups in the average column.

Site	Natural (n=4)	Living (n=4)	Hardened (n=4)	Average (n=12)
Hancock County	8196.58	8870.23	8308.84	8458.55 ± 208.38^{c}
Swift Tract	3350.18	3281.83	3220.86	3285.29 ± 37.35^{b}
Alonzo Landing	61.56	59.06	42.76	54.46 ± 5.89^{a}
Camp Wilkes	312.40	304.80	251.92	289.71 ± 19.02^{a}
Ocean Springs	35.22	26.66	52.41	38.10 ± 7.57^{a}
Grand Bay	16.40	22.05	14.38	17.61 ± 2.29^{a}

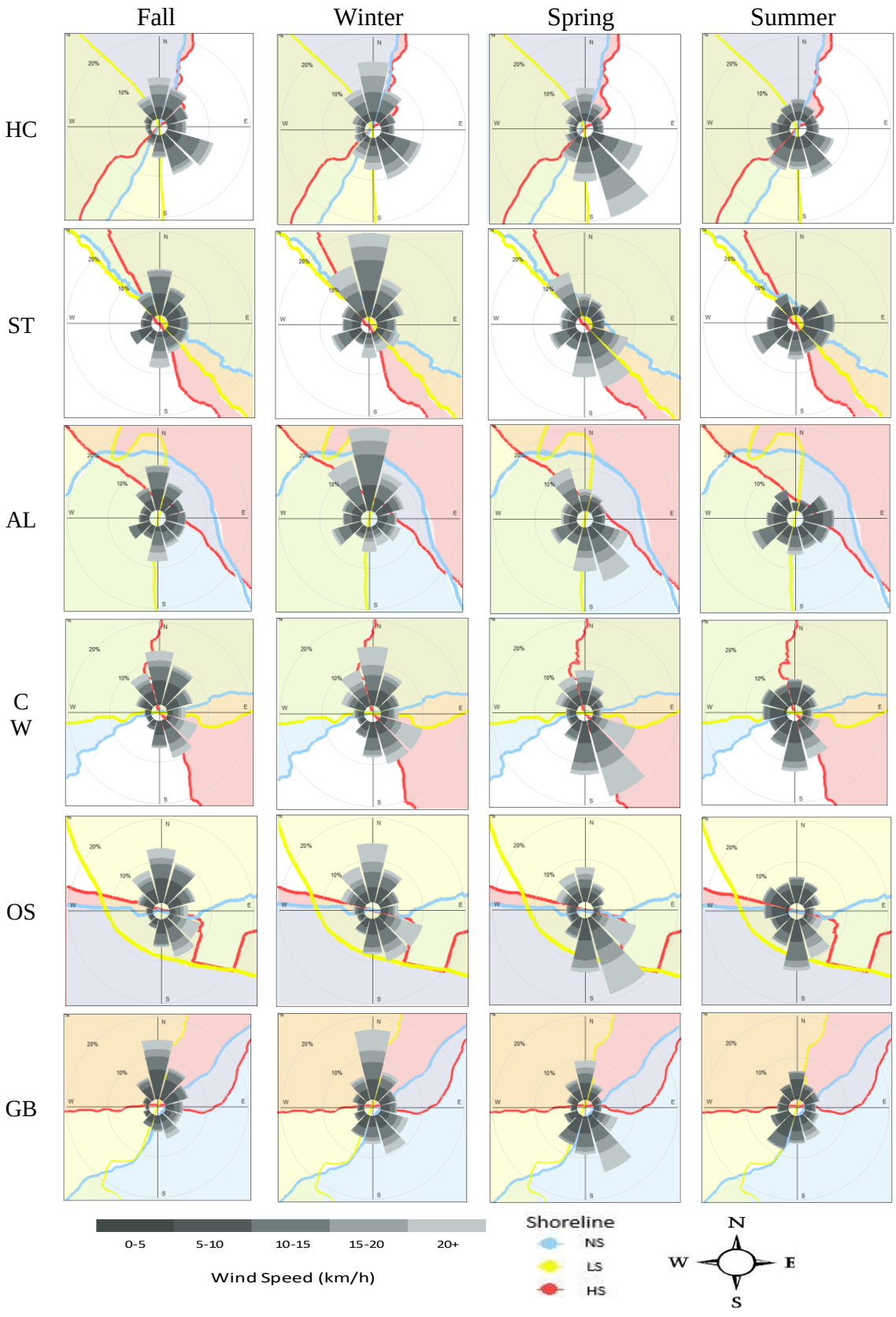
Fall
Winter
Spring
Summer
HC
ST
AL
C
W
OS
GB
0-5
5-10
10-15
15-20
20+
Wind Speed (km/h)
Shoreline
NS
LS
HS
N
W
E
S

Figure 14. Wind rose diagram for Hancock County (HC), Swift Tract (ST), Alonzo Landing (AL), Camp Wilkes (CW), Ocean Springs (OS) for each season. Each image has the three different shorelines; natural (blue), living (yellow), and hardened (red) with the shorelines oriented by compass bearings. The shaded section of each color represents the land.

The mean relative exposure was significantly different between the two energy groups (F (1, 1134) = 98.94, $p < 0.00$). The high wave energy sites (M = 3932.43, SE = 636.58) included HC, ST and AL and had significantly greater exposure than the low wave energy sites (M = 115.14, SE = 23.41) that included CW, OS, and GB (Table 3). This finding suggests that relative exposure may be influenced by fetch distance, wind energy/direction, and shoreline orientation. The highest relative exposure occurs when a shoreline is facing perpendicular to a long fetch distance that is also in the direction of the strongest seasonal winds. This allows the formation of large waves that crash onto the shoreline and can cause edge erosion.

Table 3. Average (±SE) Relative Exposure for natural, living, and hardened shorelines for each wave power group and the average (±SE) for each wave energy group. Significant differences in means are indicated by superscript letter groups in the average column.

Energy	Natural (n=12)	Living (n=12)	Hardened (n=12)	Average (n=36)
High	3,869 ± 1,092	4,070 ± 1,127	3,857 ± 1,184	3,932 ± 636.58[b]
Low	121.34 ± 41.28	117.84 ± 41.74	106.24 ± 42.12	115.14 ± 23.41[a]

3.2.2 Erosion Rates and Shoreline Slope

Shorelines with high relative exposure also experienced more rapid erosion rates in the period from 2011 to 2019. The average annual erosion rate over this eight-year period was calculated by Juneau (2021), who found that the shoreline erosion at NS (*M* = 0.70 m/yr, *SE* = 0.13 m/yr) averaged over the six sites had the highest mean annual erosion rate (Table 4). In comparison the LS (*M* = 0.25 m/yr, *SE* = 0.06 m/yr) had intermediate mean annual erosion rates, and the HS (*M* = -0.02 m/yr, *SE* = 0.01 m/yr) had the lowest annual rate of erosion, however, this analysis used an erosion rate value of 0m at the LS and HS at HC. The reason for this was the installation of a large geo-tube (~ 3 m dia x 615 m long) that substantially moved the LS offshore out into former subtidal elevations, as well as the installation of a rock jetty at the HS that ran perpendicular to the shoreline instead of parallel.

The mean annual erosion rate was significantly different among the six sites and shorelines (F (10, 54) = 25.39, $p < 0.00$). For the NS, HC (*M* = 1.69 m/yr, *SE* = 0.08 m/yr) had the highest erosion rate (Table 4, Figure 13). The next highest were ST (*M* = 0.93 m/yr, *SE* = 0.10 m/yr) and AL (*M* = 1.04 m/yr, *SE* = 0.23 m/yr), followed by CW (*M* = 0.45 m/yr, *SE* = 0.03 m/yr), OS (*M* = 0.14 m/yr, *SE* = 0.03 m/yr), and GB (*M* = -0.07 m/yr, *SE* = 0.03 m/yr). The high rate of shoreline retreat at the various NS indicates retrograding facies are common in the study region and suggests marsh edge erosion is a frequent problem. Erosion rates of natural shorelines may be influenced by relative exposure and wave power.

Table 4. Average erosion rates (m/yr ± SE) for the three different shorelines at each site, as well as the average (±SE) for each site and each type of shoreline. All Sites excludes the living shoreline and hardened shoreline at Hancock County. Significant letters are from the two-way ANOVA with the parameters being site and shoreline with all shorelines included.

Site	Natural	Living	Hardened	By Site
Hancock County	1.69 ± 0.09^{e}	0.00 ± 0.00^{a}	0.00 ± 0.00^{a}	0.56 ± 0.24
Swift Tract	0.93 ± 0.10^{d}	0.42 ± 0.04^{bc}	-0.01 ± 0.02^{a}	0.45 ± 0.12
Alonzo Landing	1.04 ± 0.23^{d}	0.71 ± 0.05^{cd}	-0.06 ± 0.03^{a}	0.56 ± 0.16
Camp Wilkes	0.45 ± 0.03^{bc}	0.30 ± 0.16^{b}	-0.19 ± 0.06^{a}	0.19 ± 0.10
Ocean Springs	0.14 ± 0.03^{ab}	0.10 ± 0.04^{ab}	0.04 ± 0.02^{ab}	0.09 ± 0.02
Grand Bay	-0.07 ± 0.03^{a}	-0.02 ± 0.02^{a}	0.18 ± 0.10^{ab}	0.03 ± 0.05
All Sites	0.70 ± 0.13	0.25 ± 0.06	-0.01 ± 0.03	

Table 5. Average erosion rates (m/yr ± SE) for the three different shorelines for the two energy groupings, as well as the average (±SE) for each energy group. Significant letters are from the two-way ANOVA with the parameters being energy and shoreline with all shorelines included.

Energy	Natural	Living	Hardened	By Energy
High	1.22 ± 0.13^{c}	0.38 ± 0.09^{b}	-0.02 ± 0.01^{a}	0.52 ± 0.10
Low	0.17 ± 0.07^{ab}	0.13 ± 0.06^{ab}	0.01 ± 0.06^{a}	0.10 ± 0.04

For the LS (*M* = 0.25 m/yr, *SE* = 0.06 m/yr) HC was an outlier site that was previously left out by Juneau (2021) because of the circumstances by which it was created, which caused it to have gained 3.25 m/yr (*SE* = 0.05 m/yr) (Table 4). The site that had the significantly highest LS erosion rate was AL (*M* = 0.71 m/yr, *SE* = 0.05 m/yr). The site that had the lowest LS erosion rate was GB, which gained 0.02 m/yr of shoreline. The other three sites were not significantly different to each other: ST (*M* = 0.42 m/yr, *SE* = 0.04 m/yr), CW (*M* = 0.30 m/yr, *SE* = 0.16 m/yr), OS (*M* = 0.10 m/yr, *SE*

= 0.04 m/yr (Table 4). The mean erosion rates were significantly lower at the LS shorelines compared to the adjacent NS counterparts, apart from OS and GB. This finding indicates that the implementation of a LS may reduce the rate of shoreline erosion compared to the adjacent NS at most project sites.

For the HS the only significantly difference was between CW (*M* = -0.19 m/yr, *SE* = 0.06 m/yr) and GB (*M* = 0.18 m/yr, *SE* = 0.10 m/yr). Again, HC's HS was left out by Juneau (2021) and is subsequently also being left out of these results because the shoreline and rock jetty at this site are not parallel to each other, like was found at the other five sites. The other shorelines had erosion rates intermediate between CW and GB, AL (*M* = -0.06 m/yr, *SE* = 0.03 m/yr), OS (*M* = 0.04 m/yr, *SE = 0.03* m/yr), ST (*M* = -0.01, *SE* = 0.02 m/yr) and HC (*M* = 0.00, *SE* = 0.00 m/yr). All five of these sites had a type of retaining wall (wooden bulkhead or rocky riprap) that held the shoreline position constant over time. This finding indicates that the HS (excluding HC) had little erosion over time. It is very possibly erosion was zero and any change detected was because of geospatial error and variation that could have been due to changes in the different images used to delineate the shoreline.

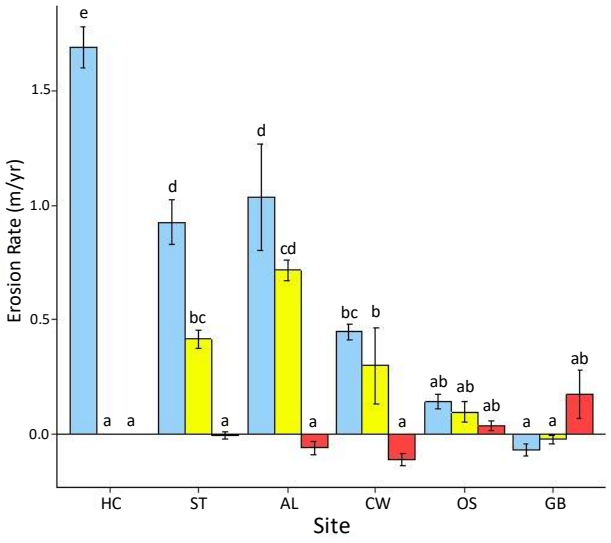

Figure 15. Erosion rates (m/yr) for the different six sites and three shoreline types with natural shorelines (blue), living shorelines (yellow), and hardened shorelines (red). The LS and HS for HC were zeroed. Tukey's HSD post-hoc letter groups show the significant differences for the three shorelines and sites.

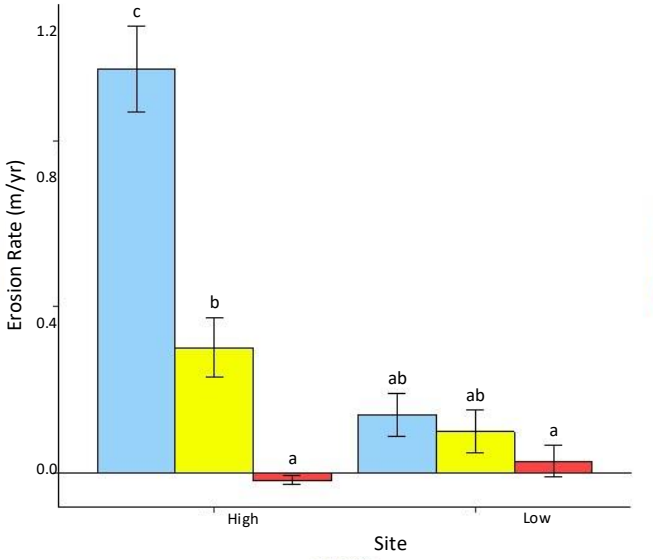

Figure 16. Erosion rates (m/yr) for the different two energy groups and three shoreline types with natural shorelines (blue), living shorelines (yellow), and hardened shorelines (red). This excludes the living shoreline for HC because it had a high rate of accretion. Tukey's HSD post-hoc letter groups show the significant differences for the three shorelines and energy groups.

The mean slope at the three shoreline types were also significantly different ($F(2,33) = 19.88$, $p < 0.00$) according to Juneau (2021). The HS (M = 24.99 cm, SE = 2.01 cm) had a significantly steeper slope than either the NS (M = 12.84 cm, SE = 1.43 cm) or LS (M = 10.62 cm, SE = 1.37 cm), which did not differ from each other (Table 6, Figure 17). At all sites, except for HC and GB, the LS had a gentler slope than the adjacent NS from the same site (Figure 18). The LS at HC is one of the shorelines left out from the elevation data in Juneau (2021) because the geo-tube acts more like a HS, with a rapid elevation increase (~2m) from the water's edge. The LS at GB is a marsh restoration project with a rocky berm and located alongside a boat ramp so the adjacent navigational channel may have been dredged in the past resulting in a steep slope, as well as affecting the LS due to frequent boat wakes. These findings indicate that shoreline slope is often affected by manmade structures especially in the HS and in some LS sites. Shoreline slope and mean erosion rates may in turn affect sediment composition, turbidity, and vegetation found at the site.

Table 6. The average slope (±SE) for the natural, living, and hardened shorelines at all six sites. Significant letters are between the six sites within each of the three treatment types.

Site	Natural (cm/m)	Living (cm/m)	Hardened (cm/m)
Hancock County	7.83 ± 0.33^{ab}	12.63 ± 6.13^{bc}	22.67 ± 1.00^{cd}
Swift Tract	15.25 ± 0.42^{bc}	10.75 ± 0.92^{ab}	30.08 ± 0.75^{d}
Alonzo Landing	20.75 ± 3.58^{cd}	11.83 ± 2.00^{ab}	25.25 ± 4.08^{cd}
Camp Wilkes	8.75 ± 1.75^{ab}	4.75 ± 2.08^{a}	29.33 ± 0.33^{d}
Ocean Springs	14.00 ± 0.33^{bc}	8.42 ± 2.42^{ab}	12.25 ± 2.75^{bc}
Grand Bay	10.50 ± 1.17^{ab}	15.33 ± 2.83^{bc}	30.33 ± 0.50^{d}

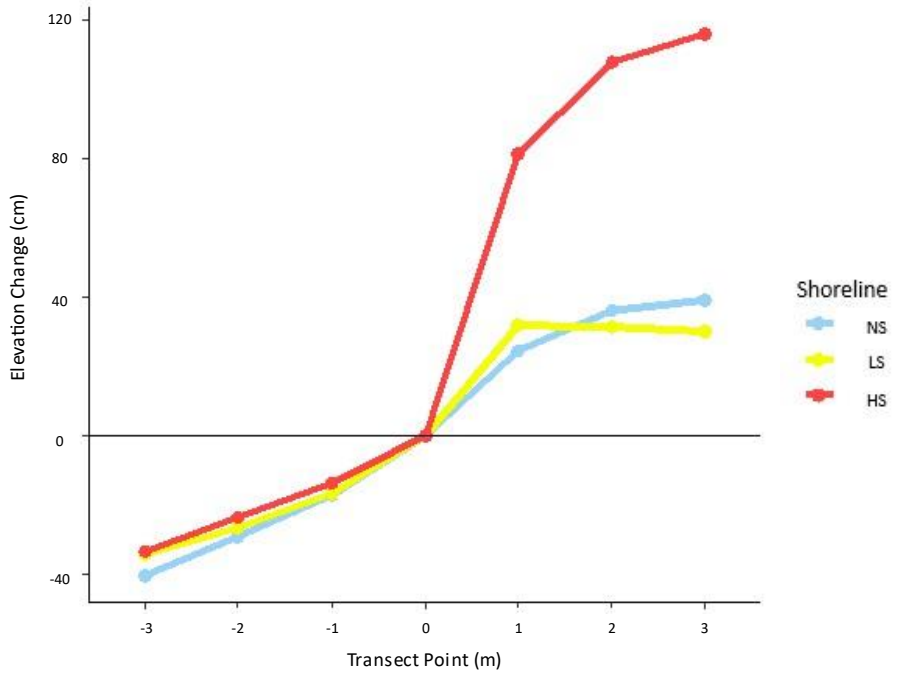

Figure 17. A graph of the average elevation change (cm/m) for natural (blue), living (yellow), and hardened (red) shorelines. The coordinate (0,0) represents the mean water level at the shoreline at the time of sampling. Negative elevation point distances are seaward, while positive transect point distances are landward.

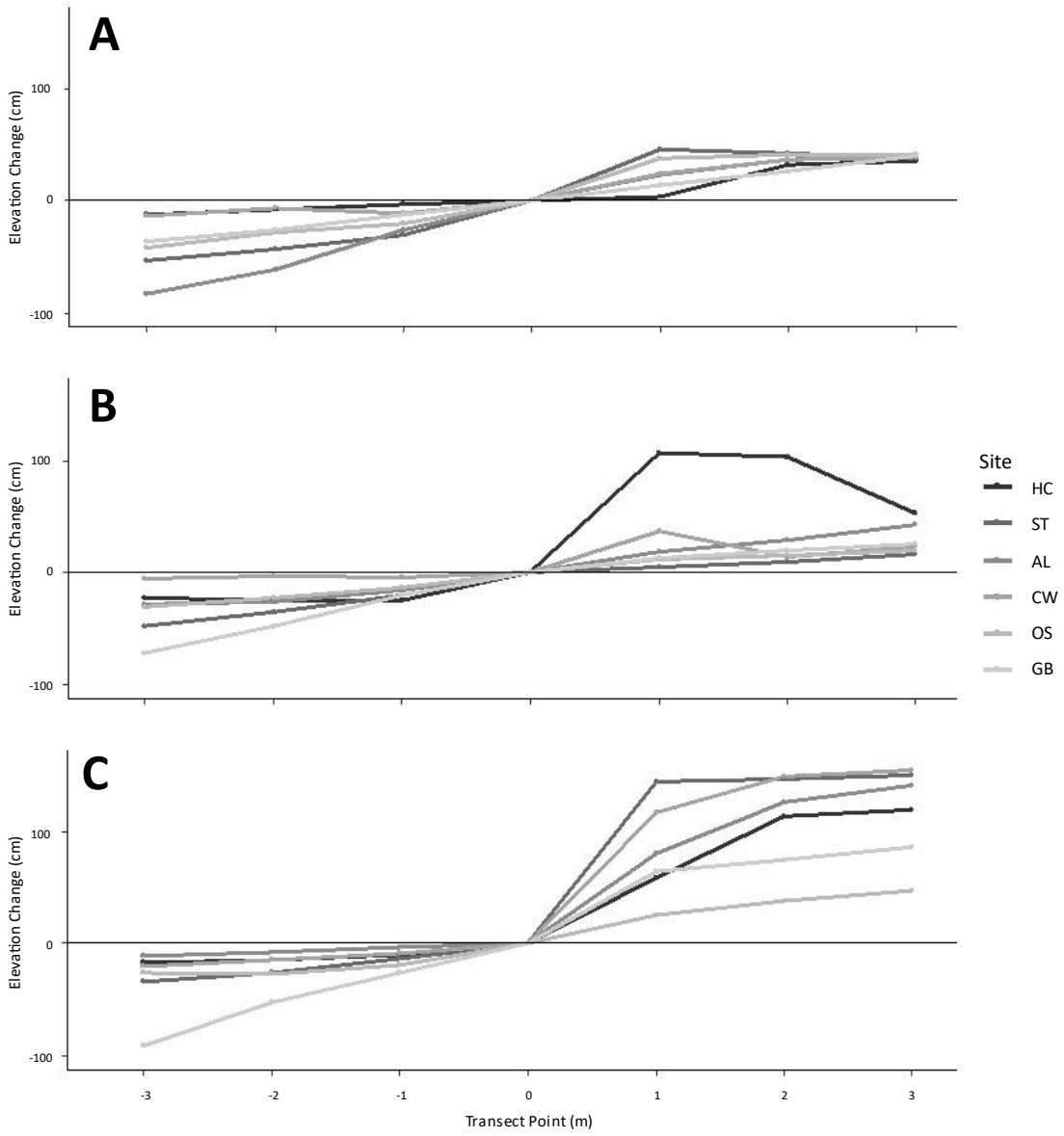

Figure 18. A graph of the average elevation change (cm/m) for the six different sites, separated by (A) natural, (B) living, and (C) hardened shorelines. The coordinate (0,0) represents the mean water level at the shoreline at the time of sampling. Negative elevation points are seaward, while positive transect points are landward.

3.2.3 Sediment Bulk Density and Organic Matter Content

Bulk density and OM were calculated by averaging the three different depths. The mean BD was significantly different among the three shoreline types (F (2,262) = 66.53, $p < 0.00$). Bulk density was lowest in the NS (M = 0.60 g/cm^3, SE = 0.04 g/cm^3) and highest in the HS (M = 1.25 g/cm^3, SE = 0.03 g/cm^3), with LS (M = 0.89 g/cm^3, SE = 0.05 g/cm^3) intermediate. This indicates that the NS had the most porous sediments followed by the LS. The HS had the least porous sediments, which can stunt root growth for vegetation. This shows that the shoreline type plays a role in the BD, a proxy for porosity, of the intertidal sediments.

Bulk density was significantly different among the six sites and shorelines (F (10,247) = 13.35, $p < 0.00$). For the NS the lowest BD among the NS was at CW (M = 0.25 g/cm^3, SE = 0.01 g/cm^3), followed by OS (M = 0.42 g/cm^3, SE = 0.02 g/cm^3), HC (M = 0.60 g/cm^3, SE = 0.02 g/cm^3), AL (M = 0.63 g/cm^3, SE = 0.11 g/cm^3) and ST (M = 0.64 g/cm^3, SE = 0.10 g/cm^3) (Table 7). The NS at GB (M = 1.06 g/cm^3, SE = 0.11 g/cm^3) was significantly different from all other NS. The mean BD for GB was almost twice as high as at the second highest site, ST.

For the LS, ST (M = 0.47 g/cm^3, SE = 0.12 g/cm^3) had the lowest BD among the LS followed by AL (M = 0.76 g/cm^3, SE = 0.07 g/cm^3), OS (M = 0.82 g/cm^3, SE = 0.08 g/cm^3), HC (M = 0.87 g/cm^3, SE = 0.10 g/cm^3) and CW (M = 1.05 g/cm^3, SE = 0.09 g/cm^3) (Table 7). Grand Bay's (M = 1.40 g/cm^3, SE = 0.05 g/cm^3) LS had the highest BD.

The lowest BD for the HS was at OS (M = 0.70 g/cm^3, SE = 0.06 g/cm^3) (Table 7, Fig.). The next lowest BD was GB (M = 1.24 g/cm^3, SE = 0.07 g/cm^3), HC (M = 1.25 g/cm^3, SE = 0.05 g/cm^3), ST (M = 1.37 g/cm^3, SE = 0.06 g/cm^3), and AL (M = 1.41

g/cm^3, *SE* = 0.01 g/cm^3). Camp Wilkes (*M* = 1.54 g/cm^3, *SE* = 0.01 g/cm^3) had the highest BD of all sites and shorelines. All the HS sites, except for OS, had low BD.

The mean BD was significantly different in the two energy groups when separated by shoreline type. The BD for the NS low energy sites (*M* = 0.58 g/cm^3, *SE* = 0.07 g/cm^3), NS high energy sites (*M* = 0.62 g/cm^3, *SE* = 0.05 g/cm^3), and the LS high energy sites (*M* = 0.70 g/cm^3, *SE* = 0.06 g/cm^3) were similar (Table 8, Figure 19). The LS at the low energy sites (*M* = 1.08 g/cm^3, *SE* = 0.06 g/cm^3) was like the HS at the low energy sites (*M* = 1.16 g/cm^3, *SE* = 0.06 g/cm^3). The highest BD was at the HS high energy sites (*M* = 1.34 g/cm^3, *SE* = 0.03 g/cm^3). This finding indicates that BD may be influenced by the type of shoreline and the amount of energy that shoreline receives. In the higher energy sites, the NS and LS act the same as the NS at the low energy sites, having more porous sediment and allowing water and roots to migrate within it, so it may be expected for these shorelines to have finer sediment particles.

Table 7. Average (±SE) of the sediment composition (BD, OM) collected at six sites, with three shoreline types at each site. Significant differences in means are indicated by superscript letter groups in each column for the different types of shorelines.

Site	Bulk Density (g/cm^3)	Organic Matter (%)
Natural		
Hancock County	0.60 ± 0.02^{b}	13.10 ± 1.23^{b}
Swift Tract	0.64 ± 0.10^{b}	22.57 ± 2.97^{c}
Alonzo Landing	0.63 ± 0.11^{b}	16.14 ± 2.47^{bc}
Camp Wilkes	0.25 ± 0.01^{a}	37.49 ± 1.89^{d}
Ocean Springs	0.42 ± 0.02^{ab}	13.85 ± 1.04^{b}
Grand Bay	1.06 ± 0.11^{c}	4.02 ± 0.63^{a}
Living		
Hancock County	0.87 ± 0.10^{b}	12.48 ± 2.95^{a}
Swift Tract	0.47 ± 0.12^{a}	48.37 ± 7.76^{b}
Alonzo Landing	0.76 ± 0.07^{ab}	9.43 ± 1.29^{a}
Camp Wilkes	1.05 ± 0.09^{bc}	6.59 ± 1.50^{a}
Ocean Springs	0.82 ± 0.08^{ab}	7.16 ± 1.53^{a}
Grand Bay	1.40 ± 0.05^{c}	2.46 ± 0.38^{a}
Hardened		
Hancock County	1.25 ± 0.05^{b}	1.61 ± 0.84^{ab}
Swift Tract	1.37 ± 0.06^{bc}	2.48 ± 0.65^{ab}
Alonzo Landing	1.41 ± 0.01^{bc}	0.33 ± 0.20^{a}
Camp Wilkes	1.54 ± 0.01^{c}	2.32 ± 0.16^{ab}
Ocean Springs	0.71 ± 0.06^{a}	7.04 ± 0.83^{c}
Grand Bay	1.24 ± 0.07^{b}	3.49 ± 0.63^{b}

Table 8. Average (±SE) of the three sediment size fractions collected for high and low energy groups, with three shoreline types at each group. Significant differences in means are indicated by superscript letter groups in each column.

Shoreline	Bulk Density (g/cm^3)	Organic Matter (%)
High Energy		
Natural	0.62 ± 0.05^{a}	17.27 ± 1.45^{b}
Living	0.70 ± 0.06^{a}	23.74 ± 3.89^{b}
Hardened	1.34 ± 0.03^{c}	1.47 ± 0.38^{a}
Low Energy		
Natural	0.58 ± 0.07^{a}	18.45 ± 2.24^{b}
Living	1.08 ± 0.06^{b}	5.58 ± 0.81^{a}
Hardened	1.16 ± 0.06^{bc}	4.28 ± 0.46^{a}

The mean OM was significantly different among the three shoreline types: NS, LS, and HS (F (2, 262) = 28.68, $p < 0.00$). The OM at HS (M = 2.88 %, SE = 0.33%) was significantly lower than the LS (M = 15.09 %, SE = 2.29%) and NS (M = 17.86 %, SE = 1.33%) that were similar (Table 7). The finding of low OM at HS indicates that there is little organic content in the sediment, while LS had over five times as much organic matter and NS had over six times as much organic matter as the HS in this study. This indicates that the OM content of the sediment may be positively influenced by having marsh vegetation present (NS and LS).

The mean OM was significantly different among the six sites (F (5, 259) = 11.98, $p < 0.00$). The OM was the lowest at GB (M = 3.38 %, SE = 0.34%) (Table 7). Organic matter content for AL (M = 8.61%, SE = 1.36%), HC (M = 9.07 %, SE = 1.34%), and OS (M = 9.49 %, SE = 0.83%) were grouped between GB and CW (M = 15.47 %, SE =

2.49%). The significantly highest OM was ST (*M* = 24.47 %, *SE* = 3.92%). This finding indicates that location may influence the organic matter content found.

The mean OM was significantly different among the six different sites and shorelines (F (10, 247) = 23.13, $p < 0.00$). The OM at the NS for GB (*M* = 4.02 %, *SE* = 0.63%) was significantly lower than the other NS (table 7), followed by HC (*M* = 13.10 %, *SE* = 1.23%), OS (*M* = 13.85 %, *SE* = 1.04%), AL (*M* = 16.14 %, *SE* = 2.47%), and ST (*M* = 22.57 %, *SE* = 2.97%). The highest OM was at CW (*M* = 37.49 %, *SE* = 1.89%) which is more than double the next highest OM for NS (ST). This indicates that the OM for NS can vary greatly and not all of them have equal organic matter content.

The OM at the LS for ST (*M* = 48.37 %, *SE* = 7.76%) was significantly higher than HC (*M* = 12.48%, *SE* = 2.95%), AL (*M* = 9.43 %, *SE* = 1.29%), OS (*M* = 7.16 %, *SE* = 1.53%), CW (*M* = 6.59 %, *SE* = 1.50%), and GB (*M* = 2.46 %, *SE* = 0.38%) which were all similar (table 7). This indicates that among the LS the OM may be affected by the implementation of the LS and may affect the organic matter content by slightly lowering it.

The OM among the HS was lowest at AL (*M* = 0.33 %, *SE* = 0.20%), followed by HC (*M* = 1.61 %, *SE* = 0.84%), CW (*M* = 2.32 %, *SE* = 0.16%), ST (*M* = 2.48 %, *SE* = 0.65%), and GB (*M* = 3.49%, *SE* = 0.63%). The significantly highest OM among the HS was at OS (*M* = 7.04 %, *SE* = 0.83%). The highest OM for HS was still lower than all the sites at the NS and LS, except for GB. This indicates that the structures implemented at the HS decrease the deposition and accumulation of organic matter content at their base, which may also be seen as a higher percent of the sand fraction.

The mean OM was significantly different for the three shoreline types by two energy groups (F (2, 259) = 17.14, $p < 0.00$). The LOI at the LS for the high energy sites (M = 23.74 %, SE = 3.89%) and NS for both the low energy sites (M = 18.45 %, SE = 2.24%) and high energy sites (M = 17.27 %, SE = 1.45%) were significantly higher than the OM at the LS for the low energy sites (M = 5.58 %, SE = 0.81%) and the HS for both the low energy sites (M = 4.28 %, SE = 0.46%) and high energy sites (M = 1.47 %, SE = 0.38%) group (table 8). This finding indicates that the energy groups may not influence OM in NS or HS, but they do at LS.

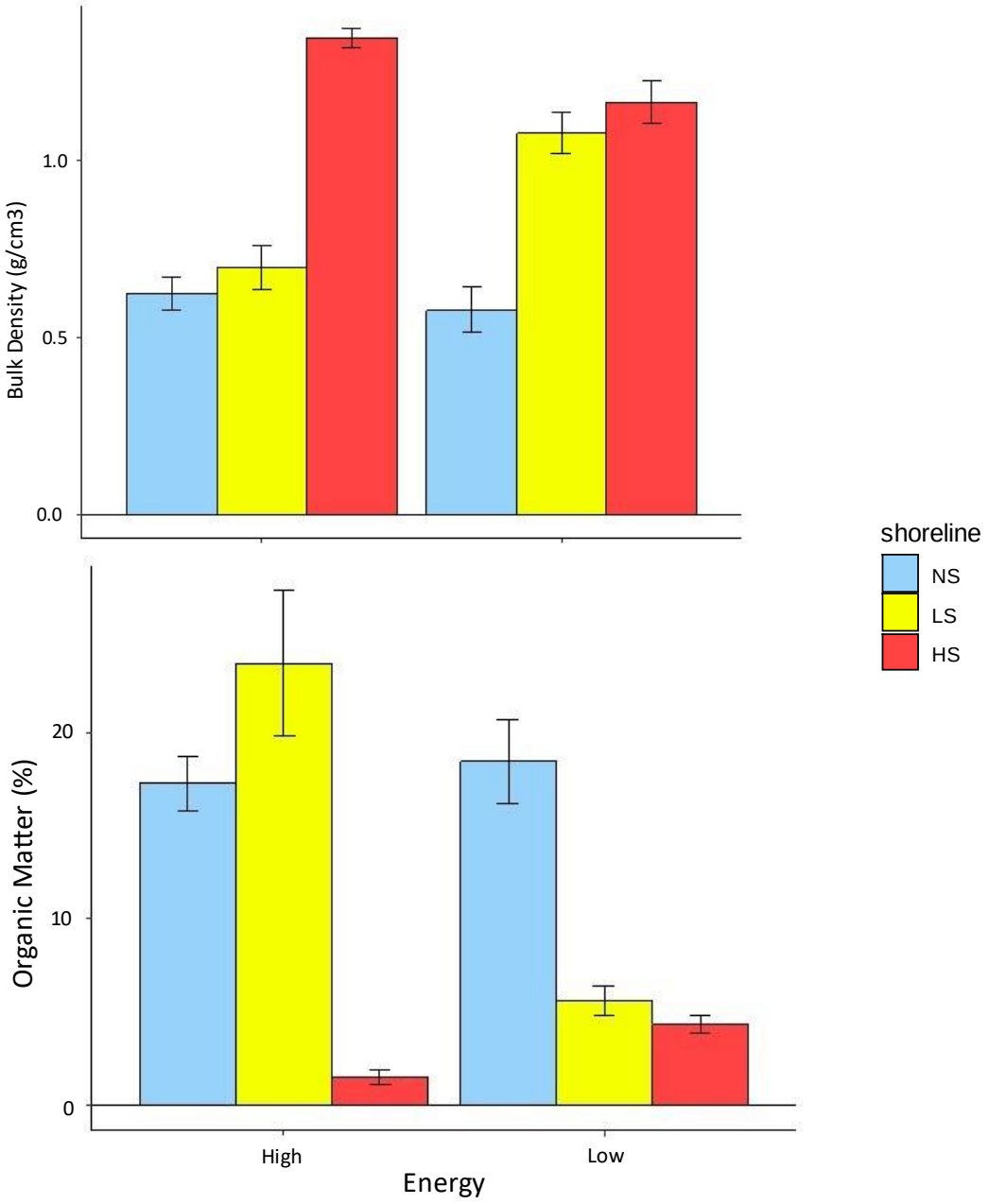

Figure 19. Bulk density (g/cm^3) and organic matter (%) for the different two energy groups and three shoreline types with natural shorelines (blue), living shorelines (yellow), and hardened shorelines (red).

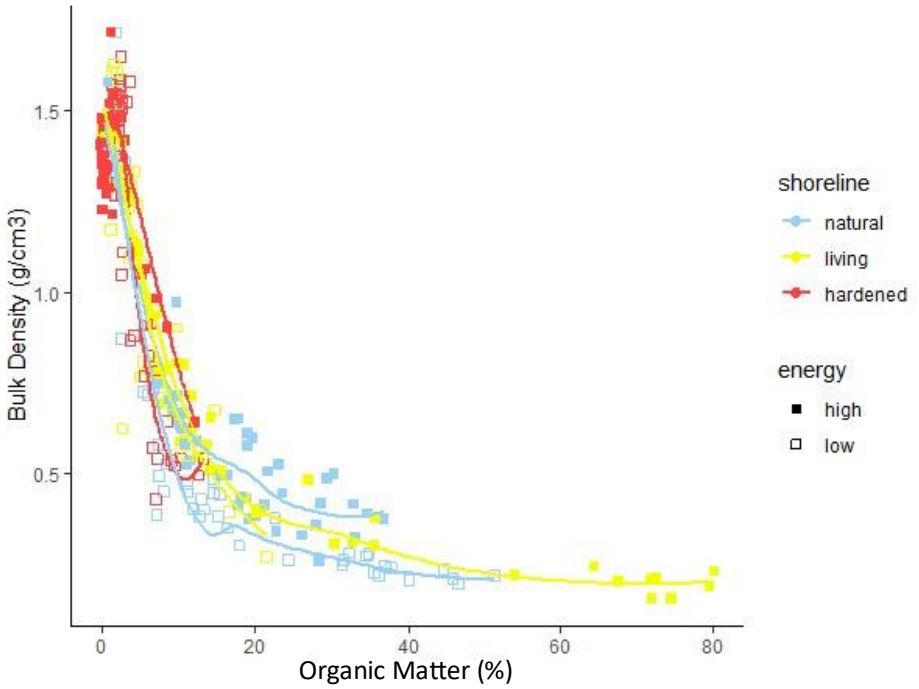

Figure 20. Scatterplot of OM to BD for the two energy groups and three shoreline types. Symbols and colors indicate sample origin, filled symbols indicate high energy sites and hollow symbols indicate low energy.

The scatterplot (Figure 20) shows that BD and OM have an inverse relationship with BD increasing as OM declines. The HS had higher BD and lower OM, the LS had the most variability, with ST having the highest OM, and the NS were clustered with lower BD and higher OM.

The HS averaged higher BD (M = 1.25 g/cm^3, SE = 0.03 g/cm^3) and lower OM (M = 2.88 %, SE = 0.33%), while the NS averaged lower BD (M = 0.60 g/cm^3, SE = 0.04 g/cm^3) and higher OM (M = 17.86 %, SE = 1.33%) with the LS intermediate, especially for OM. The BD averaged by shoreline type exhibited an increase from NS (M = 0.60 g/cm^3, SE = 0.04 g/cm^3) to LS (M = 0.89 g/cm^3, SE = 0.05 g/cm^3), to HS (M = 1.25 g/cm^3, SE = 0.03 g/cm^3). Of all six sites, GB had the highest average BD (M = 1.23

g/cm^3, *SE* = 0.05 g/cm^3), whereas OS had the lowest average BD (*M* = 0.65 g/cm^3, *SE* = 0.04 g/cm^3). In contrast to BD, the OM averages decreased from NS (*M* = 17.86 %, *SE* = 1.33%) to LS (*M* = 15.09%, *SE* = 2.29 %), to HS (*M* = 2.88 %, *SE* = 0.33%). Of all six sites GB had the lowest average OM (*M* = 3.32 %, *SE* = 0.34%), whereas ST had the highest average OM (*M* = 24.47 %, *SE* = 3.92%).

When the six sites are regrouped into the two high and low energy groups (Table 8) similar patterns emerge. The energy groups and the different shorelines were significantly different for both BD (*F* (2, 259) = 14.01, *p* < 0.00) and OM (*F* (2,259) = 16.92, *p* < 0.00). The BD at the low energy sites averaged 0.58 g/cm^3 (NS, *SE* = 0.07 g/cm^3), 1.08 g/cm^3 (LS, *SE* = 0.06 g/cm^3), and 1.16 g/cm^3 (HS, *SE* = 0.06 g/cm^3). The BD in the high energy sites averaged 0.62 g/cm^3 (NS, *SE* = 0.05 g/cm^3), 0.70 g/cm^3 (LS, *SE* = 0.06 g/cm^3), and 1.34 g/cm^3 (HS, *SE* = 0.03 g/cm^3). The low energy sites had significantly lower OM at the LS (*M* = 5.58%, *SE* = 0.81%) and HS (*M* = 4.28%, *SE* = 0.46%), compared to the NS (*M* = 18.45%, *SE* = 2.24%). The high energy sites had lower OM at the HS (*M* = 1.47%, *SE* = 0.38%), compared to the LS (*M* = 23.74%, *SE* = 3.89%) and NS (*M* = 17.27%, *SE* = 1.45%). Comparing the two energy groupings, the high energy sites for LS had an 18.16 % increase in OM, whereas there was a decrease of 1.18 % (NS) and 2.81 % (HS) compared to the respective low energy sites.

3.2.4 Sediment Grain Size

Sediment depth in the top 30 cm significantly affected grain size composition, with the percent sand declining (*F* (2, 262) = 5.06, *p* = 0.01) and silt/clay increasing with depth (*F* (2, 261) = 5.36, *p* < 0.01); percent pebbles and coarse sand was low (<10%) and

not influenced by depth (Figure 21). These results suggest sand grains were more abundant in the upper portion of the sediment cores, potentially because of wave energy winnowing the finer silt and clay particles, which then tend to accumulate at deeper depths (>10cm) or are transported to lower energy conditions in deeper water depths offshore. Similar trends were observed with higher sediment OM found in the deeper core depths (Figure 5). For the rest of the sediment grain size data analysis the three depths were averaged.

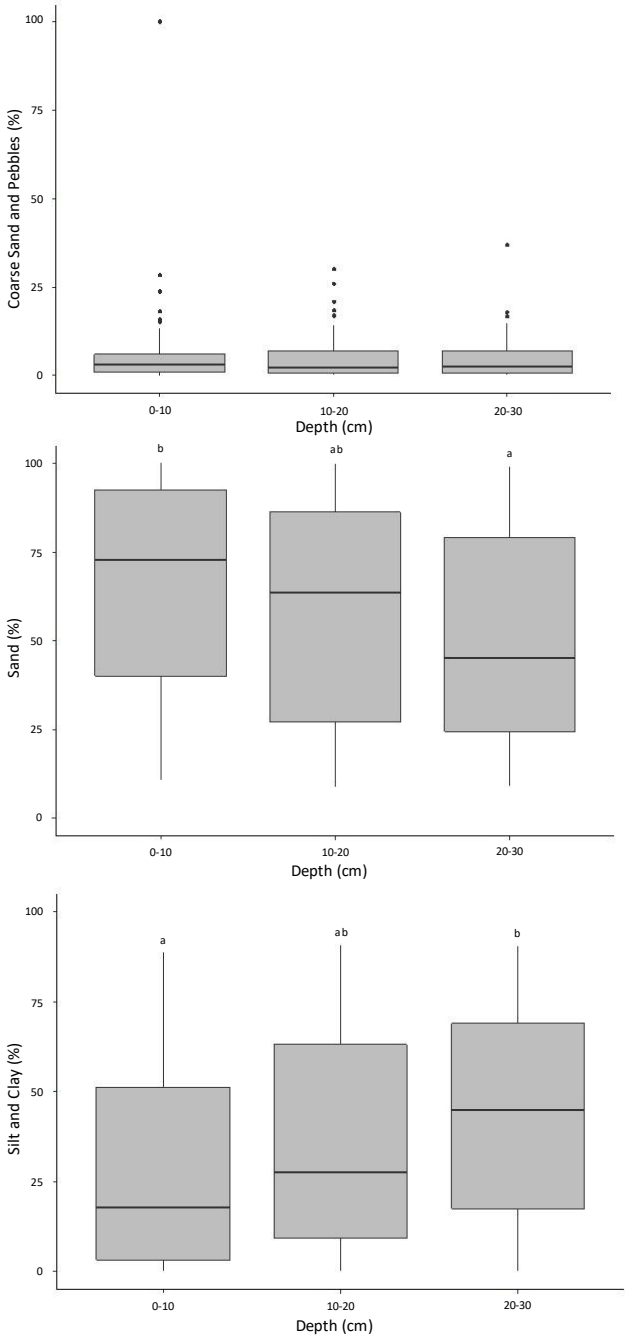

Figure 21. Boxplot of the different depth fractions (cm) for the different sediment features grouped across all six sites: percent of coarse sand and pebbles, percent of sand, and percent of silt and clay. Significant differences by depth are indicated by Tukey's HSD post-hoc letter groups.

When sediment grain size data was analyzed by shoreline type (NS, LS, and HS), the NS (M = 59.67%, SE = 2.92%) had the highest percentage silt/clay (Table 9, Figure 17). The silt/clay fraction was lower in the LS (M = 29.50%, SE = 2.56%) sites and least at the HS (M = 19.23%, SE = 2.29%) sites. Sand content was highest in the HS (M = 76.65%, SE = 2.45%) sites and lowest in the NS (M = 35.19%, SE = 2.75%) sites, with LS intermediate (M = 65.89%, SE = 2.71%) (Table 5). The HS had the highest percent of sand at all sites, except OS and GB where the LS had ~15 % more sand. Percent sand was the dominant sediment grain size in both HS and LS except at OS, which had slightly more silt than sand. Ocean Springs Inner harbor had one of the lowest average wave powers but does have frequent vessel traffic.

Sediment composition at the six sites differed significantly for the percent of coarse sand and pebbles (F (5, 258) = 2.92, p = 0.01), sand (F (5, 259) = 9.52, p < 0.00), and silt and clay (F (5, 258) = 9.43, p < 0.00) size fractions, primarily based on the exposure to high and low energy groups (Table.C.6). The sand fraction in both energy groups increased from the NS to LS to HS, the low energy sites had a lower sand percent value for each shoreline: NS (M = 33.29%, SE = 3.22%) and HS (M = 60.64%, SE = 3.12%) and the sand fraction was greater in the high energy sites; NS (M = 37.09%, SE = 4.49%) and HS (M = 92.66%, SE = 1.84%). At the LS shoreline type, sand was greater (M = 70.63%, SE = 3.26%) in the low energy than the high energy sites (M = 60.78%, SE = 4.15%). Finally, the silt/clay fraction decreased from NS to HS, with LS intermediate. The NS had less than a one percent difference of silt/clay between the high (M = 59.96%, SE = 4.75%) and low (M = 59.38%, SE = 3.50%) energy sites (Table 8, Figure 22). LS had ~10% difference with the high energy sites (M = 34.21%, SE = 3.89%) containing

more silt/clay than the low energy sites (*M* = 25.33%, *SE* = 3.13%), while the HS had ~30% difference with low energy sites (*M* = 34.62%, *SE* = 3.07%) containing more silt/clay than the high energy sites (*M* = 3.83%, *SE* = 1.06%). The percent sand exhibited an inverse relationship to the percent silt and clay in both energy groups, except for the HS, with the low energy sites having a higher percent of silt and clay than the LS. This could be because the sediment core for the LS at GB was taken from within the emergent marsh vegetation and not from the subtidal, where oyster shells were used as fill to stabilize the shoreline.

Sediment grain size data indicated that the sand vs. slit/clay fractions were the major change observed in the sediment composition across all sites and shoreline types. There was an inverse relationship between these two grain size classes, with higher sand content resulting in less silt/clay and vice versa. The sand fraction was higher in the shallow (<10cm) portion of the sediment core when averaged across all six sites. The sand fraction was greater in the HS and reduced at the LS and NS, with the NS shoreline type on average having the largest silt/clay fraction. Finally, high energy sites tended to have more sandy sediments than low energy sites.

Table 9. Average (±SE) of the three sediment size fractions collected at six sites, with three shoreline types at each site. Significant differences in means are indicated by superscript letter groups in each column for the different types of shorelines.

Site	Coarse Sand and Pebbles (%)	Fine Sand (%)	Silt and Clay (%)
Natural			
Hancock County	1.11 ± 0.17^{a}	19.25 ± 4.64^{a}	79.64 ± 4.63^{d}
Swift Tract	1.81 ± 0.58^{a}	30.03 ± 7.65^{a}	68.16 ± 8.12^{bcd}
Alonzo Landing	5.94 ± 1.23^{a}	61.99 ± 6.27^{b}	32.07 ± 6.10^{a}
Camp Wilkes	18.29 ± 5.99^{b}	37.07 ± 8.30^{a}	48.67 ± 8.13^{ab}
Ocean Springs	1.95 ± 0.22^{a}	21.28 ± 2.27^{a}	76.76 ± 2.38^{cd}
Grand Bay	5.78 ± 1.97^{a}	41.53 ± 2.72^{ab}	52.70 ± 3.26^{ac}
Living			
Hancock County	0.94 ± 0.39^{a}	52.88 ± 6.12^{ab}	46.18 ± 5.91^{c}
Swift Tract	10.17 ± 1.30^{c}	47.90 ± 7.73^{a}	42.38 ± 7.03^{bc}
Alonzo Landing	4.97 ± 0.69^{b}	83.06 ± 3.12^{c}	12.62 ± 2.66^{a}
Camp Wilkes	2.36 ± 0.38^{ab}	74.99 ± 5.18^{bc}	22.65 ± 5.07^{ab}
Ocean Springs	5.19 ± 1.02^{b}	59.62 ± 6.42^{ac}	34.98 ± 6.66^{ac}
Grand Bay	4.91 ± 1.28^{b}	76.88 ± 2.99^{bc}	18.21 ± 2.78^{a}
Hardened			
Hancock County	4.11 ± 2.46^{ac}	90.20 ± 4.87^{cd}	5.72 ± 2.77^{a}
Swift Tract	7.13 ± 0.91^{bc}	88.40 ± 1.78^{cd}	5.30 ± 1.28^{a}
Alonzo Landing	0.52 ± 0.12^{a}	99.38 ± 0.27^{d}	0.47 ± 0.14^{a}
Camp Wilkes	2.84 ± 1.63^{ab}	75.17 ± 3.78^{bc}	21.99 ± 2.82^{b}
Ocean Springs	9.24 ± 2.02^{c}	44.77 ± 4.08^{a}	45.99 ± 5.47^{c}
Grand Bay	2.12 ± 0.77^{ab}	61.99 ± 5.28^{b}	35.89 ± 5.47^{bc}

Table 10. Mean (±SE) of three sediment size fractions collected for high and low energy groups, with three shoreline types for each group. Significant differences in averages are indicated by superscript letter groups in each column.

Shoreline	Coarse Sand and Pebbles (%)	Fine Sand (%)	Silt and Clay (%)
High Energy			
Natural	2.96 ± 0.55^{b}	37.09 ± 4.49^{a}	59.96 ± 4.75^{c}
Living	5.37 ± 0.77^{ab}	60.78 ± 4.15^{b}	34.21 ± 3.89^{b}
Hardened	3.92 ± 0.95^{ab}	92.66 ± 1.84^{c}	3.83 ± 1.06^{a}
Low Energy			
Natural	8.67 ± 2.31^{a}	33.29 ± 3.22^{a}	59.38 ± 3.50^{c}
Living	4.04 ± 0.55^{ab}	70.63 ± 3.26^{b}	25.33 ± 3.13^{b}
Hardened	4.74 ± 1.01^{ab}	60.64 ± 3.12^{b}	34.62 ± 3.07^{b}

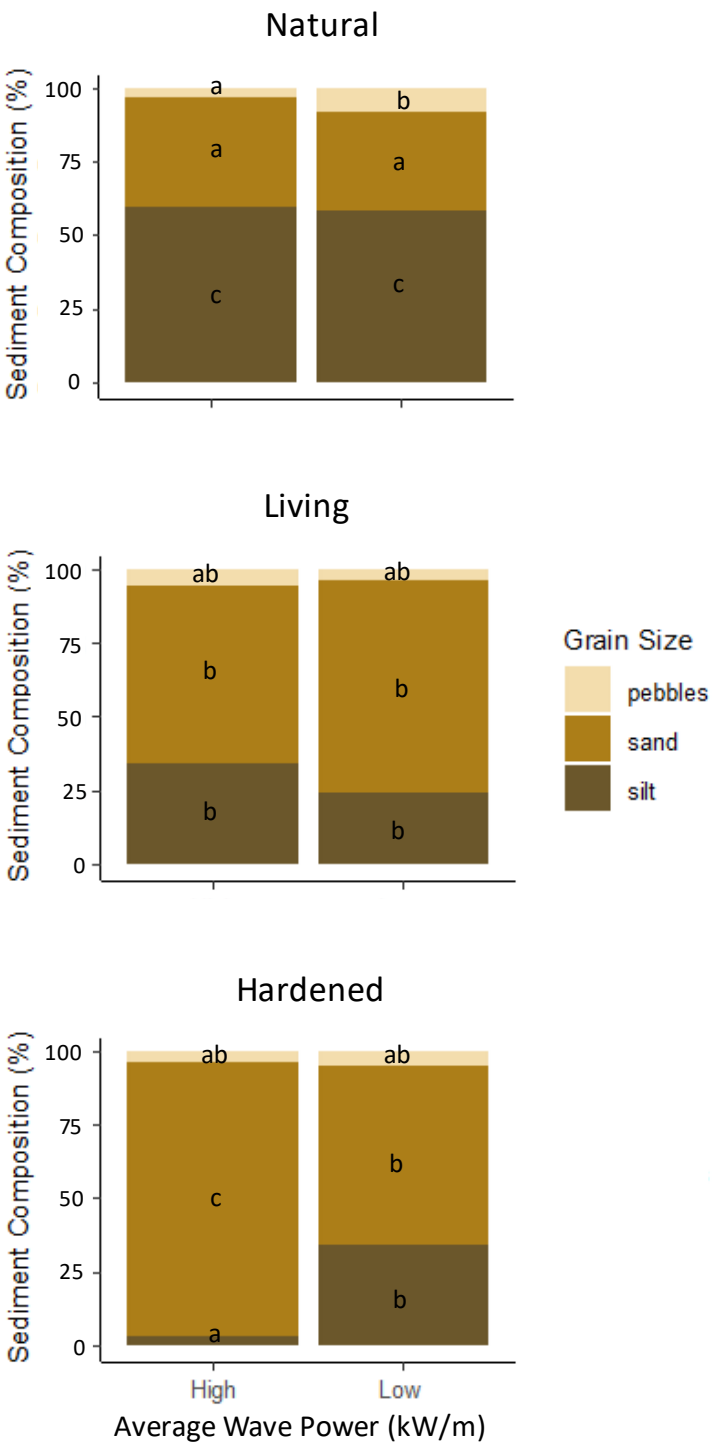

Figure 22. Sediment grain size composition at three shoreline types (NS, LS, HS) collected from the high and low energy groups. Tukey's HSD post-hoc letter groups show the significant differences for the three shorelines and energy groups by the different sediment fractions (pebbles, sand, and silt).

3.3 Vegetation

3.3.1 Species Richness

A total of 39 plant species were found within the 180 quadrats (Table 11). Species richness was not significantly different among the six sites ($F(5,12) = 1.75$, $p = 0.20$) or among the shorelines ($F(2,15) = 0.18$, $p = 0.86$), this could be because the HS had both the highest (CW) and lowest (HC and AL) number of species. All 17 species found at the CW HS were not found at the CW NS or LS, accounting for 59% of the species variability at CW.

Table 11. List of all the species found at the six different sites.

Abbreviation	Species Name	Common Name
AMAR	*Amaranthus spp.*	NA
ASTE	*Aster spp.*	NA
BAHA	*Baccharis halimifolia*	Groundsel tree
BAMO	*Bacopa monnieri*	Water hyssop
BOFR	*Borrichia frutescens*	Sea ox-eye
DISP	*Distichlis spicata*	Saltgrass
ELEO	*Eleocharis spp.*	NA
FICA	*Fimbristylis castanea*	Marsh fimbry
HYBO	*Hydrocotyle bonariensis*	Largeleaf pennywort
ILVO	*Ilex vomitoria*	Yaupon holly
IMCY	*Imperata cylindrica*	Cogongrass
IPSA	*Ipomea sagittata*	Saltmarsh morning-glory
IVFR	*Iva frutescens*	Jesuit's bark
JURO	*Juncus roemerianus*	Black needlerush
LAPA	*Lathyrus palustris*	Marsh pea
LICA	*Lilaeopsis carolinensis*	Carolina grasswort
MYCE	*Myrica cerifera*	Southern wax myrtle
PADI	*Paspalum distichum*	Knotgrass
PARE	*Panicum repens*	Torpedo grass
PIEL	*Pinus elliottii*	Slash pine
QUE1	*Quercus spp. 1*	Aquatic oak
QUE2	*Quercus spp. 2*	Oak
RUTR	*Rubus trivialis*	Southern dewberry
SALA	*Sagittaria lancifolia*	Bull tongue arrowhead
SCAM	*Schoenoplectus americanus*	Chairmakers bulrush
SCRO	*Schoenoplectus robustus*	Sturdy bulrush
SMRO	*Smilax rotundifolia*	Roundleaf greenbrier
SOSE	*Solidago sempervirens*	Goldenrod
SPAL	*Spartina alterniflora*	Smooth cordgrass
SPCY	*Spartina cynosuroides*	Big cordgrass
SPPA	*Spartina patens*	Saltmeadow cordgrass
SPSP	*Spartina spartinae*	Gulf cordgrass
SYTE	*Symphyotrichum tenuifolium*	Perennial saltmarsh American aster
TRPA	*Tripolium pannonicum*	Seashore aster
TRSE	*Triadica sebifera*	Chinese tallow tree
TURF	Unknown	Turf grass
UNK1	Unknown 1	NA
UNK2	Unknown 2	Weed
UNK3	Unknown 3	Purple vine

Species richness was significantly different between the two energy groups ($F(1,16) = 5.43$, $p = 0.03$). The species richness for the low energy sites ($M = 7.89$ species, $SE = 1.29$ species) was ~50 % higher than the high energy sites ($M = 3.89$ species, $SE = 1.17$ species). The site with the highest species richness was CW (28 species), followed by GB (14 species), OS (13 species), HC (10 species), AL (9 species), and ST (5 species) (Table 12). These results indicate that species richness may be influenced by the energy groups, with low energy tending to increase the number of species found.

Table 12. Vegetation data by site and shoreline for the average species richness, total percent cover (±SE), dominant marsh species cover, the Shannon H index, and the Simpson's D index. Significant differences in means are indicated by superscript letter groups in the average percent cover column.

Site	Species Richness	Avg Percent Cover (%)	Dominant Sp Cover (%)	Shannon Index	Simpson Index
			Natural		
Hancock County	4	67.00 ± 8.50^{cd}	67.00 ± 26.89^{d}	0.82	0.47
Swift Tract	4	63.50 ± 9.19^{cd}	61.00 ± 9.42^{cd}	0.57	0.30
Alonzo Landing	9	54.60 ± 7.43^{bc}	46.85 ± 7.25^{cd}	1.63	0.75
Camp Wilkes	7	73.90 ± 4.^{03cd}	72.10 ± 4.25^{d}	1.03	0.49
Ocean Springs	5	82.20 ± 3.53^{cd}	79.45 ± 3.88^{e}	1.17	0.65
Grand Bay	3	63.00 ± 6.72^{cd}	63.00 ± 6.72^{cd}	0.78	0.44
			Living		
Hancock County	9	52.25 ± 5.38^{bc}	40.00 ± 5.31^{c}	1.73	0.78
Swift Tract	2	59.50 ± 12.81^{cd}	59.50 ± 12.81^{cd}	0.06	0.02
Alonzo Landing	6	78.00 ± 5.07^{cd}	72.00 ± 4.48^{d}	1.52	0.75
Camp Wilkes	8	66.00 ± 6.23^{cd}	53.00 ± 10.57^{c}	1.12	0.59
Ocean Springs	8	69.80 ± 5.12^{cd}	35.15 ± 5.21^{bc}	1.40	0.68
Grand Bay	7	64.50 ± 9.73^{cd}	60.00 ± 10.06^{cd}	1.05	0.54
			Hardened		
Hancock County	0	0.00 ± 0.00^{a}	0.00 ± 0.00^{a}	0.00	0.00
Swift Tract	1	95.00 ± 0.00^{d}	0.00 ± 0.00^{a}	0.00	0.00
Alonzo Landing	0	0.00 ± 0.00^{a}	0.00 ± 0.00^{a}	0.00	0.00
Camp Wilkes	16	32.40 ± 7.93^{ab}	1.10 ± 3.48^{a}	2.19	0.84
Ocean Springs	9	86.00 ± 3.79^{cd}	78.40 ± 3.04^{e}	1.31	0.67
Grand Bay	7	63.00 ± 4.23^{cd}	25.90 ± 8.96^{b}	1.51	0.73

Table 13 Vegetation data by energy groups and shoreline for the average species richness, total percent cover (±SE), dominant marsh species cover, the Shannon H index, and the Simpson's D index. Significant differences in means are indicated by superscript letter groups in the average percent cover and in dominant marsh species cover column.

Shoreline	Species Richness	Avg Percent Cover (%)	Dominant Sp. Cover (%)	Shannon Index	Simpson Index
High Energy					
Natural	10	61.70 ± 4.78^{b}	58.28 ± 5.97^{b}	1.20	0.59
Living	10	63.25 ± 5.17^{b}	57.17 ± 9.31^{b}	1.65	0.73
Hardened	1	31.67 ± 8.32^{a}	0.00 ± 0.00^{d}	0.00	0.00
Low Energy					
Natural	10	72.83 ± 3.11^{b}	71.52 ± 4.76^{a}	1.52	0.72
Living	18	66.67 ± 4.08^{b}	49.38 ± 7.40^{bc}	1.74	0.75
Hardened	25	60.17 ± 5.19^{b}	35.13 ± 22.79^{c}	2.35	0.87

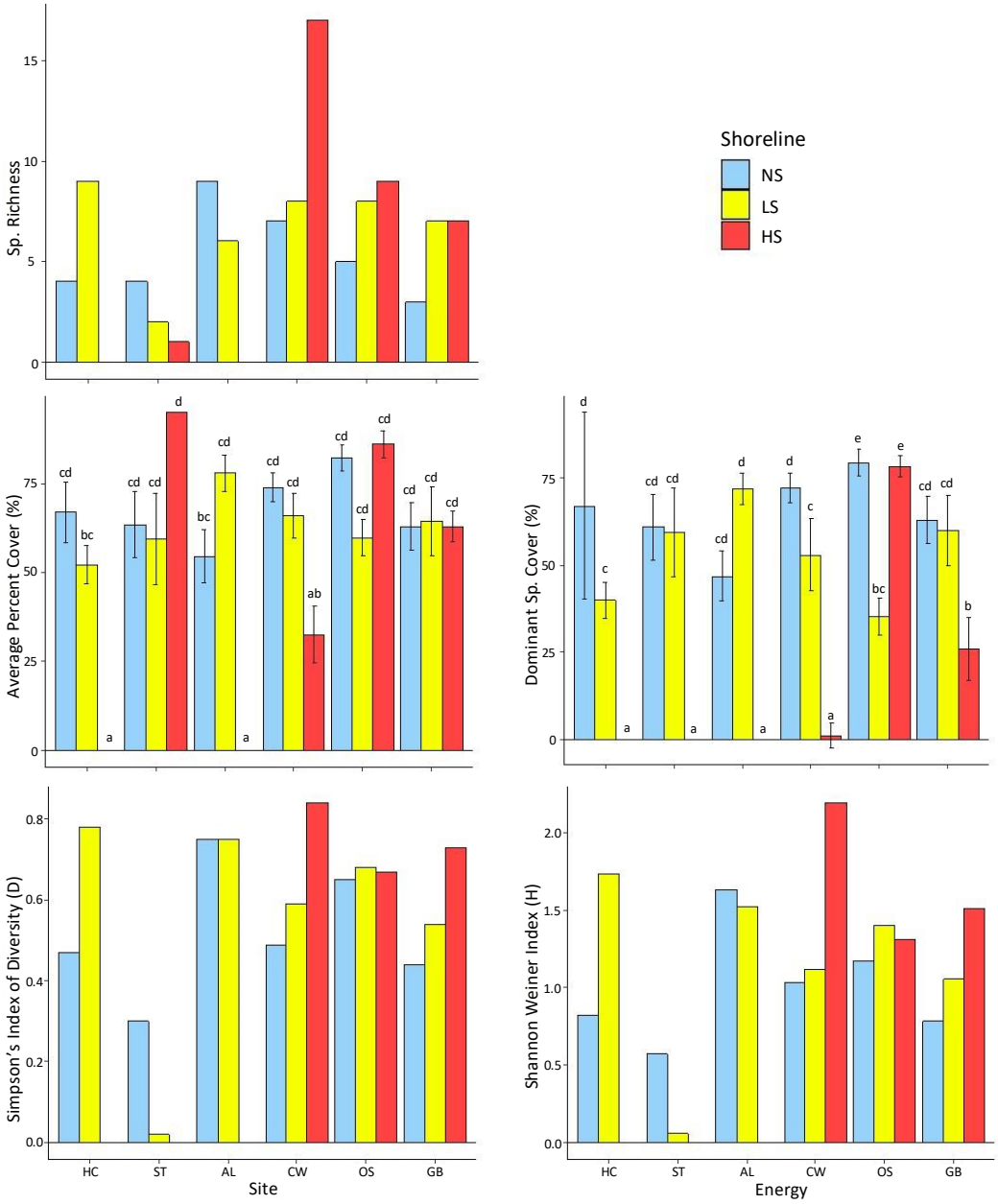

Figure 23. Species richness, average percent cover (%, ± SE), average dominant marsh species cover (%, ± SE), Simpson's Index of Diversity (D), and the Shannon Weiner Index (H) for the natural (blue), living (yellow), and hardened (red) shorelines at each site. Tukey's HSD post-hoc letter groups show the significant differences for the three shorelines and sites for average percent cover and dominant marsh species cover.

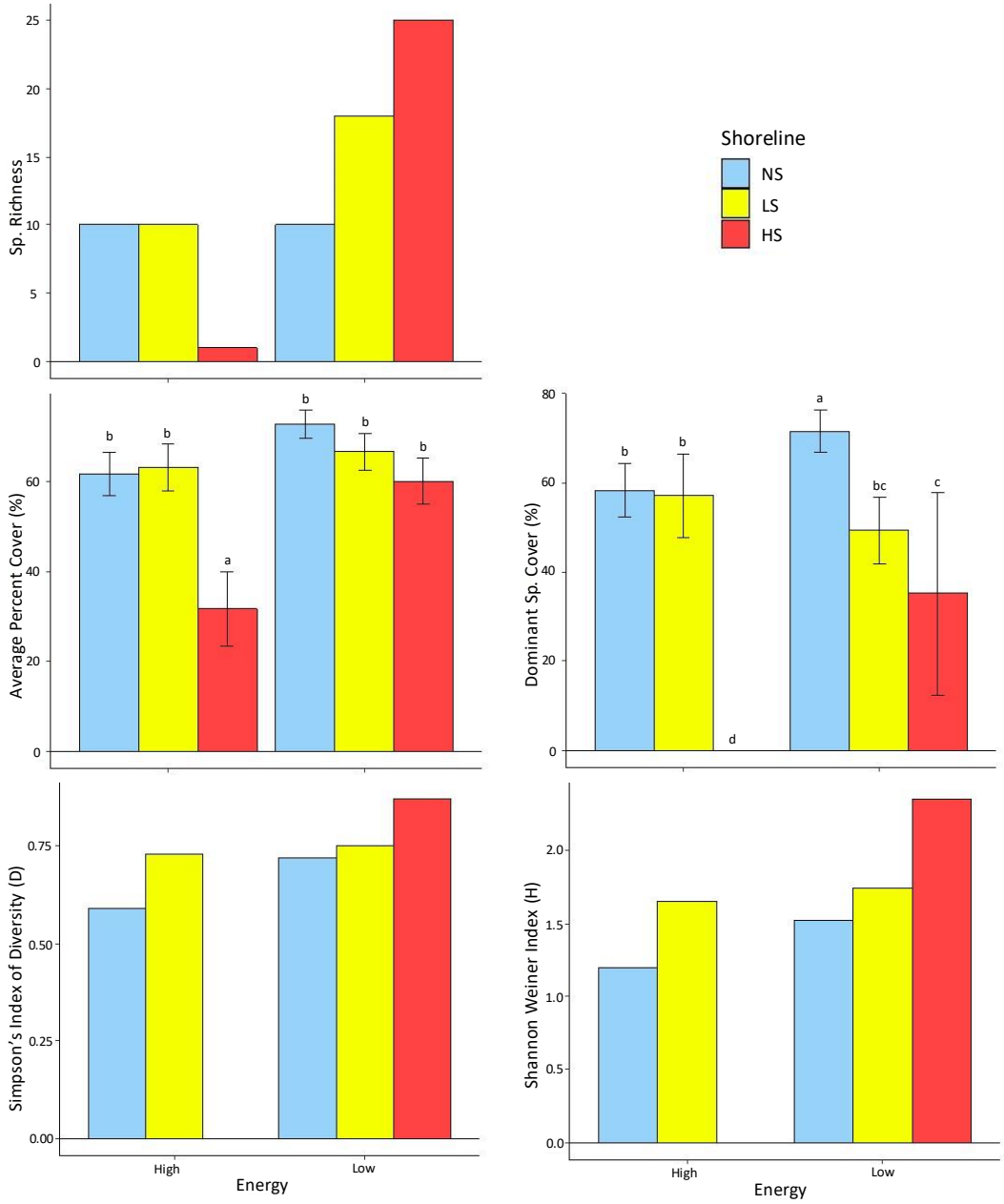

Figure 24. Species richness, average percent cover (%, ± SE), average dominant marsh species cover (%, ± SE), Simpson's Index of Diversity (D), and the Shannon Weiner Index (H) for the natural (blue), living (yellow), and hardened (red) shorelines for the different energy groups. Tukey's HSD post-hoc letter groups show the significant differences for the three shorelines and energy groups for average percent cover and dominant marsh species cover.

3.3.2 Percent Cover

Vegetation percent cover was significantly different among the three shorelines ($F(2, 177) = 8.84$, $p < 0.00$). The NS ($M = 67.37\%$, $SE = 2.93\%$) had the highest average percent cover and was similar to the LS ($M = 65.01\%$, $SE = 3.27\%$), but the HS ($M = 46.07\%$, $SE = 5.20\%$) was significantly lower (Figure 24). It makes sense that the NS and LS would tend have a higher average percent cover because the NS consist of vegetation and the LS either already had vegetation or more vegetation was planted after construction. Percent cover was highest for the HS at ST ($M = 95\%$, $SE = 0.00\%$) because it solely contained planted turf grass. The HS at both HC and AL contained no vegetation ($M = 0.00\%$, $SE = 0.00\%$). These findings indicate that percent cover may be affected by humans either planting vegetation or removing vegetation to build a HS.

Vegetation percent cover was significantly different among the six sites ($F(5, 174) = 8.79$, $p < 0.00$). The highest average percent cover was found at OS ($M = 79.33\%$, $SE = 2.67\%$), which was not significantly different from ST ($M = 72.67\%$, $SE = 5.87\%$). The lowest percent cover was at HC ($M = 39.75\%$, $SE = 6.24\%$), which was not significantly different from AL ($M = 44.20\%$, $SE = 6.72\%$). The intermediate group consist of GB ($M = 63.50\%$, $SE = 4.04$) and CW ($M = 57.43\%$, $SE = 4.83\%$) because they were not significantly different from the sites with high or low percent cover. Vegetation percent cover was significantly different between the two energy groups ($F(1, 178) = 9.93$, $p < 0.00$). The low energy sites ($M = 66.76\%$, $SE = 2.46\%$) had a higher percent cover of vegetation than the high energy sites ($M = 52.21\%$, $SE = 3.91\%$). These results show that both site and energy may affect the percent cover of vegetation.

Of the 39 species found, nine of them are considered dominant marsh species in Mississippi by Eleuterius (1972). There was a significant difference between the shoreline types of the percent dominant marsh species present ($F(2, 177) = 46.03$, $p < 0.00$). The NS had the highest percent of dominant marsh species ($M = 72.83\%$, $SE = 9.06\%$), which was not significantly different from the LS ($M = 55.77\%$, $SE = 14.07\%$), but both were significantly different from the HS ($M = 14.13\%$, $SE = 7.60\%$).

The percent of dominant marsh species was significant among the different energy groups and shorelines ($F(2, 174) = 10.16$, $p < 0.00$). The highest percent of dominant marsh species was at the NS for the low energy sites ($M = 71.52\%$, $SE = 4.76\%$), while the lowest was at the HS for the high energy sites (0.00%, SE = 0.00%). The low energy HS ($M = 39.47\ \%$, $SE = 22.79\ \%$) had the second lowest percent of dominant marsh species, followed by the low energy LS ($M = 49.38\ \%$, $SE = 7.40\ \%$) and the high energy LS ($M = 57.17\%$, $SE = 9.31\ \%$) and NS ($M = 58.28\%$, $SE = 5.97\ \%$). This finding shows that energy and type of shoreline play a role in the percent of dominant vegetation found.

3.3.3 Diversity

Simpson's Index of Diversity (D) and the Shannon Weiner Index (H) placed the site/shoreline combination in the same order of diversity as the species richness data (Table 12). In both the Simpson's D and the Shannon H indices, the NS and LS follow the same pattern, while the HS varied (Figure 20). High and low energy groups showed high variability in diversity for HS and only less variability for LS (Figure 21). The NS at the low energy sites had similar species with a high percent cover causing them to have a

low S index but a higher H index value. The H index varied greatly for HS when grouped by energy. The higher energy sites had zero to one species and the low energy sites 7-17 species with varying percent cover.

A Bray Curtis dissimilarity matrix was plotted using NMDS (k = 2, stress = 0.079) to represent the relationship of the different species of vegetation between the different sites and shoreline types (Figure 25). The HS at HC and AL were removed from the data set because there was no vegetation at those sites. The matrix had a non-metric fit $R^2 = 0.994$ and a linear fit $R^2 = 0.985$. The NS and LS are tightly clumped, while the HS is sparse. Using the same matrix results, the data was grouped by high and low energy.

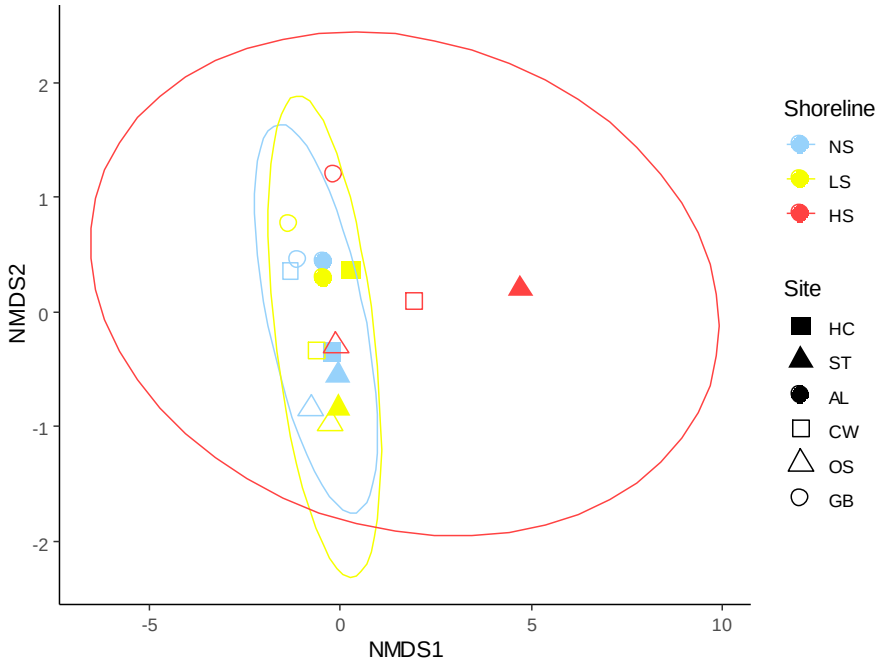

Figure 25. Non-metric multidimensional scaling plot of the vegetation diversity found at the different shorelines per site.

3.4 Data Interactions

To visualize data interactions among the different factors (hydrographic, geomorphic, and vegetation) an MDS (Figure 27, k = XX, stress= 0.95) and a PCA were conducted (Figure 28). Hydrographic features that were included in both the MDS and the PCA were the average wave power and turbidity. The geomorphic features included were relative exposure, average erosion rate, average slope, percent of sand, and organic matter. The vegetative features included were species richness, percent of dominant species, and percent cover. Some features were left out to simplify the model, and when made with the features included the results were similar. The features that were left out were: average fetch distance, bulk density, percent of pebbles and coarse sand, percent silt, Shannon-Weiner Index, and the Simpson's Index of Diversity. The average fetch distance was left out because it was used to calculate the relative exposure. Percent of pebbles and coarse sand were left out because they were small values that did not differ. Percent silt was removed because it was the inverse of percent sand, and the same for organic matter and bulk density. The alpha diversity indices were not included because the vegetation had multiple factors that all contributed to the diversity. These features also had high correlations of >0.9 to some of the other features (Figure 26) resulting in potential over fitting of the ordination.

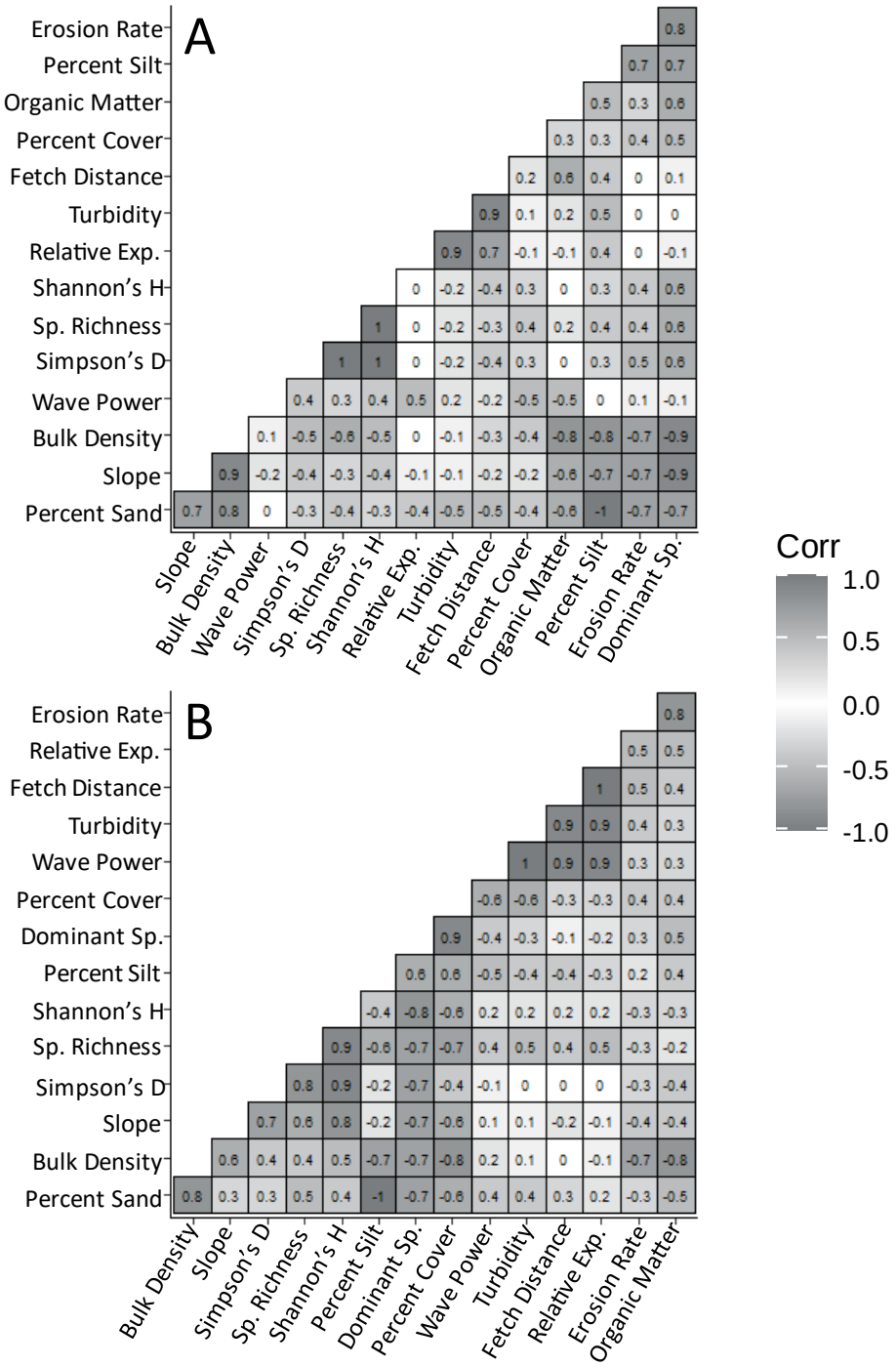

Figure 26. Correlation matrices for high (A) and low (B) energy groups containing the different variables: erosion rate, percent silt, organic matter, average percent cover, average fetch distance, turbidity, relative exposure, Shannon-Weiner Index, species richness, Simpson's Index of Diversity, average wave power, bulk density, slope, percent sand, and percent of dominant species.

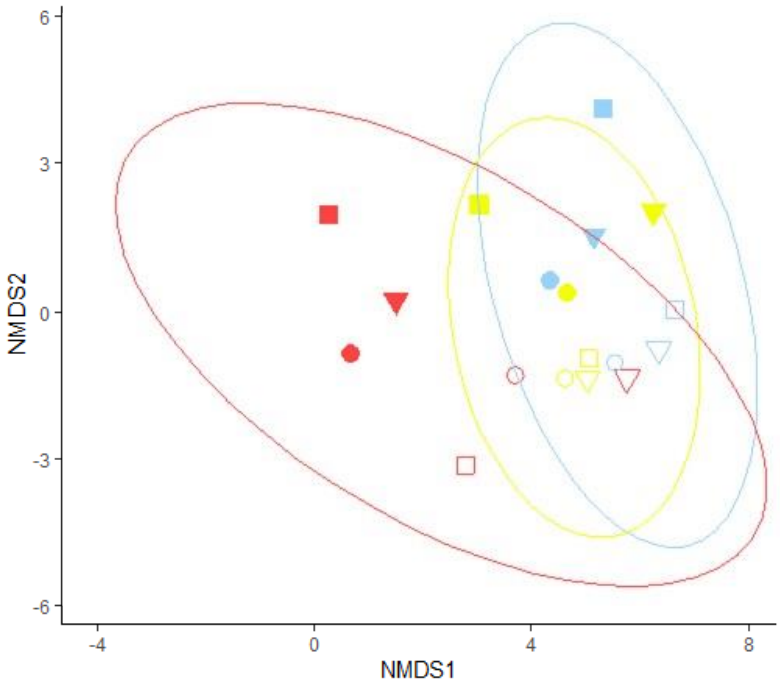

Figure 27. Non-metric multidimensional scaling plot representing relationship between for the different shorelines and sites, determined by the variables: average wave power, turbidity, relative exposure, average erosion rate, average slope, percent of sand, organic matter, species richness, percent of dominant species, and percent cover.

The MDS and the PCA show a similar pattern in the dataset (Figures 27 and 28). The MDS was created using Euclidean distance (Figure 27). There is a large overlap between the NS and the LS. The HS is overlapping them at the low energy sites in the bottom right corner. However, at the high energy sites the HS vary greatly from the NS and LS. The axis NMDS1 shows a greater separation for type of shoreline, while the axis NMDS2 shows separation by the different energy groups.

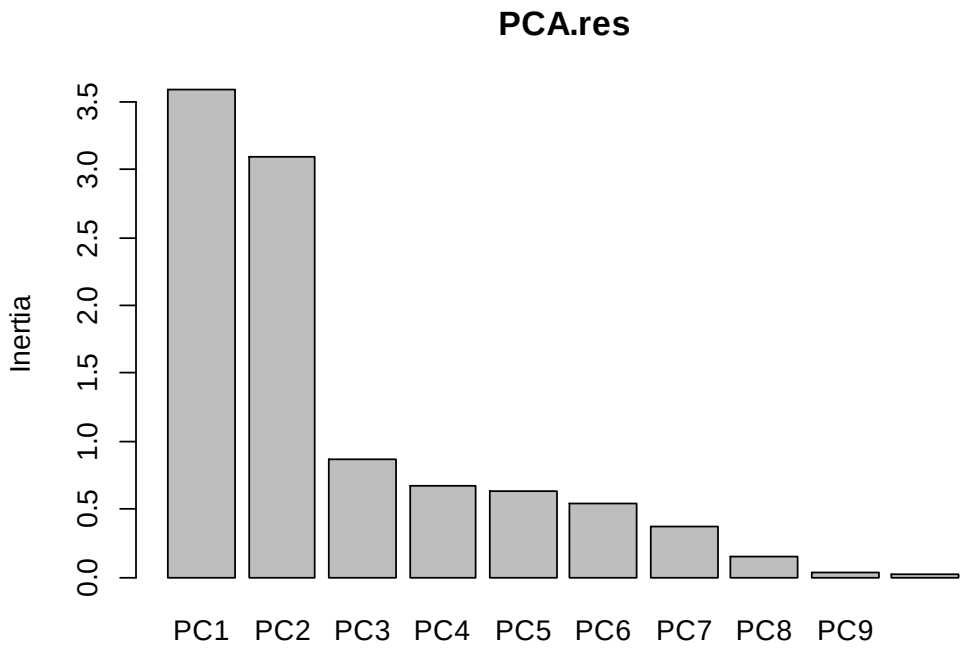

Figure 28. Scree plot for the principal component analysis (PCA).

Approximately 75% of the estimated variance is explained by the first three axes of the PCA (Figure 28) , the first axis (PC1) explains 35.9% and the second axis (PC2) explains 31.0%, and the third axis (PC3) explains 8.70% of the estimated variance in the total dataset. The PCA plots show that the LS and NS are similar while they have a strong separation from the HS. There is strong separation amongst the high energy sites, while the low energy sites are more clumped together.

Table 14. Principle component analysis contributions (eigenvectors) for each factor used for the first three dimensions (PC1, PC2, and PC3). The factors include percent of dominant marsh species, percent cover for all species, average slope, percent of sand in the sediment, average wave power, turbidity, relative exposure, percent organic matter, species richness, and erosion rates.

Factor	PC1	PC2	PC3
Percent Dominant	21.01	4.04	0.67
Percent Cover	14.70	0.16	0.40
Avg Slope	14.00	4.30	7.21
Percent Sand	12.89	7.81	2.41
Avg Wave Power	11.58	14.27	1.48
Turbidity	8.97	19.57	0.21
Relative Exposure	7.00	16.29	3.40
Organic Matter	4.80	10.72	2.55
Species Richness	3.45	5.17	72.02
Erosion Rate	1.58	17.66	9.65

In the PCA (Figure 29), PC1 represents the percent of dominant vegetative species percent cover of vegetation, and the average slope of the shoreline. This axis shows a pattern of low energy groups' LS and NS to high energy groups' HS. PC2 represents the turbidity, erosion rate, relative exposure, and average wave power. This axis mostly represents energy and shape of the shorelines, it shows a gradient between high and low energy groups as well as from HS to LS to NS. PC3 represents species richness. This axis shows the HS, as well as the low energy sites' NS and LS are more similar than the high energy sites' NS and LS.

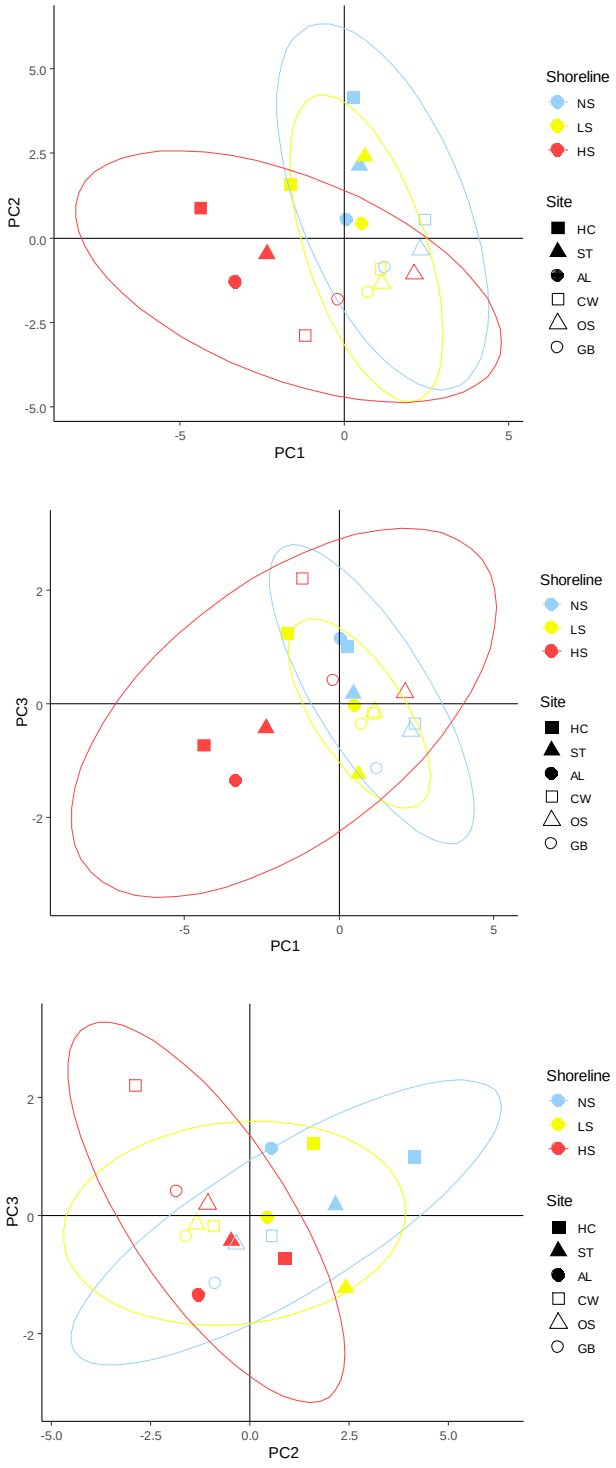

Figure 29. Principal Component Analysis for the three shoreline types at each site. High energy sites have solid shapes, while low energy sites are open symbols. PC1 represents the percent of dominant vegetative species, percent cover of vegetation, and the average slope of the shoreline. PC2 represents the turbidity, erosion rate, relative exposure, and average wave power. PC3 represents species richness.

The PCA results help to analyze the main driving features in the data collected from the six study sites. Areas with high turbidity, erosion rates, wave power and relative exposure have steeper slopes and a higher percent of sand, but lower percent cover and percent of dominant vegetative species. I created a conceptual model to show this relationship (Figure 29). This model divides the results into four quadrants, the upper left quadrant is where HS can be found in high energy locations while the lower right quadrant is where NS and LS can thrive under low energy conditions. The other two quadrants show the intermediate conditions.

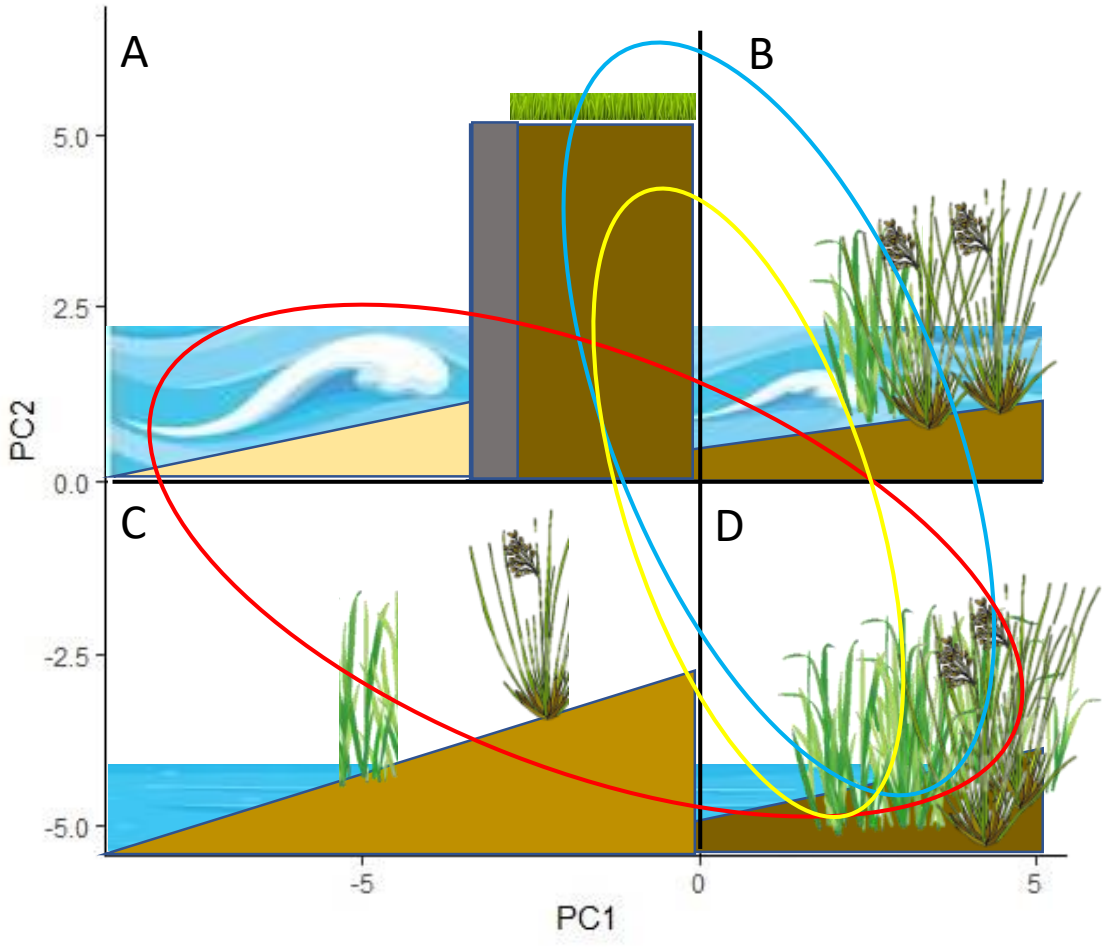

Figure 30. A conceptual model representing the results found with the PCA. The ellipses are from the PCA and show the different types of shorelines: natural (blue), living (yellow), and hardened (red). Quadrant A represents high energy hitting a hardened structure with sandy sediment at the base and has no native vegetation. Quadrant B represents high energy with the less sand but features a steeper slope with native vegetation. Quadrant C is a low energy shoreline but with a steep slope, moderate sand content and less native vegetation. Quadrant D represents a low energy shoreline, with mostly silt/clay sediments but little sand, and lots of native vegetation.

CHAPTER 4 - DISCUSSION

4.1 Summary

There are many different views on how to protect our coastline from erosion, which can vary by the goal of the property in question. This research is done in hopes to find a way to combine the goals of ecological restoration and prevention of property erosion. I focused on two manmade methods of protecting a shoreline when the natural marsh fails; one of which is a hardened structure and the other, a living shoreline, which has a natural component of marsh vegetation. The LS is a method that tries to maintain natural coastal processes while also dissipating wave impacts on the shoreline (Erdle et al., 2006).

This study looked at natural, living, and hardened shorelines from two different energy groups to see how the hydrographic, geomorphic, and vegetative processes affect them. Predominantly high vs. predominantly low wave energy exerted on a shoreline influenced all the other variables studied. Site played a role in all the variables, except for species richness and the percent of dominant marsh species present. Shoreline type (NS, LS, HS) affected the erosion rate, slope, sediment variables, and the percent cover, percent of dominant marsh species present.

For the energy division I used the average wave power because it shows the amount of impact a shoreline is receiving, but use of this method would depend on field sampling abilities and access to equipment. A suitable alternative to using the average wave power would be turbidity if field sampling is an option. However, for initial analysis or when there is no access to the required technology, relative exposure and fetch distance could also be calculated using Google Earth Pro. When using the relative exposure, it is

important to be aware that currents and boat traffic do play a role in the energy impact the shoreline receives.

4.2 Hydrographic Features

The hydrographic data, using the single YSI, was collected by site and combined with the three wave gauges collected in front of each shoreline type. I used the data from the average wave power to divide the sites into high (HC, ST, and AL) and low energy sites (CW, OS, and GB). I used the average wave power because it represented the water motion impacts that the shoreline was receiving, according to Leonardi et al., (2016) wave energy and erosion have a linear relationship and may help indicate under which wave energy conditions the different types of shorelines diverge. Studies have shown that shorelines that receive lower wave energy are less likely to require human interference, although conditions at some sites may be increased by human interference (Erdle et al., 2006). At the high energy sites (6.91 kW/m), the average wave power was five times greater than at the low energy sites (1.31 kW/m). This division found by the wave power data was used to divide the rest of the data into two groups for further analysis.

Measuring turbidity reflects the number and type of particles in the water column, usually caused by rougher water conditions. High wave energy can disturb the sediment, suspending it into the water column, however, vegetation can reduce this disturbance since the below ground biomass stabilizes the sediment (Bilkovic et al., 2016), and emergent stems can reduce water velocities (Gedan et al., 2011). The high energy sites (16.86 NTU) were found to have almost five times greater turbidity than the low energy sites (3.46 NTU). The turbidity and wave power were highly correlated (r = 0.85),

showing a potentially strong relationship between them (Figure 26). I also found higher turbidity in the winter (10.32 NTU) than in the summer (9.03 NTU), which is likely caused by the winter having high wind speed and frequency of northern wind, while the summer has lower speed and wind frequency of southeastern winds (Figure 14). Two of the three high energy sites, HC and AL, showed the greatest difference between the two seasons, which could be caused by the orientation of these two shorelines relative to the dominant winds.

4.3 Geomorphic Features

The geomorphic data was collected for the three different shoreline types (natural, living, and hardened) at each site. The relative exposure was calculated using the method of La Peyre et al. (2014) to explain the wave power and turbidity found at each site based on fetch distance, wind speed, and wind direction. No difference was found among the different types of shorelines at a given site because the wind data within a site was collected from the same data frame. Sites with a maximum fetch distance less than 804.67 m (0.5 mi) were considered low energy and less likely to require human interference, although there are other factors that could increase the erosion (Duhring et al., 2006; Erdle et al., 2006). Based on Erdle et al. (2006) half of the sites in our study fit that criterion: AL (298.02 m), GB (107.96 m) and OS (107.01 m); while the three other sites would be considered high energy: HC (31944.13 m), ST (56663.05 m) and CW (1484.64 m, Table.C.2). These results were also reflected in the relative exposure for the different sites (Table 2). This contradicts the energy groups because AL and CW are switched, implying that there may be other factors affecting the wave energy exerted on

these shorelines. This is probably caused by the short fetch distances found at AL but magnified by high wave power caused by both tidal currents and a car ferry terminal that is located a short distance away. At CW there are emergent marsh islands and sand bars that can buffer the wave energy coming in from the more exposed water body.

The erosion rates were only taken for the last decade (2011-2019) by Juneau (2021) because not all the living shorelines had been implemented in the prior decades (1992 – 2005, 2005 - 2011) she had calculated. However, by only using data with all three shoreline types represented at the different sites it is easier to compare the erosion rates among them. The NS (0.70 m/yr) had a higher erosion rate than LS (0.25 m/yr) and HS (-0.02 m/yr). It was expected that the HS would have little to no erosion because it is a permanent or mostly permanent structure. The high erosion rates at the NS were also expected because otherwise there would be no need to protect the shorelines from erosion, most of the NS had a scarp at the vegetation base (Figure 3) indicative of ongoing edge erosion. The large scarps found at the high energy sites show how the roots help contain the sediment under less severe conditions (Bilkovic & Mitchell, 2018). At all the sites, apart from GB, the rate of erosion decreased with the implementation of the LS compared to the adjacent NS. The reason that GB did not show less erosion at the LS compared to the NS could be caused by increased boat traffic because it is located next to a boat launch. The erosion results fit the expected trade off that LS are a compromise to maintain a natural ecosystem while lessening the rate of erosion, while the HS are a proven technique to stop the rate of erosion in this study (Bilkovic et al., 2016; Polk & Eulie, 2018; Swann, 2008). One potential error when measuring the erosion rate of a shoreline is that there may be fill or removal of sediment by humans that is not well

documented. Therefore, it is important to view erosion as more of a rate of change in shoreline position over time.

Shorelines with steeper slopes tend to reflect the impacts of higher wave energy and have larger grain-size sediments and higher edge erosion rates (Nelson, 2008). Steep slopes make it more difficult for vegetation to grow and the implementation of a breakwater structure may help facilitate conditions suitable for vegetation expansion (Erdle et al., 2006). I found that HS (28.87 cm/m) had a significantly steeper slope, because most of them were solid walls with a large drop-off. The slope of the NS (14.62 cm/m) and LS (12.70 cm/m) were not different from each other. However, when comparing the NS and LS by site, the slope decreases from the NS and LS, apart from at GB and HC. This difference may be explained because the LS at GB is next to a boat ramp and HC has the geo-tube that have a significant drop. The lower slopes at the LS counterpart could also be due to sediment fill when the LS structure was built. Erdle et al. (2006) found that sites with greater fetch may need human interference to add fill to the shoreline.

Sediment grain size can be affected by the energy that impacts the shoreline, which in turn can affect the ability of vegetation to thrive (Bozek & Burdick, 2005). I found that there was a difference based on energy, site, and shoreline type on sediment grain size composition. Sediment influx is an important factor because every site is going to have different sources of sediment. The high energy sites' portion of silt/clay decreased from NS to LS to HS. The results for the high energy shorelines coincide with findings by Mitchell & Bilkovic (2019) that the sediment at the LS will be similar to those at the NS. In contrast, the low energy sites' portion of silt/clay decreased from NS

to HS to LS. The sediment grain size for the low energy shorelines reflects the findings of Feagin et al.(2009), that the higher percent of sand found at the HS, followed by the LS could be caused by scouring at the base of the hardened structures (Basco, 2006; Roberts, 2010). This difference could also be due to the use of sand as a sediment fill during the LS reconstruction. The NS had the smallest difference in sediment composition between the high and low energy sites, whereas the greatest difference was at the HS sites. This finding agrees with Bozek and Burdick (2005) that high energy sites will have coarser, more sandy sediment, as well as Feagin et al. (2009) who found coarser sediment at restored sites.

Bulk density is important for the ability of plant roots to grow and expand into the sediments and tends to reflect the percent of sand in the sediment (Vymazal, 2013). In The organic matter content in the sediment that is available for plants is also reflective of the silt/clay content because the pore space available allows for organisms to break down materials (Davis et al., 2015). The NS were found to have the lowest sediment BD, followed by LS and then HS. The inverse pattern was seen for the organic matter content in the soil. I found that both BD and OM are not influenced by the energy groups at the NS and HS but are at the LS. For both these parameters, the LS at the high energy sites were more like the NS, while the low energy sites were more closely related to the HS.

4.4 Vegetation

Vegetation can protect a shoreline from erosion, filter runoff, and provides both food and habitat for different organisms (Craft et al., 2009; Wu et al., 2012; Bilkovic and Mitchell, 2018). I used multiple methods to test and evaluate the vegetation diversity for

the shorelines at each site. Species richness was found to only be affected by the energy groups, with the low energy sites having higher richness. Percent cover was viewed in two ways, total percent cover and the percent cover of the dominant marsh species identified by Eleuterius (1972). The NS and LS were found to have a higher total percent cover than the HS. Total percent cover was also found to be higher at the low energy sites. The dominant marsh species coverage found that both NS and LS had over 55 % cover of dominant marsh species, while HS had less than 15 %. It is perhaps not surprising that the HS have less dominant marsh species, not only because of anthropogenic removal but the steeper slopes remove the vegetation from the harsher conditions allowing for more competitive non-marsh species to thrive (Pennings et al., 2005). The lower percent cover and dominant species at the HS removes a vital part of the ecosystem created by a natural marsh and endangers species that are endemic to marshes (D. M. Bilkovic & Roggero, 2008).

To look at diversity I used alpha diversity within the community and beta diversity between the communities (Bozek & Burdick, 2005). The energy groups for the HS varied in alpha diversity, the low energy sites showed high diversity while the high energy sites showed no diversity. Both the LS and NS had similar trends for both energy groups. Beta diversity showed high similarity between the NS and LS, but with greater variability in species present at the HS. The variability seen for plant diversity in the HS is mostly due to either the removal of all vegetation or the dense planting of turf grass representing a low diversity habitat, compared against a wooded upland vegetation community with many plant species present.

4.5 Data Interactions and Conceptual Model

Low energy sites amongst the three different shoreline types had similar spatial patterns in response to vegetation qualities, energy, and shape of the shoreline. Based on the conceptual model (Figure 30) these results show that the LS and NS are indicative of shallow slopes with higher vegetation diversity and coverage. These shoreline conditions also tend to support higher organic matter and finer sediment composition. The presence of vegetation and the high sediment organic matter are part of what make a natural marsh a key habitat to many species. Based on the results in this study, the LS provide similar food and protective habitat to nearby NS, as had been found in other studies (Balouskus & Targett, 2016; Bilkovic & Roggero, 2008; Partyka et al., 2017).

The erosion rate of the coastline and its geographic shape were mostly affected by the wave energy groups. As shown in the conceptual model (Figure 30), the energy exerted on the shorelines affected the sediment, morphology and vegetation found at the different shoreline types. Shorelines that received high energy had fewer dominant marsh species and this is probably because they tended to have steeper slopes, meaning the vegetation present is not required to be salt or inundation tolerant.

This conceptual model can be used to help predict where the implementation of a LS will help retain the shoreline and ecosystem at similar sites within the northern Gulf of Mexico. Other locations in the Gulf of Mexico or elsewhere may have different drivers or the effect from those drivers could vary from the data collected at the six case study sites. According to the conceptual model, a living shoreline will do best at a site that is receiving high or low energy impacts as long as it has a gradual slope. The gradual slope does not have to be natural; many LS involve the creation of a more gradual slope.

It is important to consider that there will be variability and error in the data collected for multiple reasons. One potential cause of error could be due to the weather at the time of sampling, in order to go out on the water to deploy the wave gauges, the water had to be calm and the gauges had a short battery period. With the gauges the data could also vary if we had sampled more frequently, collecting data for representative time periods in all four seasons.

CHAPTER 5 - CONCLUSION

The goal of this study was to evaluate how hydrological, geological, and biological parameters can affect different shoreline types (natural marsh, living shorelines, and hardened shorelines). This information can help coastal managers better identify conditions at potential sites where a living shoreline project may be effective. Based on this study, I conclude that the amount of energy impacting a shoreline can serve as a good proxy for the environmental conditions that can benefit the potential implementation of a living shoreline. Depending on research tools available, methods for obtaining this data would be either field sampling to measure the average wave power, or computer calculations to derive the relative exposure from fetch distance, however, neither method alone is completely accurate and other factors are involved in affecting project success. The low energy coastline groups exhibited less turbidity, less erosion, sediments with a higher percent of silt/clay, more sediment organic matter, and a higher diversity and percent cover of vegetation. I also found that high energy sites can cause a greater variability in the responses of the factors measured among the three different shoreline types than there was at the low energy sites.

The main difference found between NS and LS was that the LS had a slower erosion rate. If a project goal is to stop erosion of a shoreline, then a HS would be the best method, however, if the project involves maintaining a similar ecosystem to a NS, then a LS is a better alternative. The LS in this study did not stop erosion, but lessened the rate compared to the adjacent NS control. Other than erosion, the LS and NS were similar in slope, sediment grain size, soil BD, organic matter content, percent cover of vegetation, and the percent of dominant marsh vegetation. This study showed that a LS is

a potentially good alternative to help maintain a similar ecosystem to the NS while also slowing erosion rates.

Only two of the LS in this case study had been implemented longer than five years at the time of sampling. It is important to understand that restoration projects undergo succession, and this is a short time frame. With increased and more frequent sampling of LS after they are implemented the rate of succession could be identified for the different factors. With that in mind there are studies that have looked at LS after longer periods of implementation.

Living shorelines are better for the environment and help lessen the rate of erosion, however, many people still implement HS, especially on small scale projects. This often happens on personal property where people want immediate access to the water instead of multiple meters of tall vegetation separating them. Unfortunately, many of these property owners are unaware of the benefits that marshes provide. Another reservation cited by property owners on the use of LS for shoreline protection is the uncertainty about the cost (Whalen et al., 2012).

This research is important because the elevation, currents, and substrate of the U.S. Eastern and Gulf coasts makes these regions particularly vulnerable to storms and sea level rise. This research has increased our knowledge on what environmental conditions may be most suitable for living shorelines to help to decrease erosion rates (Arkema et al., 2013). Further research for the implementation of LS could focus on: (1) following the data from LS sites after implementation for multiple years, (2) differences in the responses of the various types of LS constructions, (3) whether using alternate types of sediment fill for a LS can make a difference (4) and the cost effectiveness of the

most successful of the different types of LS constructions over the long term (> 5 years). Those studies could help weigh the benefits of maintaining the different types of shorelines to the cost of erosion losses to habitats or property.

APPENDIX A – Wave gauge Kruskal-Wallis rank sums test table. Turbidity, relative exposure, shoreline slope, bulk density, organic matter, sediment grain size, species richness, total average percent cover, percent cover of dominant marsh species summary and ANOVA tables

Table.A.1 Kruskal-Wallis rank sums test for the average wave power by energy.

	X^2	DF	Pr(>F)
Kruskal-Wallis	19.36	1	1.08e-05

Table.A.2 Kruskal-Wallis rank sums test for the average wave power by site

	X^2	DF	Pr(>F)
Kruskal-Wallis	21.49	5	0.0006539

Table.A.3 ANOVA of turbidity by site and season

	Df	Sum Sq	Mean Sq	F value	Pr(>F)
Site	5	465508	93102	306.975	2e-16
Season	1	951	951	3.134	0.0767
Interaction	5	134052	26810	88.399	2e-16
Residuals	7833	2375650	303		

Table.A.4 One-way ANOVA of Relative Exposure by Site

	DF	Sum Sq	Mean Sq	F value	Pr(>F)
Site	5	43597343	8719469	59.57	2e-16
Residuals	1130	165405955	146377		

Table.A.5 ANOVA of erosion by site and shoreline

	Df	Sum Sq	Mean Sq	F value	Pr(>F)
Site	5	3.46	0.69	25.39	4.49e-13
Shoreline	2	6.06	3.03	111.23	2e-16
Interaction	10	6.87	0.69	25.20	2e-16
Residuals	54	1.47	0.03		

Table.A.6 One-way ANOVA of slope by shoreline.

	DF	Sum Sq	Mean Sq	F value	Pr(>F)
Shoreline	2	1435	717.5	22.53	6.77e-07
Residuals	33	1051	31.8		

Table.A.7 One-way ANOVA of bulk density by shoreline.

	DF	Sum Sq	Mean Sq	F value	Pr(>F)
Shoreline	2	19.35	9.674	66.53	2e-16
Residuals	262	38.10	0.145		

Table.A.8 ANOVA bulk density by site and shoreline.

	Df	Sum Sq	Mean Sq	F value	Pr(>F)
Shoreline	2	19.348	9.674	120.53	2e-16
Site	5	7.561	1.512	18.84	7.36e-16
Interaction	10	10.711	1.071	13.35	2e-16
Residuals	247	19.824	0.080		

Table.A.9 ANOVA of bulk density by energy and shoreline.

	Df	Sum Sq	Mean Sq	F value	Pr(>F)
Shoreline	2	19.35	9.674	73.159	2e-16
Energy	1	0.13	0.133	1.006	0.317
Interaction	2	3.71	1.857	14.044	1.62e-06
Residuals	259	34.25	0.132		

Table.A.10 One-way ANOVA of organic matter by shoreline.

	DF	Sum Sq	Mean Sq	F value	Pr(>F)
Shoreline	2	11329	5664	28.68	5.46e-12
Residuals	262	51749	198		

Table.A.11 One-way ANOVA of organic matter by site.

	DF	Sum Sq	Mean Sq	F value	Pr(>F)
Site	5	11845	2369.1	11.98	1.93e-10
Residuals	259	51233	197.8		

Table.A.12 ANOVA of organic matter by site and shoreline.

	Df	Sum Sq	Mean Sq	F value	Pr(>F)
Shoreline	2	11329	5664	67.59	2e-16
Site	5	11663	2333	27.83	2e-16
Interaction	10	19386	1939	23.13	2e-16
Residuals	247	20700	84		

Table.A.13 ANOVA of organic matter by energy and shoreline.

	Df	Sum Sq	Mean Sq	F value	Pr(>F)
Shoreline	2	11329	5664	32.943	1.79e-13
Energy	1	1321	1321	7.685	0.00597
Interaction	2	5894	2947	17.139	1.02e-07
Residuals	259	44534	172		

Table.A.14 One-way ANOVA of depth by percent sand.

	Df	Sum Sq	Mean Sq	F value	Pr(>F)
Depth	2	9058	4529	5.06	0.00698
Residuals	262	234510	895		

Table.A.15 One-way ANOVA of depth by percent silt and clay.

	Df	Sum Sq	Mean Sq	F value	Pr(>F)
Depth	2	9291	4645	5.363	0.00522
Residuals	261	226094	866		

Table.A.16 One-way ANOVA of coarse sand and pebbles by site.

	Df	Sum Sq	Mean Sq	F value	Pr(>F)
Site	5	935	186.97	2.924	0.0138
Residuals	258	16499	63.95		

Table.A.17 One-way ANOVA of percent sand by site.

	Df	Sum Sq	Mean Sq	F value	Pr(>F)
Site	5	37818	7564	9.521	2.37e-08
Residuals	259	199029	771		

Table.A.18 One-way ANOVA of percent silt and clay by site.

	Df	Sum Sq	Mean Sq	F value	Pr(>F)
Site	5	36355	7271	9.425	2.88e-08
Residuals	258	199029	771		

Table.A.19 One-way ANOVA of species richness by site.

	DF	Sum Sq	Mean Sq	F value	Pr(>F)
Site	5	113.2	22.63	1.75	0.198
Residuals	174	351.7	2.021		

Table.A.20 One-way ANOVA of species richness by shoreline.

	DF	Sum Sq	Mean Sq	F value	Pr(>F)
Shoreline	2	6.33	3.167	0.181	0.836
Residuals	15	262.17	17.478		

Table.A.21 One-way ANOVA of species richness by energy.

	DF	Sum Sq	Mean Sq	F value	Pr(>F)
Energy	1	68.06	68.06	5.432	0.0332
Residuals	178	393.1	2.21		

Table.A.22 One-way ANOVA of percent cover by shoreline.

	Df	Sum Sq	Mean Sq	F value	Pr(>F)
Shoreline	2	16361	8180	8.836	0.00022
Residuals	177	163863	926		

Table.A.23 One-way ANOVA of percent cover by site.

	Df	Sum Sq	Mean Sq	F value	Pr(>F)
Site	5	36334	7267	8.788	1.88e-07
Residuals	174	143889	827		

Table.A.24 One-way ANOVA of percent cover by energy.

	Df	Sum Sq	Mean Sq	F value	Pr(>F)
Energy	1	8527	8527	9.934	0.0019
Residuals	178	170697	959		

Table.A.25 One-way ANOVA of percent of dominant marsh species by shoreline.

	Df	Sum Sq	Mean Sq	F value	Pr(>F)
Shoreline	2	73013	3657	46.03	<2e-16
Residuals	177	140364	793		

Table.A.26 ANOVA of percent of dominant marsh species by energy and shoreline.

	Df	Sum Sq	Mean Sq	F value	Pr(>F)
Shoreline	1	8235	8325	12.11	0.000634
Energy	2	73013	36507	53.69	<2e-16
Interaction	2	5894	2947	17.139	1.02e-07
Residuals	174	118313	680		

Table.A.27 Kruskal-Wallis rank sums test for the significant wave period by site.

	X^2	DF	Pr(>F)
Kruskal-Wallis	17.93	5	0.003042

Table.A.28 Kruskal-Wallis rank sums test for the significant wave period by energy.

	X^2	DF	Pr(>F)
Kruskal-Wallis	13.11	1	0.0002934

Table.A.29 Kruskal-Wallis rank sums test for the average wave height by sites.

	X^2	DF	Pr(>F)
Kruskal-Wallis	21.24	5	0.0007283

Table.A.30 Kruskal-Wallis rank sums test for the average wave height by energy.

	X^2	DF	Pr(>F)
Kruskal-Wallis	18.16	1	2.029e-05

Table.A.31 Kruskal-Wallis rank sums test for the maximum wave height by site.

	X^2	DF	Pr(>F)
Kruskal-Wallis	22.97	5	0.0003418

Table.A.32 Kruskal-Wallis rank sums test for the maximum wave height by energy.

	X^2	DF	Pr(>F)
Kruskal-Wallis	20.18	1	7.056e-06

Table.A.33 Kruskal-Wallis rank sums test for the significant wave height by site.

	X^2	DF	Pr(>F)
Kruskal-Wallis	20.15	5	0.001171

Table.A.34 Kruskal-Wallis rank sums test for the significant wave height by energy.

	X^2	DF	Pr(>F)
Kruskal-Wallis	17.05	1	3.651e-05

Table.A.35 One-way ANOVA of bulk density by depth.

	Df	Sum Sq	Mean Sq	F value	Pr(>F)
Depth	2	0.15	0.0732	0.334	0.716
Residuals	262	57.30	0.21870		

Table.A.36 One-way ANOVA of organic matter by depth.

	Df	Sum Sq	Mean Sq	F value	Pr(>F)
Depth	2	1067	533.3	2.253	0.107
Residuals	262	2011	236.7		

APPENDIX B – Data analysis for the other data calculated from the wave gauges: average wave power, significant wave period, average wave height, maximum wave height, significant wave height, and wave percentiles

Table.B.1 Average wave power, signficant wave period, average wave height, maximum wave height, and signficant wave height for the six sites. Significant differences by site are indicated by Wilcoxon Rank Test letter groups.

Site	Average Wave Power (kW/m)	Significant Wave Period (s)	Average Wave Height (m)	Maximum Wave Height (m)	Significant Wave Height (m)
Hancock County	8.94 ± 1.78^{a}	2.72 ± 0.29^{ab}	0.08 ± 0.01^{ab}	0.39 ± 0.09^{a}	0.12 ± 0.01^{a}
Swift Tract	5.27 ± 1.09^{a}	2.73 ± 0.08^{ab}	0.07 ± 0.01^{abc}	0.38 ± 0.06^{a}	0.09 ± 0.01^{ab}
Alonzo Landing	7.35 ± 2.22^{a}	4.39 ± 0.79^{a}	0.06 ± 0.00^{abc}	0.32 ± 0.15^{a}	0.09 ± 0.01^{ab}
Camp Wilkes	1.98 ± 0.18^{bc}	2.06 ± 0.20^{ab}	0.05 ± 0.00^{bcd}	0.11 ± 0.01^{b}	0.06 ± 0.00^{b}
Ocean Springs	0.53 ± 0.15^{cd}	0.43 ± 0.43^{b}	0.03 ± 0.01^{de}	0.03 ± 0.01^{b}	0.01 ± 0.01^{b}
Grand Bay	1.12 ± 0.46^{bcd}	1.67 ± 0.46^{ab}	0.04 ± 0.01^{cde}	0.05 ± 0.01^{b}	0.04 ± 0.01^{b}

Table.B.2 Average wave power, signficant wave period, average wave height, maximum wave height, and signficant wave height for the high and low wave power groups.

Wave Power Group	Average Wave Power (kW/m)	Significant Wave Period (s)	Average Wave Height (m)	Maximum Wave Height (m)	Significant Wave Height (m)
High	6.91 ± 0.95	3.13 ± 0.28	0.07 ± 0.00	0.36 ± 0.05	0.10 ± 0.01
Low	1.31 ± 0.23	1.49 ± 0.26	0.04 ± 0.00	0.07 ± 0.01	0.04 ± 0.01

The significant wave period was statistically different among the six sites (H (5) = 17.93, $p < 0.00$). The significant wave period at AL (M = 4.39 s, SE = 0.79 s) was greater than at ST (M = 2.73 s, SE = 0.08 s), HC (M = 2.72 s, SE = 0.29 s), CW (M = 2.06 s, SE = 0.20 s), GB (M = 1.67 s, SE = 0.46 s), and OS (M = 0.43 s, SE = 0.43 s) (Fig. B1). Of the sites the only two that were significantly different from each other were AL and OS

(Table B1). The significant wave period was also significantly different between the high and low WP groups (H (1) = 13.11, $p < 0.00$) with the high WP group (M = 3.13 s, SE = 0.28 s) greater than the low WP group (M = 1.49 s, SE = 0.26 s). The significant wave period is the wave period for the top one third of the wave height. This indicated that the significant wave period is affected by the wave height.

The average wave height was significantly different among the six sites (H (5) = 21.24, $p < 0.00$) and the two WP groups (H (1) = 18.16, $p < 0.00$). Hancock County (M = 0.08 m, SE = 0.01 m) had the greatest average wave height of all six sites, followed by ST (M = 0.07 m, SE = 0.01 m), and AL (M = 0.06 m, SE = 0.00 m) which were not significantly different from each other (Fig B1). The lowest average wave height was at OS (M = 0.03 m, SE = 0.01 m) and was significantly different from HC, ST, and AL. Between the high and low averages were CW (M = 0.05 m, SE = 0.00 m) and GB (M = 0.04 m, SE = 0.01). The high WP group (M = 0.07 m, SE = 0.00 m) was greater than the low WP group (M = 0.04 m, SE = 0.00 m). The results from the average wave height data indicate that site shoreline orientation and available shoreline perpendicular fetch distance may influence the formation of wave height.

The maximum wave height was significantly different among the six (H (5) = 22.97, $p < 0.00$) and the two WP groups (H (1) = 20.18, $p < 0.00$). The maximum wave height was greatest at HC (M = 0.39 m, SE = 0.09 m), followed by ST (M = 0.38 m, SE = 0.06 m), AL (M = 0.32 m, SE = 0.15 m), CW (M = 0.11 m, SE = 0.01 m), GB (M = 0.04 m, SE = 0.01 m), and OS (M = 0.03 m, SE = 0.01 m) (Fig. B1). Statistical grouping for the maximum wave height grouped HC, ST, and AL together and CW, OS, and GB

together. The maximum wave height for the high WP group (M = 0.36 m, SE = 0.05 m) was more than five times greater than the low WP group (M = 0.07 m, SE = 0.01 m).

Finally, the significant wave height was also significantly different among the six sites (H (5) = 20.15, $p < 0.00$) and the two WP (H (1) = 17.05, $p < 0.00$). The significant wave height is the average wave height for the top third of all wave heights. Hancock County (M = 0.12 m, SE = 0.01 m) had the greatest significant wave height and was significantly different from CW (M = 0.06 m, SE = 0.00 m), GB (M = 0.04 m, SE = 0.01 m), and OS (M = 0.01 m, SE = 0.01 m). Swift Tract (M = 0.09 m, SE = 0.01 m) and AL (M = 0.09 m, SE = 0.01 m) were between the two groups. The high WP group (M = 0.10 m, SE = 0.01 m) had more than double the significant wave height than the low WP group (M = 0.04 m, SE = 0.01). This finding indicates that the significant wave height may be influenced by the available fetch distance and wind power.

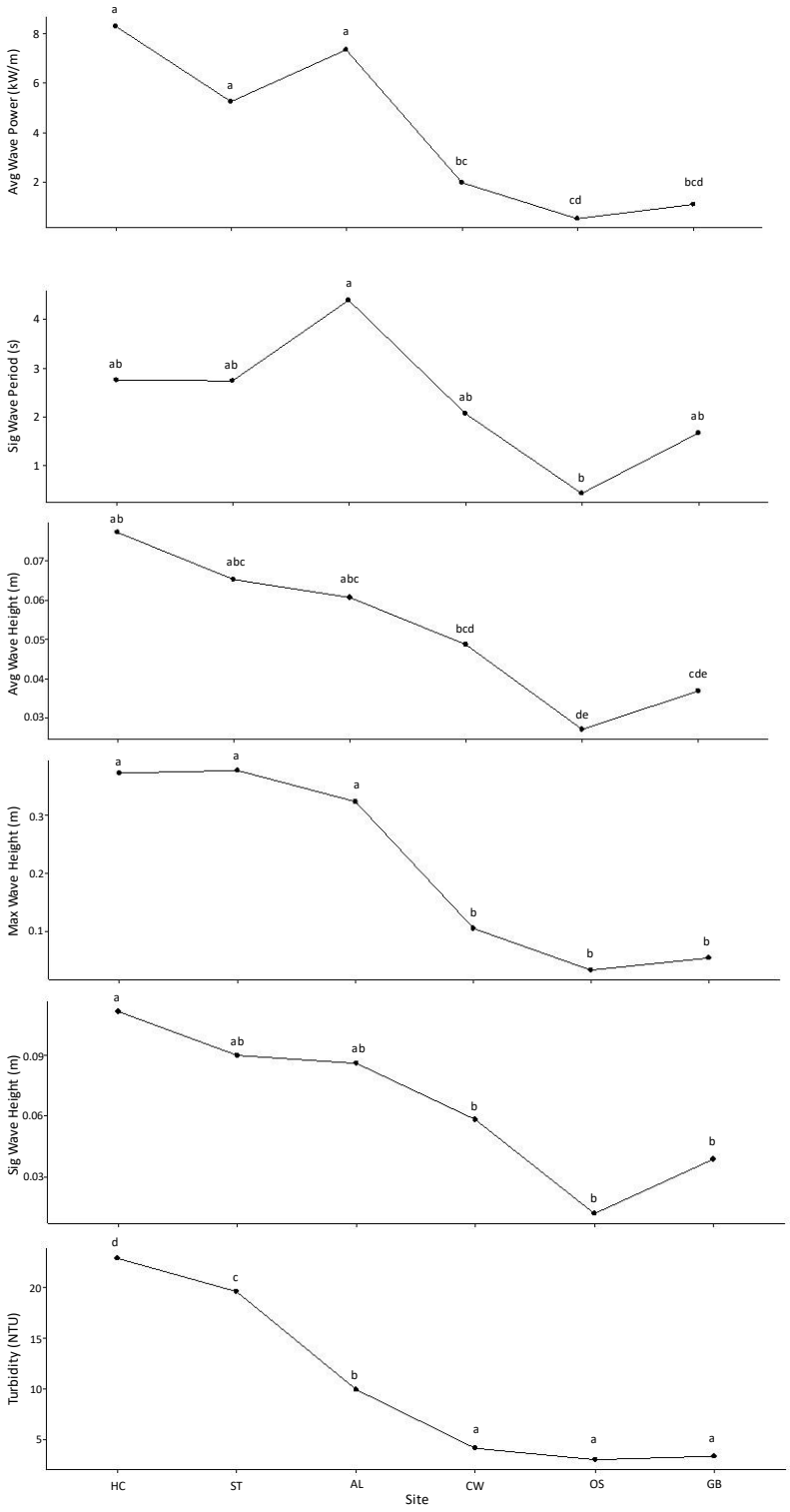

Figure.B.1 Average wave power (kW/m), significant wave period (s), average wave height (m), maximum wave height (m), significant wave height (m), and turbidity (NTU)

for the six sites. Significant differences by site are indicated by Wilcoxon Rank Test letter groups.

The average wave height, significant wave height, significant wave period, and maximum wave height all decreased with average wave power (Fig B1). Shoreline (NS, LS, HS) had no significant effect on any of these parameters. Season (summer vs winter) only had an effect on the average wave power, significant wave height and average wave height but there was no visible pattern seen across sites.

The wave height percentiles show that the three high WP sites (HC, ST, and AL) have higher wave heights than the low WP sites (CW, OS, and GB) (Fig. B2). The jump between the 99^{th} and 100^{th} percentile is largest at ST (0.24 m), followed by HC (0.18 m), AL (0.16 m), CW (0.02 m), OS (0.004 m), and GB (0.004 m). The high WP group showed a jump between the 99^{th} and 100^{th} of 0.19 m, which was almost 19 times greater than the low WP group (0.01 m) (Fig B3). This data is another way to represent the wave gauge data and show the difference between the six sites and how the wave energy may affect other factors in the water, such as turbidity.

Table.B.3. Wave Height Percentiles for the three different types of shorelines (NS, LS, and HS) for all six sites during winter and summer of 2020.

Site	Shoreline	Season	10	20	30	40	50	60	70	80	90	95	99	100
Hancock County	Natural	Winter	0.05	0.06	0.07	0.08	0.09	0.11	0.12	0.13	0.16	0.18	0.22	0.32
		Summer	0.04	0.05	0.05	0.05	0.06	0.06	0.07	0.08	0.10	0.12	0.15	0.29
	Living	Winter	0.04	0.05	0.05	0.05	0.06	0.07	0.08	0.09	0.12	0.15	0.21	0.40
		Summer	0.04	0.04	0.05	0.05	0.05	0.05	0.06	0.07	0.08	0.08	0.10	0.16
	Hardened	Winter	0.05	0.06	0.07	0.08	0.08	0.09	0.10	0.11	0.12	0.15	0.29	0.69
		Summer	NA	NA	NA	NA	NA	NA	NA	NA	NA	NA	NA	NA
Swift Tract	Natural	Winter	NA	NA	NA	NA	NA	NA	NA	NA	NA	NA	NA	NA
		Summer	0.04	0.05	0.06	0.06	0.07	0.08	0.09	0.11	0.13	0.15	0.19	0.49
	Living	Winter	0.04	0.04	0.04	0.04	0.05	0.05	0.05	0.05	0.06	0.06	0.08	0.15
		Summer	0.04	0.04	0.05	0.05	0.05	0.06	0.06	0.07	0.08	0.09	0.11	0.34
	Hardened	Winter	0.04	0.05	0.05	0.05	0.06	0.06	0.07	0.08	0.09	0.10	0.10	0.44
		Summer	0.04	0.05	0.06	0.06	0.07	0.08	0.09	0.10	0.12	0.14	0.17	0.47
Alonzo Landing	Natural	Winter	NA	NA	NA	NA	NA	NA	NA	NA	NA	NA	NA	NA
		Summer	NA	NA	NA	NA	NA	NA	NA	NA	NA	NA	NA	NA
	Living	Winter	NA	NA	NA	NA	NA	NA	NA	NA	NA	NA	NA	NA
		Summer	0.04	0.04	0.05	0.05	0.05	0.06	0.06	0.07	0.09	0.10	0.12	0.18
	Hardened	Winter	0.04	0.04	0.05	0.05	0.05	0.06	0.06	0.07	0.08	0.09	0.11	0.16
		Summer	0.04	0.04	0.05	0.05	0.05	0.06	0.06	0.07	0.10	0.13	0.25	0.63
Camp Wilkes	Natural	Winter	0.04	0.04	0.04	0.04	0.05	0.05	0.05	0.05	0.06	0.07	0.08	0.12
		Summer	0.04	0.04	0.04	0.04	0.04	0.05	0.05	0.05	0.06	0.08	0.10	0.11
	Living	Winter	0.04	0.04	0.04	0.04	0.04	0.04	0.05	0.05	0.05	0.06	0.06	0.07
		Summer	0.04	0.04	0.04	0.05	0.05	0.05	0.05	0.06	0.07	0.07	0.09	0.13
	Hardened	Winter	0.04	0.04	0.04	0.04	0.04	0.05	0.05	0.05	0.06	0.06	0.08	0.08
		Summer	0.04	0.04	0.04	0.04	0.05	0.05	0.05	0.05	0.06	0.07	0.09	0.12
Ocean Springs	Natural	Winter	0.00	0.00	0.00	0.00	0.02	0.02	0.02	0.02	0.02	0.02	0.02	0.02
		Summer	NA	NA	NA	NA	NA	NA	NA	NA	NA	NA	NA	NA
	Living	Winter	0.00	0.00	0.00	0.00	0.02	0.02	0.02	0.02	0.02	0.02	0.02	0.02
		Summer	NA	NA	NA	NA	NA	NA	NA	NA	NA	NA	NA	NA
	Hardened	Winter	0.00	0.00	0.00	0.00	0.02	0.02	0.02	0.02	0.02	0.02	0.02	0.02
		Summer	0.04	0.04	0.04	0.04	0.04	0.04	0.04	0.05	0.05	0.05	0.05	0.06
Grand Bay	Natural	Winter	0.00	0.00	0.00	0.00	0.02	0.02	0.02	0.02	0.02	0.02	0.02	0.02
		Summer	0.02	0.02	0.02	0.02	0.02	0.02	0.02	0.02	0.02	0.02	0.03	0.03
	Living	Winter	0.04	0.04	0.04	0.04	0.05	0.05	0.06	0.07	0.08	0.09	0.09	0.09
		Summer	0.04	0.04	0.04	0.04	0.04	0.04	0.04	0.05	0.05	0.05	0.06	0.07
	Hardened	Winter	NA	NA	NA	NA	NA	NA	NA	NA	NA	NA	NA	NA
		Summer	0.04	0.04	0.04	0.04	0.04	0.04	0.04	0.05	0.05	0.05	0.05	0.05

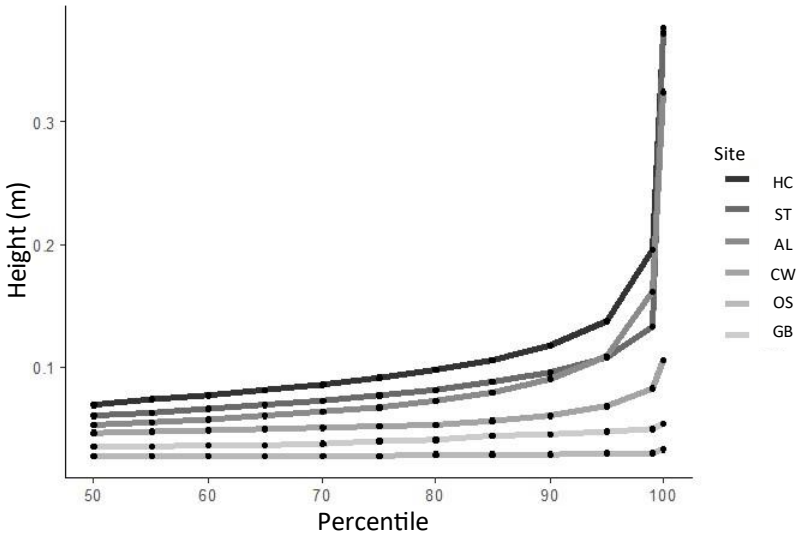

Figure.B.2 Wave height percentiles from 50-100% showing the height (m) for the six sites: Hancock County (HC), Swift Tract (ST), Alonzo Landing (AL), Camp Wilkes (CW), Ocean Springs (OS), and Grand Bay (GB).

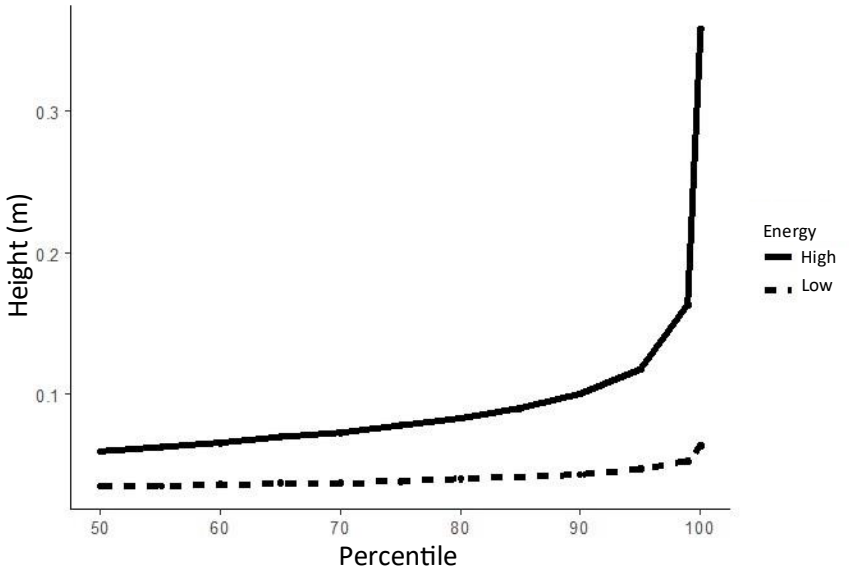

Figure.B.3 Wave height percentiles from 50-100% showing the height (m) for high and low wave power groups.

APPENDIX C - More detailed tables and figures for the results.

Table.C.1 Wave gauge data results, heights are in cm, and wave period is in seconds.

Hours of collection were calculated at timeanddate.com, which rounds down.

Site	Shoreline	Season	Avg Wave Height	Sig Wave Height	Max Wave Height	Sig Wave Period	Avg Wave Power	Hours Collected
Hancock County	Natural	Winter	0.10	0.15	0.32	2.89	14.28	13
		Summer	0.07	0.09	0.29	2.91	5.71	151
	Living	Winter	0.72	0.11	0.40	3.43	9.69	141
		Summer	0.06	0.07	0.16	2.92	4.01	151
	Hardened	Winter	0.09	0.13	0.69	1.66	7.78	81
		Summer	NA	NA	NA	NA	NA	NA
Swift Tract	Natural	Winter	NA	NA	NA	NA	NA	NA
		Summer	0.08	0.12	0.49	2.75	8.22	100
	Living	Winter	0.05	0.06	0.15	2.49	2.37	100
		Summer	0.06	0.08	0.34	2.98	4.12	100
	Hardened	Winter	0.06	0.08	0.44	2.74	4.28	100
		Summer	0.08	0.11	0.47	2.69	7.34	100
Alonzo Landing	Natural	Winter	NA	NA	NA	NA	NA	NA
		Summer	NA	NA	NA	NA	NA	NA
	Living	Winter	NA	NA	NA	NA	NA	NA
		Summer	0.06	0.08	0.18	5.81	6.67	137
	Hardened	Winter	0.06	0.08	0.16	3.07	3.89	75
		Summer	0.07	0.10	0.63	4.30	11.49	119
Camp Wilkes	Natural	Winter	0.05	0.06	0.12	1.49	1.54	137
		Summer	0.05	0.06	0.11	2.50	2.52	156
	Living	Winter	0.05	0.06	0.07	1.80	1.55	137
		Summer	0.05	0.06	0.13	1.95	2.19	156
	Hardened	Winter	0.05	0.06	0.08	2.78	2.36	137
		Summer	0.05	0.06	0.12	1.85	1.70	156
Ocean Springs	Natural	Winter	0.02	NA	0.02	NA	0.40	87
		Summer	NA	NA	NA	NA	NA	NA
	Living	Winter	0.02	NA	0.02	NA	0.40	87
		Summer	NA	NA	NA	NA	NA	NA
	Hardened	Winter	0.02	NA	0.02	NA	0.34	87
		Summer	0.04	0.05	0.07	1.70	1.00	138
Grand Bay	Natural	Winter	0.02	NA	0.02	NA	0.12	112
		Summer	0.02	0.02	0.03	1.68	0.24	143
	Living	Winter	0.06	0.08	0.09	2.19	2.62	112
		Summer	0.04	0.05	0.07	1.71	1.00	143
	Hardened	Winter	NA	NA	NA	NA	NA	NA
		Summer	0.04	0.05	0.05	2.75	1.60	143

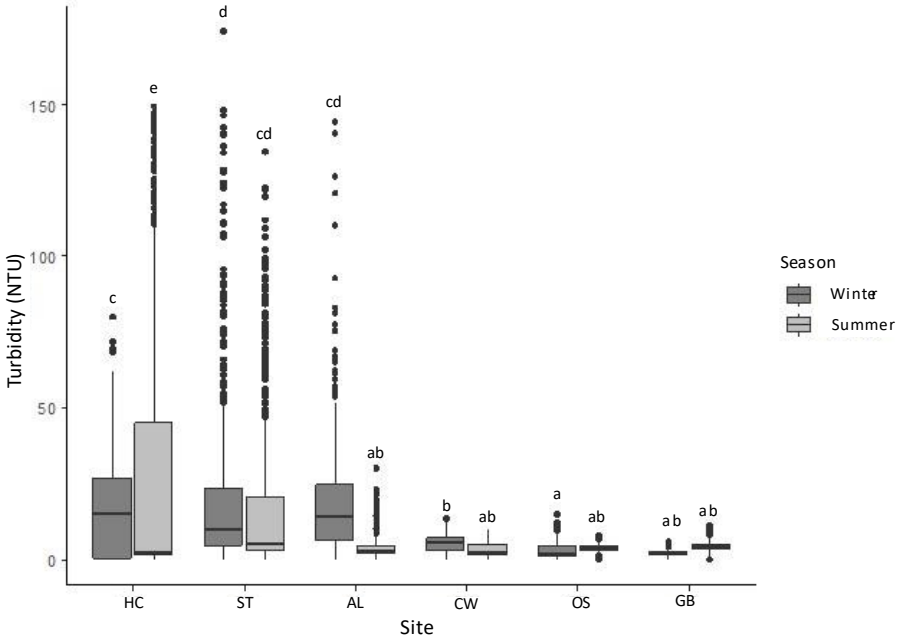

Figure.C.1 Boxplot of turbidity (NTU) separated by season and site. Significant differences by season and site are indicated by Tukey's HSD post-hoc letter groups.

Table.C.2 Maximum fetch distance (m) for natural, living, and hardened shorelines at each and the average maximum fetch for each site. Fetch average is the mean of all the fetch transects at the site that did not equal zero (n=19).

Site	Natural (m)	Living (m)	Hardened (m)	Avg max (m)
Hancock County	34,608	33,569	27,626	31,944
Swift Tract	34,952	106,542	28,495	56,663
Alonzo Landing	245.54	388.11	260.41	298.02
Camp Wilkes	1252.08	2156.56	1045.28	1484.64
Ocean Springs	108.17	225.16	197.55	176.96
Grand Bay	45.06	189.51	86.47	107.01

Table.C.3 Average fetch distance (m) for natural, living, and hardened shorelines at each and the average fetch for each site. The avg fetch distance is the mean of all the fetch transects at the site that did not equal zero.

Site	Natural (m)	Living (m)	Hardened (m)	Avg max (m)
Hancock County	17,794	15,221	14,486	15,972
Swift Tract	12,686	26,221	15,061	17,777
Alonzo Landing	125.42	176.59	174.40	159.51
Camp Wilkes	439.00	574.22	360.60	457.18
Ocean Springs	45.62	71.60	98.09	71.77
Grand Bay	25.46	71.14	41.62	46.08

Table.C.4 Mean Relative Exposure (±SE) for natural, living, and hardened shorelines for each season and wave power group (n=3).

Shoreline	Fall	Winter	Spring	Summer
High Energy				
Natural	3,834 ± 2,214	3,960 ± 2,286	4,468 ± 2,580	3,215 ± 1,856
Living	4,000 ± 2,309	2,907 ± 2,198	4,498 ± 2,597	3,977 ± 2,296
Hardened	3,057 ± 1,765	3,088 ± 1,783	5,411 ± 3,124	3,874 ± 2,237
Low Wave Power				
Natural	103.17 ± 82.05	113.00 ± 91.95	145.77 ± 107.12	123.44 ± 101.64
Living	99.41 ± 72.20	140.58 ± 111.85	96.79 ± 65.35	134.58 ± 124.67
Hardened	59.98 ± 25.88	68.22 ± 31.05	176.90 ± 162.90	119.85 ± 80.48

Table.C.5 Relative Exposure for natural, living, and hardened shorelines at each site for each season.

Shoreline	Fall	Winter	Spring	Summer
Hancock County				
Natural	9,861	9,566	6,889	6,471
Living	8,981	6,915	10,647	8,937
Hardened	7,706	7,441	12,835	5,253
Swift Tract				
Natural	1,577	2,235	6,458	3,130
Living	2,960	4,432	2,768	2,967

Hardened	1,434	1,768	3,345	6,337
Alonzo Landing				
Natural	64.24	79.68	57.04	45.26
Living	57.92	73.24	80.10	24.98
Hardened	30.19	55.28	54.16	31.41
Camp Wilkes				
Natural	266.88	296.72	359.46	326.53
Living	243.79	364.26	227.28	383.88
Hardened	101.00	125.55	502.65	278.46
Ocean Springs				
Natural	31.13	28.19	52.15	29.43
Living	25.65	29.65	37.97	13.38
Hardened	66.81	60.22	18.33	64.27
Grand Bay				
Natural	11.48	14.09	25.70	14.37
Living	28.79	27.81	25.12	6.47
Hardened	12.13	18.90	9.71	16.80

Table.C.6 Mean (± SE) of the percent coarse sand and pebbles, percent sand, percent silt/clay, bulk density, and organic matter (OM) for the different depths for the shorelines at all six sites. n=5.

Shoreline	Depth	Coarse Sand and Pebbles (%)	Sand (%)	Silt and Clay (%)	Bulk Density (g/cm^3)	OM (%)
Hancock County						
Natural	0-10	1.02 ± 0.40	29.15 ± 13.33	69.84 ± 13.27	0.68 ± 0.02	10.91 ± 1.83
	10-20	1.12 ± 0.27	13.66 ± 2.47	85.22 ± 2.57	0.57 ± 0.04	11.99 ± 1.52
	20-30	1.21 ± 0.26	14.93 ± 2.36	83.86 ± 2.53	0.54 ± 0.03	16.41 ± 2.43
Living	0-10	0.84 ± 0.61	57.45 ± 11.40	41.71 ± 10.97	0.88 ± 0.21	11.72 ± 5.21
	10-20	1.09 ± 0.80	48.04 ± 9.52	50.87 ± 9.08	0.81 ± 0.16	13.56 ± 5.16
	20-30	0.88 ± 0.75	53.15 ± 12.69	45.96 ± 12.40	0.91 ± 0.19	12.16 ± 6.08
Hardened	0-10	0.36 ± 0.22	98.62 ± 0.53	1.11 ± 0.36	1.31 ± 0.01	0.40 ± 0.14
	10-20	0.90 ± 0.35	96.85 ± 0.85	2.24 ± 0.67	1.32 ± 0.03	0.52 ± 0.19
	20-30	11.07 ± 6.74	75.12 ± 12.75	13.81 ± 7.42	1.13 ± 0.13	3.92 ± 2.30
Swift Tract						
Natural	0-10	2.81 ± 1.58	40.35 ± 17.01	56.84 ± 18.36	0.77 ± 0.19	19.24 ± 6.47
	10-20	1.43 ± 0.68	27.97 ± 16.09	70.60 ± 16.65	0.75 ± 0.21	18.88 ± 5.41
	20-30	1.19 ± 0.42	21.77 ± 4.72	77.04 ± 4.93	0.41 ± 0.03	29.60 ± 1.75

Living	0-10	5.28 ± 0.64	82.01 ± 11.09	14.08 ± 11.09	0.97 ± 0.22	10.96 ± 5.31
	10-20	14.55 ± 2.16	35.00 ± 7.66	50.45 ± 8.51	0.24 ± 0.04	59.13 ± 6.70
	20-30	10.69 ± 1.31	26.86 ± 1.06	62.62 ± 1.95	0.20 ± 0.01	75.02 ± 1.89
Hardened	0-10	6.86 ± 2.16	88.58 ± 2.17	4.56 ± 0.98	1.40 ± 0.04	1.29 ± 0.38
	10-20	7.27 ± 1.37	90.60 ± 1.35	2.58 ± 1.18	1.27 ± 0.12	3.40 ± 1.55
	20-30	7.26 ± 1.49	86.04 ± 4.93	8.77 ± 3.13	1.45 ± 0.12	2.76 ± 1.15
Alonzo Landing						
Natural	0-10	4.33 ± 1.09	54.08 ± 13.04	41.59 ± 12.27	0.62 ± 0.21	16.42 ± 4.93
	10-20	6.22 ± 2.16	62.63 ± 12.49	31.15 ± 12.43	0.59 ± 0.19	16.79 ± 4.31
	20-30	7.28 ± 3.00	69.26 ± 7.59	23.46 ± 6.69	0.68 ± 0.20	15.20 ± 4.57
Living	0-10	3.81 ± 0.61	93.69 ± 4.34	4.30 ± 3.23	0.76 ± 0.17	9.64 ± 2.71
	10-20	6.49 ± 1.37	74.97 ± 4.23	18.54 ± 3.85	0.66 ± 0.07	11.02 ± 2.12
	20-30	4.53 ± 1.39	79.87 ± 3.02	15.61 ± 4.35	0.88 ± 0.13	7.19 ± 1.66
Hardened	0-10	0.59 ± 0.28	99.35 ± 0.23	0.31 ± 0.16	1.43 ± 0.02	0.10 ± 0.01
	10-20	0.36 ± 0.07	99.73 ± 0.73	0.61 ± 0.36	1.41 ± 0.02	0.80 ± 0.57
	20-30	0.61 ± 0.25	99.05 ± 0.38	0.51 ± 0.20	1.39 ± 0.01	0.08 ± 0.02
Camp Wilkes						
Natural	0-10	30.68 ± 17.35	70.02 ± 17.60	11.37 ± 11.37	0.24 ± 0.01	39.56 ± 2.42
	10-20	12.47 ± 3.94	19.91 ± 2.22	67.62 ± 6.03	0.28 ± 0.03	35.76 ± 4.65
	20-30	11.71 ± 1.78	21.27 ± 1.29	67.02 ± 2.68	0.23 ± 0.01	37.16 ± 2.87
Living	0-10	2.89 ± 0.69	58.59 ± 10.00	38.52 ± 9.75	0.61 ± 0.10	13.21 ± 2.36
	10-20	1.52 ± 0.36	87.37 ± 5.02	11.11 ± 4.68	1.27 ± 0.05	3.09 ± 0.72
	20-30	2.65 ± 0.81	79.01 ± 6.84	18.33 ± 7.23	1.29 ± 0.09	3.47 ± 1.09
Hardened	0-10	5.92 ± 4.54	74.28 ± 11.57	19.8 ± 7.83	1.53 ± 0.02	2.02 ± 0.42
	10-20	2.1 ± 1.85	76.7 ± 3.04	21.2 ± 3.57	1.54 ± 0.03	2.42 ± 0.12
	20-30	0.49 ± 0.21	74.53 ± 2.48	24.97 ± 2.48	1.54 ± 0.02	2.53 ± 0.19
Ocean Springs						
Natural	0-10	2.36 ± 0.37	26.82 ± 3.79	70.82 ± 4.04	0.44 ± 0.04	11.56 ± 1.84
	10-20	1.83 ± 0.49	20.30 ± 3.85	77.87 ± 4.00	0.39 ± 0.04	16.36 ± 2.14
	20-30	1.66 ± 0.28	16.74 ± 3.44	81.60 ± 3.48	0.42 ± 0.01	13.61 ± 0.76
Living	0-10	3.39 ± 0.39	73.15 ± 9.53	19.39 ± 11.23	1.10 ± 0.11	3.22 ± 1.06
	10-20	7.46 ± 2.06	63.65 ± 9.77	28.88 ± 8.54	0.75 ± 0.10	7.47 ± 2.34
	20-30	4.16 ± 1.68	37.65 ± 8.35	58.19 ± 7.26	0.57 ± 0.11	11.70 ± 3.31
Hardened	0-10	11.24 ± 1.92	49.80 ± 5.22	38.96 ± 7.11	0.72 ± 0.11	7.82 ± 1.79
	10-20	10.47 ± 5.14	41.47 ± 8.05	48.06 ± 12.08	0.66 ± 0.08	7.75 ± 1.53
	20-30	6.01 ± 2.99	43.03 ± 8.54	50.95 ± 9.93	0.76 ± 0.12	5.55 ± 0.90
Grand Bay						
Natural	0-10	8.26 ± 5.15	50.78 ± 1.76	40.96 ± 5.25	0.90 ± 0.19	4.18 ± 1.28
	10-20	2.35 ± 0.44	39.56 ± 5.38	58.09 ± 5.12	1.13 ± 0.24	4.03 ± 1.29
	20-30	6.72 ± 3.03	34.25 ± 3.20	59.04 ± 2.48	1.16 ± 0.18	3.84 ± 0.95
Living	0-10	4.21 ± 1.94	74.93 ± 4.31	20.87 ± 3.76	1.33 ± 0.07	2.83 ± 0.44
	10-20	4.99 ± 1.92	76.78 ± 6.07	18.23 ± 5.23	1.40 ± 0.10	2.41 ± 0.79
	20-30	6.44 ± 5.53	82.02 ± 0.37	11.53 ± 5.90	1.60 ± 0.00	1.64 ± 0.29
Hardened	0-10	4.68 ± 1.84	73.50 ± 5.14	21.82 ± 4.73	1.28 ± 0.01	2.63 ± 0.32

	10-20	0.72 ± 0.22	68.31 ± 8.48	30.96 ± 8.65	1.30 ± 0.10	2.99 ± 0.74
	20-30	0.97 ± 0.53	44.14 ± 8.46	54.89 ± 8.47	1.15 ± 0.20	4.85 ± 1.68

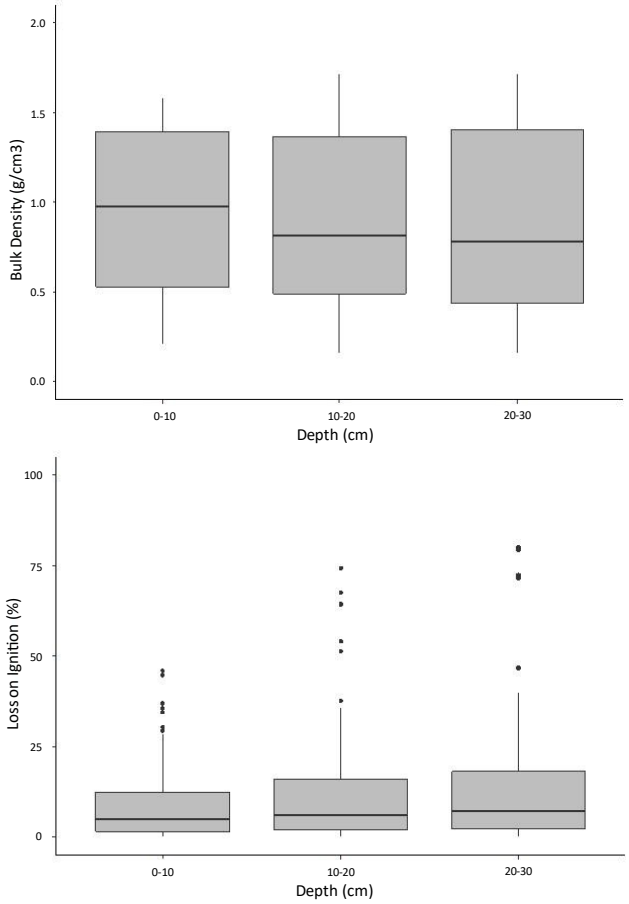

Figure.C.2 Boxplot of the different depth fractions (cm) for the different sediment features grouped across all six sites: bulk density and organic matter.

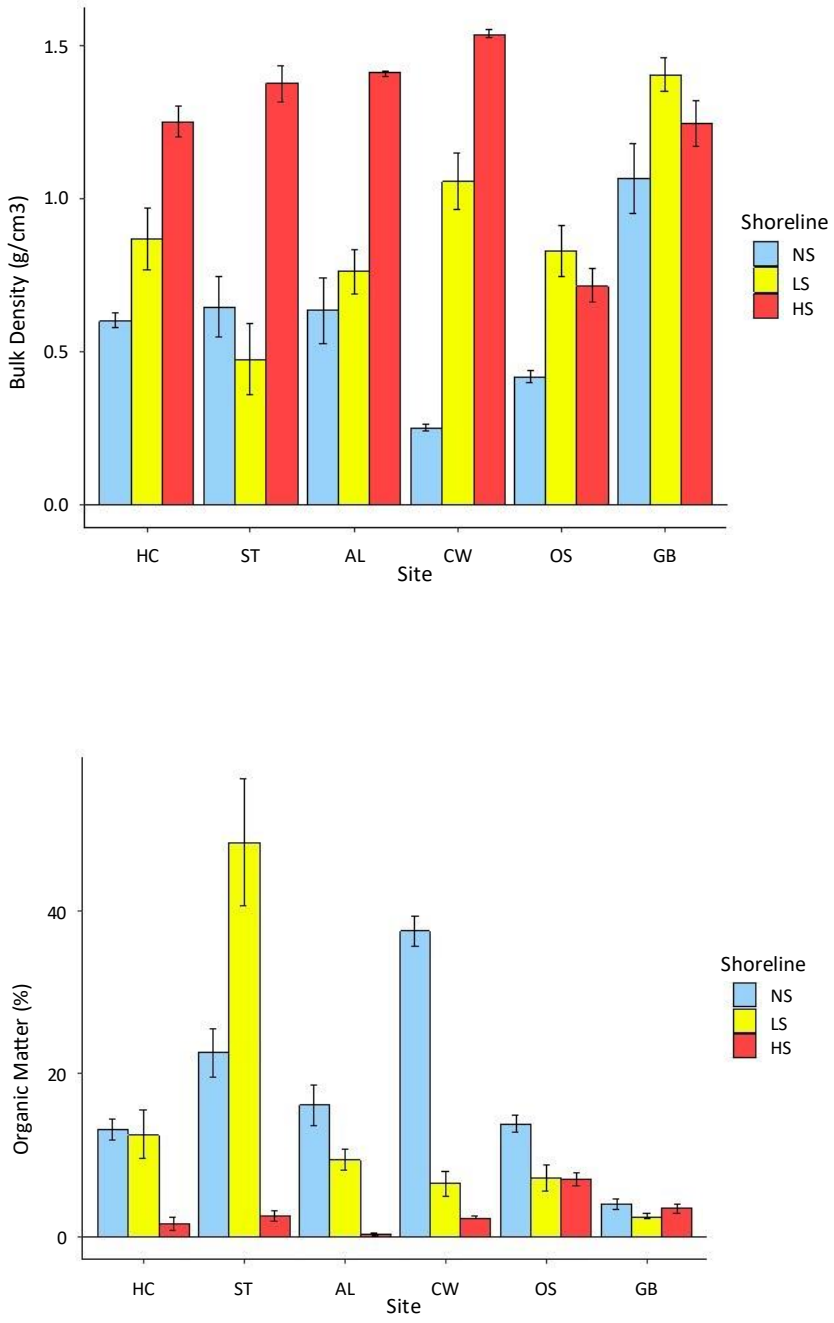

Figure.C.3 Bulk density (g/cm^3) and organic matter (%) for the different six different sites and three shoreline types with natural shorelines (blue), living shorelines (yellow), and hardened shorelines (red).

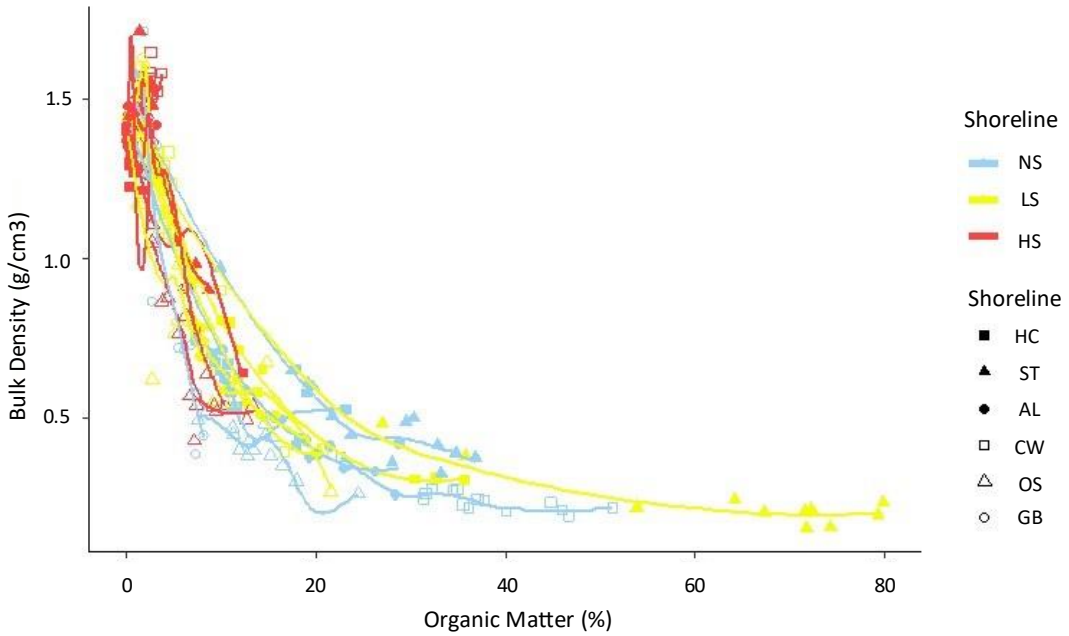

Figure.C.4 Scatterplot of OM to BD for all six sites and three shoreline types. Symbols and colors indicate sample origin, filled symbols indicate high energy sites.

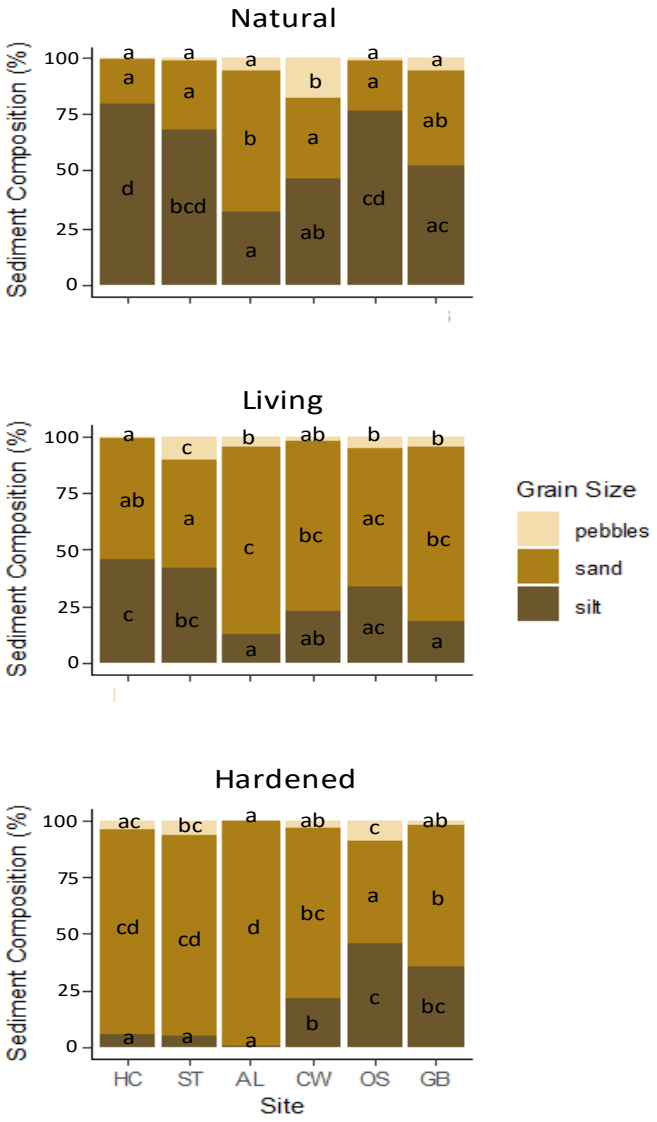

Figure.C.5 Sediment grain size composition at three shoreline types collected from six sites: Hancock County marsh (HC), Swift Tract (ST), Alonzo Landing (AL), Camp Wilkes (CW), Ocean Springs harbor (OS), and Grand Bay (GB). Significant differences by sediment fraction are indicated by Tukey's HSD post-hoc letter groups

Table.C.7 Vegetation data by site and shoreline for the average total percent cover, species richness, species found, average percent cover (±SE) for each of the species, the maximum and minimum percent cover each for each of the species, the Shannon H index, and the Simpson D index.

Shoreline	Avg. Total % Cover	Species Richness	Species	Avg % Cover ± SE	Max	Min	Shannon's H	Simpson's D Index
Hancock County								
Natural	67.00	4.00	SPAL	0.46 ± 0.13	0.85	0.00	0.82	0.47
			SPPA	0.15 ± 0.09	0.85	0.00		
			JURO	0.06 ± 0.05	0.50	0.00		
			DISP	0.00 ± 0.00	0.05	0.00		
Living	52.25	9.00	SPPA	0.18 ± 0.05	0.50	0.00	1.73	0.78
			SCRO	0.14 ± 0.02	0.25	0.00		
			SPAL	0.08 ± 0.03	0.25	0.00		
			PADI	0.05 ± 0.03	0.30	0.00		
			PARE	0.03 ± 0.03	0.30	0.00		
			IVFR	0.02 ± 0.02	0.15	0.00		
			BOFR	0.02 ± 0.01	0.10	0.00		
			SYTE	0.01 ± 0.01	0.05	0.00		
			DISP	0.01 ± 0.01	0.05	0.00		
Hardened	0.00	0.00	NA	0.00 ± 0.00	0.00	0.00	0.00	1.00
Swift Tract								
Natural	63.50	4.00	SPAL	0.53 ± 0.09	0.95	0.15	0.57	0.30
			SPPA	0.09 ± 0.07	0.75	0.00		
			BAHA	0.02 ± 0.01	0.10	0.00		
			AMAR	0.01 ± 0.01	0.05	0.00		
Living	59.50	2.00	SPAL	0.59 ± 0.13	0.95	0.00	0.06	0.02
			SPPA	0.01 ± 0.00	0.05	0.00		
Hardened	0.00	0.00	TURF	0.95 ± 0.00	0.95	0.95	0	0
Alonzo Landing								
Natural	54.60	9.00	JURO	0.20 ± 0.07	0.60	0.00	1.63	0.75
			SPPA	0.14 ± 0.04	0.35	0.00		
			SPAL	0.11 ± 0.02	0.20	0.01		
			BAHA	0.04 ± 0.03	0.25	0.00		
			SYTE	0.02 ± 0.01	0.10	0.00		
			FICA	0.02 ± 0.02	0.15	0.00		
			PARE	0.02 ± 0.02	0.15	0.00		
			BOFR	0.01 ± 0.01	0.05	0.00		
			DISP	0.01 ±0.01	0.05	0.00		
Living	78.00	6.00	SPPA	0.26 ± 0.05	0.45	0.00	1.52	0.75
			JURO	0.22 ± 0.06	0.50	0.00		
			SPAL	0.17 ± 0.04	0.45	0.00		
			DISP	0.08 ± 0.04	0.35	0.00		
			BOFR	0.05 ± 0.02	0.15	0.00		
			SYTE	0.01 ± 0.01	0.05	0.00		
Hardened	0.00	0.00	NA	0.00 ± 0.00	0.00	0.00	0.0	1.0

Camp Wilkes								
Natural	73.50	7.00	JURO	0.52 ± 0.04	0.70	0.40	1.03	0.49
			SALA	0.09 ± 0.03	0.30	0.00		
			SPAL	0.08 ± 0.02	0.20	0.00		
			SPCY	0.03 ± 0.01	0.10	0.00		
			PADI	0.01 ± 0.01	0.05	0.00		
			TRPA	0.01 ± 0.01	0.05	0.00		
			DISP	0.01 ± 0.01	0.10	0.00		
Living	66.00	8.00	SPAL	0.39 ± 0.11	0.90	0.00	1.12	0.59
			JURO	0.15 ± 0.07	0.70	0.00		
			PADI	0.11 ± 0.06	0.50	0.00		
			ELEO	0.00 ± 0.00	0.03	0.00		
			HYCO	0.00 ± 0.00	0.03	0.00		
			PARE	0.01 ± 0.01	0.05	0.00		
			BAMO	0.01 ± 0.01	0.05	0.00		
			ASTE	0.00 ± 0.00	0.10	0.00		
Hardened	31.50	17.00	RUTR	0.10 ± 0.07	0.75	0.00	2.19	0.84
			PIEL	0.04 ± 0.03	0.35	0.00		
			TRSE	0.04 ± 0.03	0.30	0.00		
			ILVO	0.04 ± 0.04	0.35	0.00		
			MYCE	0.03 ± 0.02	0.15	0.00		
			SOSE	0.02 ± 0.02	0.15	0.00		
			TURF	0.02 ± 0.02	0.15	0.00		
			UNK1	0.01 ± 0.00	0.05	0.00		
			BAHA	0.01 ± 0.01	0.10	0.00		
			SCAM	0.01 ± 0.01	0.10	0.00		
			UNK2	0.01 ± 0.01	0.05	0.000		
			SMRO	0.00 ± 0.00	0.02	0.00		
			UNK3	0.00 ± 0.00	0.01	0.00		
			QUE1	0.00 ± 0.00	0.01	0.00		
			QUE2	0.00 ± 0.00	0.01	0.00		
			SCOL	0.00 ± 0.00	0.01	0.00		
			SPPA	0.00 ± 0.00	0.01	0.00		
Ocean Springs								
Natural	82.00	5.00	DISP	0.38 ± 0.05	0.50	0.00	1.17	0.65
			SPAL	0.25 ± 0.03	0.40	0.10		
			SCAM	0.17 ± 0.03	0.35	0.05		
			SOSE	0.03 ± 0.01	0.10	0.00		
			BAHA	0.01 ± 0.01	0.03	0.00		
Living	69.50	8.00	SPAL	0.35 ± 0.052	0.60	0.02	1.40	0.68
			PARE	0.13 ± 0.05	0.45	0.00		
			ASTE	0.09 ± 0.03	0.25	0.00		
			PADI	0.08 ± 0.04	0.35	0.00		
			BAHA	0.04 ± 0.03	0.30	0.00		
			SOSE	0.01 ± 0.01	0.05	0.00		
			SYTE	0.00 ± 0.00	0.02	0.00		
			LAPA	0.00 ± 0.00	0.01	0.00		
Hardened	86.00	9.00	SPAL	0.42 ± 0.11	0.90	0.00	1.31	0.67
			SPPA	0.22 ± 0.12	0.84	0.00		
			DISP	0.14 ± 0.07	0.60	0.00		
			PARE	0.06 ± 0.03	0.30	0.00		
			SALA	0.01 ± 0.01	0.05	0.00		
			BAHA	0.01 ± 0.01	0.05	0.00		
			ASTE	0.01 ± 0.01	0.05	0.00		

			SOSE	0.01 ± 0.01	0.05	0.00		
			HYCO	0.00 ± 0.00	0.01	0.00		
Grand Bay								
Natural	63.00	3.00	JURO	0.46 ± 0.10	0.95	0.05	0.78	0.44
			SPAL	0.09 ± 0.04	0.35	0.00		
			SCAM	0.09 ± 0.04	0.40	0.00		
Living	64.50	7.00	JURO	0.41 ± 0.10	0.85	0.00	1.05	0.54
			DISP	0.16 ± 0.06	0.50	0.00		
			SPAL	0.04 ± 0.02	0.20	0.00		
			SPSP	0.03 ± 0.03	0.25	0.00		
			BOFR	0.02 ± 0.01	0.10	0.00		
			LICA	0.00 ± 0.00	0.03	0.00		
			IPPU	0.00 ± 0.00	0.03	0.00		
Hardened	63.00	7.00	IMCY	0.26 ± 0.07	0.55	0.00	1.51	0.73
			JURO	0.15 ± 0.10	0.90	0.00		
			SPPA	0.11 ± 0.03	0.29	0.00		
			MYCE	0.06 ± 0.10	0.90	0.00		
			PARE	0.033 ± 0.03	0.30	0.00		
			SMRO	0.01 ± 0.01	0.10	0.00		
			RUTR	0.01 ± 0.01	0.05	0.00		

REFERENCES

Álvarez-Rogel, J., del Carmen Tercero, M., Arce, M. I., Delgado, M. J., Conesa, H. M., & González-Alcaraz, M. N. (2016). Nitrate removal and potential soil N2O emissions in eutrophic salt marshes with and without Phragmites australis. *Geoderma*, *282*, 49–58. https://doi.org/10.1016/j.geoderma.2016.07.011

Arkema, K. K., Guannel, G., Verutes, G., Wood, S. A., Guerry, A., Ruckelshaus, M., Kareiva, P., Lacayo, M., & Silver, J. M. (2013). Coastal habitats shield people and property from sea-level rise and storms. *Nature Climate Change*, *3*(10), 913–918. https://doi.org/10.1038/nclimate1944

Augustin, L. N., Irish, J. L., & Lynett, P. (2009). Laboratory and numerical studies of wave damping by emergent and near-emergent wetland vegetation. *Coastal Engineering*, *56*(3), 332–340. https://doi.org/10.1016/j.coastaleng.2008.09.004

Balouskus, R. G., & Targett, T. E. (2016). Fish and Blue Crab Density along a Riprap-Sill-Hardened Shoreline: Comparisons with Spartina Marsh and Riprap. *Transactions of the American Fisheries Society*, *145*(4), 766–773. https://doi.org/10.1080/00028487.2016.1172508

Basco, D. R. (2006). Seawall Impacts on Adjacent Beaches : Separating Fact from Fiction. *Jorunal of Coastal Research*, *II*(39), 741–744.

Bayraktarov, E., Saunders, M. I., Abdullah, S., Mills, M., Beher, J., Possingham, H. P., Mumby, P. J., & Lovelock, C. E. (2015). The cost and feasibility of marine coastal restoration. *Ecological Applications*, *26*(4), 1055–1074. https://doi.org/10.1890/15-1077.1

Bilkovic, D. M., & Mitchell, M. M. (2013). Ecological tradeoffs of stabilized salt

marshes as a shoreline protection strategy: Effects of artificial structures on macrobenthic assemblages. *Ecological Engineering*, *61*, 469–481. https://doi.org/10.1016/j.ecoleng.2013.10.011

Bilkovic, D. M., & Roggero, M. M. (2008). Effects of coastal development on nearshore estuarine nekton communities. *Marine Ecology Progress Series*, *358*, 27–39. https://doi.org/10.3354/meps07279

Bilkovic, D. M., & Mitchell, M. M. (2018). Designing Living Shoreline Salt Marsh Ecosystems to Promote Coastal Resilience. *Living Shorelines*, *April*, 293–316. https://doi.org/10.1201/9781315151465-19

Bilkovic, D. M., Mitchell, M., Mason, P., & Duhring, K. (2016). The Role of Living Shorelines as Estuarine Habitat Conservation Strategies. *Coastal Management*, *44*(3), 161–174. https://doi.org/10.1080/08920753.2016.1160201

Boerema, A., Geerts, L., Oosterlee, L., Temmerman, S., & Meire, P. (2016). Ecosystem service delivery in restoration projects: The effect of ecological succession on the benefits of tidal marsh restoration. *Ecology and Society*, *21*(2). https://doi.org/10.5751/ES-08372-210210

Bozek, C. M., & Burdick, D. M. (2005). Impacts of seawalls on saltmarsh plant communities in the Great Bay Estuary, New Hampshire USA. *Wetlands Ecology and Management*, *13*(5), 553–568. https://doi.org/10.1007/s11273-004-5543-z

Brueske, C. C., & Barrett, G. W. (1994). Effects of vegetation and hydrologic load on sedimentation patterns in experimental wetland ecosystems. *Ecological Engineering*, *3*(4), 429–447. https://doi.org/10.1016/0925-8574(94)00011-5

Cattrijsse, A., Dankwa, H. R., & Mees, J. (1997). Nursery function of an estuarine tidal

marsh for the brown shrimp Crangon crangon. *Journal of Sea Research*, *38*(1–2), 109–121. https://doi.org/10.1016/S1385-1101(97)00036-1

Chmura, G. L., Anisfeld, S. C., Cahoon, D. R., & Lynch, J. C. (2003). Global carbon sequestration in tidal, saline wetland soils. *Global Biogeochemical Cycles*, *17*(4). https://doi.org/10.1029/2002gb001917

Clewell, A. (1985). Guide to the vascular plants of the Florida panhandle. Florida State University Press, University Presses of Florida.

Correll, D., Johnston, M. (1970). Manual of the vascular plants of Texas. Texas Research Foundation.

Craft, C., Clough, J., Ehman, J., Jove, S., Park, R., Pennings, S., Guo, H., & Machmuller, M. (2009). Forecasting the effects of accelerated sea-level rise on tidal marsh ecosystem services. *Frontiers in Ecology and the Environment*, *7*(2), 73–78. https://doi.org/10.1890/070219

Craft, C., Megonigal, P., Broome, S., Stevenson, J., Freese, R., Cornell, J., Zheng, L., & Sacco, J. (2003). The pace of ecosystem development of constructed Spartina alterniflora marshes. *Ecological Applications*, *13*(5), 1417–1432. https://doi.org/10.1890/02-5086

Crum, K. P., Balouskus, R. G., & Targett, T. E. (2018). Growth and Movements of Mummichogs (Fundulus heteroclitus) Along Armored and Vegetated Estuarine Shorelines. *Estuaries and Coasts*, *41*(2018), 131–143. https://doi.org/10.1007/s12237-017-0299-x

Currin, C. A., Delano, P. C., & Valdes-Weaver, L. M. (2008). Utilization of a citizen monitoring protocol to assess the structure and function of natural and stabilized

fringing salt marshes in North Carolina. *Wetlands Ecology and Management*, *16*(2), 97–118. https://doi.org/10.1007/s11273-007-9059-1

Davis, J. L., Currin, C. A., O'Brien, C., Raffenburg, C., & Davis, A. (2015). Living shorelines: Coastal resilience with a blue carbon benefit. *PLoS ONE*, *10*(11), 1–18. https://doi.org/10.1371/journal.pone.0142595

Doody, J. P. (2004). "Coastal squeeze" - An historical perspective. *Journal of Coastal Conservation*, *10*(1–2), 129–138. https://doi.org/10.1652/1400-0350(2004)010[0129:CSAHP]2.0.CO;2

Drake, B. G. (1989). Photosynthesis of salt marsh species. *Aquatic Botany*, *34*(1–3), 167–180. https://doi.org/10.1016/0304-3770(89)90055-7

Duhring, K. A, Barnard, T. A, & Hardaway, S. (2006). *A survey of the effectiveness of existing marsh toe protection structures in Virginia*. *July*.

Eleuterius, L. (1972). The marshes of Mississippi. *Castanea*, *37*(3), 153–168. http://www.jstor.org/stable/4032384

Erdle, S., Davis, J., & Sellner, K. (2006). Management, Policy, Science, and Engineering of Nonstructural Erosion Control in the Chesapeake Bay. *Proceedings of the 2006 Living Shoreline Summit, …*. http://scholar.google.com/scholar?hl=en&btnG=Search&q=intitle:Management,+Policy,+Science,+and+Engineering+of+Nonstructural+Erosion+Control+in+the+Chesapeake+Bay#0

Feagin, R. A., Lozada-Bernard, S. M., Ravens, T. M., Möller, I., Yeager, K. M., & Baird, A. H. (2009). Does vegetation prevent wave erosion of salt marsh edges? *Proceedings of the National Academy of Sciences of the United States of America*,

106(25), 10109–10113. https://doi.org/10.1073/pnas.0901297106

Fonseca, M. S., & Cahalan, J. A. (1992). A preliminary evaluation of wave attenuation by four species of seagrass. *Estuarine, Coastal and Shelf Science*, *35*(6), 565–576. https://doi.org/10.1016/S0272-7714(05)80039-3

Gedan, K. B., Kirwan, M. L., Wolanski, E., Barbier, E. B., & Silliman, B. R. (2011). The present and future role of coastal wetland vegetation in protecting shorelines: Answering recent challenges to the paradigm. *Climatic Change*, *106*(1), 7–29. https://doi.org/10.1007/s10584-010-0003-7

Gittman, R. K., Fodrie, F. J., Popowich, A. M., Keller, D. A., Bruno, J. F., Currin, C. A., Peterson, C. H., & Piehler, M. F. (2015). Engineering away our natural defenses: An analysis of shoreline hardening in the US. *Frontiers in Ecology and the Environment*, *13*(6), 301–307. https://doi.org/10.1890/150065

Gittman, R. K., Scyphers, S. B., Smith, C. S., Neylan, I. P., & Grabowski, J. H. (2016). Ecological consequences of shoreline hardening: A meta-analysis. *BioScience*, *66*(9), 763–773. https://doi.org/10.1093/biosci/biw091

Green, B. C., Smith, D. J., & Underwood, G. J. C. (2012). Habitat connectivity and spatial complexity differentially affect mangrove and salt marsh fish assemblages. *Marine Ecology Progress Series*, *466*, 177–192. https://doi.org/10.3354/meps09791

Greenberg, R., & Maldonado, J. E. (2006). Diversity and endemism in tidal-marsh vertebrates. *Studies in Avian Biology*, *32*, 32–53.

Greenberg, R., Maldonado, J. E., Droege, S., & McDonald, M. V. (2006). Tidal Marshes: A Global Perspective on the Evolution and Conservation of Their Terrestrial Vertebrates. *BioScience*, *56*(8), 675. https://doi.org/10.1641/0006-

3568(2006)56[675:tmagpo]2.0.co;2

Herbert, D., Astrom, E., Bersoza, A. C., Batzer, A., McGovern, P., Angelini, C., Wasman, S., Dix, N., & Sheremet, A. (2018). Mitigating erosional effects induced by boat wakes with living shorelines. *Sustainability (Switzerland)*, *10*(2), 1–19. https://doi.org/10.3390/su10020436

Howes, N. C., FitzGerald, D. M., Hughes, Z. J., Georgiou, I. Y., Kulp, M. A., Miner, M. D., Smith, J. M., & Barras, J. A. (2010). Hurricane-induced failure of low salinity wetlands. *Proceedings of the National Academy of Sciences of the United States of America*, *107*(32), 14014–14019. https://doi.org/10.1073/pnas.0914582107

Johnson, D. S., Warren, R. S., Deegan, L. A., & Mozdzer, T. J. (2016). Saltmarsh plant responses to eutrophication. *Ecological Applications*, *26*(8), 2647–2659. https://doi.org/10.1002/eap.1402

Juneau, Brittany. 2021. Differences in Erosion Rates and Elevation Among Natural, Living and Hardened Shorelines in Mississippi, and Alabama. Honor's thesis. Department of Coastal Sciences, The University of Southern Mississippi

La Peyre, M. K., Humphries, A. T., Casas, S. M., & La Peyre, J. F. (2014). Temporal variation in development of ecosystem services from oyster reef restoration. *Ecological Engineering*, *63*, 34–44. https://doi.org/10.1016/j.ecoleng.2013.12.001

Leonardi, N., Ganju, N. K., & Fagherazzi, S. (2016). A linear relationship between wave power and erosion determines salt-marsh resilience to violent storms and hurricanes. *Proceedings of the National Academy of Sciences*, *113*(1), 64–68. https://doi.org/10.1073/pnas.1510095112

Madsen, J. D., Chambers, P. A., James, W. F., Koch, E. W., & Westlake, D. F. (2001).

The interaction between water movement, sediment dynamics and submersed macrophytes. *Hydrobiologia*, *444*, 71–84. https://doi.org/10.1023/A:1017520800568

Matzke, S., & Elsey-Quirk, T. (2018). Spartina patens Productivity and Soil Organic Matter Response to Sedimentation and Nutrient Enrichment. *Wetlands*, *38*(6), 1233–1244. https://doi.org/10.1007/s13157-018-1030-9

Mitchell, M., & Bilkovic, D. M. (2019). Embracing dynamic design for climate-resilient living shorelines. *Journal of Applied Ecology*, *56*(5), 1099–1105. https://doi.org/10.1111/1365-2664.13371

Mitsch, W. J., Zhang, L., Waletzko, E., & Bernal, B. (2014). Validation of the ecosystem services of created wetlands: Two decades of plant succession, nutrient retention, and carbon sequestration in experimental riverine marshes. *Ecological Engineering*, *72*, 11–24. https://doi.org/10.1016/j.ecoleng.2014.09.108

Molinaroli, E., Guerzoni, S., De Falco, G., Sarretta, A., Cucco, A., Como, S., Simeone, S., Perilli, A., & Magni, P. (2009). Relationships between hydrodynamic parameters and grain size in two contrasting transitional environments: The Lagoons of Venice and Cabras, Italy. *Sedimentary Geology*, *219*(1–4), 196–207. https://doi.org/10.1016/j.sedgeo.2009.05.013

Nelson, P. A. (2008). Ecological effects of wave energy conversion technology on California's marine and anadromous fishes. *Developing Wave Energy in Coastal California: Potential Socio-Economic and Environmental Effects*, *November*, 111–135. http://www.energy.ca.gov/2008publications/CEC-500-2008-083/CEC-500-2008-083.PDF

Nyman, J. A., Walters, R. J., Delaune, R. D., & Patrick, W. H. (2006). Marsh vertical

accretion via vegetative growth. *Estuarine, Coastal and Shelf Science*, *69*(3–4), 370–380. https://doi.org/10.1016/j.ecss.2006.05.041

O'Donnell, J. E. D. (2017). Living Shorelines: A Review of Literature Relevant to New England Coasts. *Journal of Coastal Research*, *332*(2), 435–451. https://doi.org/10.2112/jcoastres-d-15-00184.1

Oksanen, J., F.G. Blanchett, M. Friendly et al. 2020. Community Ecology Package ver. 2.5. Available at https://cran.r-project.org/web/packages/vegan/vegan.pdf

Onorevole, K. M., Thompson, S. P., & Piehler, M. F. (2018). Living shorelines enhance nitrogen removal capacity over time. *Ecological Engineering*, *120*(May), 238–248. https://doi.org/10.1016/j.ecoleng.2018.05.017

Palinkas, C. M., Sanford, L. P., & Koch, E. W. (2018). Influence of Shoreline Stabilization Structures on the Nearshore Sedimentary Environment in Mesohaline Chesapeake Bay. *Estuaries and Coasts*, *41*(4), 952–965. https://doi.org/10.1007/s12237-017-0339-6

Partyka, M. L., Peterson, M. S., Partyka, M. L., & Peterson, M. S. (2017). Habitat Quality and Salt-Marsh Species Assemblages along an Anthropogenic Estuarine Landscape *Stable URL : http://www.jstor.org/stable/40065141 Linked references are available on JSTOR for this article : Habitat Quality and Salt-Marsh Species Assemblages* . *24*(6), 1570–1581.

Pennings, S. C., Grant, M. B., & Bertness, M. D. (2005). Plant zonation in low-latitude salt marshes: Disentangling the roles of flooding, salinity and competition. *Journal of Ecology*, *93*(1), 159–167. https://doi.org/10.1111/j.1365-2745.2004.00959.x

Polk, M. A., & Eulie, D. O. (2018). Effectiveness of Living Shorelines as an Erosion

Control Method in North Carolina. *Estuaries and Coasts*, *41*(8), 2212–2222. https://doi.org/10.1007/s12237-018-0439-y

Radford A, Ahles H, Bell C (1983) Manual of the vascular flora of the Carolinas. University of North Carolina Press

Roberts, S. (2010). A report from the National Research Council—Mitigating shore erosion along sheltered coasts. *Shipman, H., Dethier, MN, Gelfenbaum, G., Fresh, KL, and Dinicola, RS, Eds, January 2010*, 85–90.

Rouge, B. (2000). *Healthy Ecosystems Grants 1 Final Report*. *Lc*, 1–14.

Ruggiero, P. (2009). Impacts of shoreline armoring on sediment dynamics. *Puget Sound Shorelines and the Impacts of Armoring—Proceedings of a State of the Science Workshop, February 2015*, 179–186.

Schmid, B. K. (2000). *Shoreline Erosion Analysis of Hancock County Marsh*. 1–3.

Scyphers, S. B., Powers, S. P., Heck, K. L., & Byron, D. (2011). Oyster reefs as natural breakwaters mitigate shoreline loss and facilitate fisheries. *PLoS ONE*, *6*(8). https://doi.org/10.1371/journal.pone.0022396

Silliman, B. R., He, Q., Angelini, C., Smith, C. S., Kirwan, M. L., Daleo, P., Renzi, J. J., Butler, J., Osborne, T. Z., Nifong, J. C., & van de Koppel, J. (2019). Field Experiments and Meta-analysis Reveal Wetland Vegetation as a Crucial Element in the Coastal Protection Paradigm. *Current Biology*, *29*(11), 1800-1806.e3. https://doi.org/10.1016/j.cub.2019.05.017

Sparks, E. L., Cebrian, J., Biber, P. D., Sheehan, K. L., & Tobias, C. R. (2013). Cost-effectiveness of two small-scale salt marsh restoration designs. *Ecological Engineering*, *53*, 250–256. https://doi.org/10.1016/j.ecoleng.2012.12.053

Sutton-Grier, A. E., Wowk, K., & Bamford, H. (2015). Future of our coasts: The potential for natural and hybrid infrastructure to enhance the resilience of our coastal communities, economies and ecosystems. *Environmental Science and Policy, 51*, 137–148. https://doi.org/10.1016/j.envsci.2015.04.006

Swann, L. (2008). The Use of Living Shorelines to Mitigate the Effects of Storm Events on Dauphin Island, Alabama, USA. *American Fisheries Society Symposium, 64*, 0–0.

Temmerman, S., Meire, P., Bouma, T. J., Herman, P. M. J., Ysebaert, T., & De Vriend, H. J. (2013). Ecosystem-based coastal defence in the face of global change. *Nature, 504*(7478), 79–83. https://doi.org/10.1038/nature12859

Temple, N. A., Sparks, E. L., Webb, B. M., Cebrian, J., Virden, M. F., Lucore, A. E., & Moss, H. B. (2021). Responses of two fringing salt marsh plant species along a wave climate gradient. *Marine Ecology Progress Series*, *675*, 53–66. https://doi.org/10.3354/meps13843

Valiela, I., & Cole, M. L. (2002). Comparative evidence that salt marshes and mangroves may protect seagrass meadows from land-derived nitrogen loads. *Ecosystems*, *5*(1), 92–102. https://doi.org/10.1007/s10021-001-0058-4

Van Raalte, C. D., Valiela, I., Carpenter, E. J., & Teal, J. M. (1974). Inhibition of nitrogen fixation in salt marshes measured by acetylene reduction. *Estuarine and Coastal Marine Science*, *2*(3), 301–305. https://doi.org/10.1016/0302-3524(74)90020-6

Vargas-Luna, A., Crosato, A., & Uijttewaal, W. S. J. (2015). Effects of vegetation on flow and sediment transport: Comparative analyses and validation of predicting

models. *Earth Surface Processes and Landforms*, *40*(2), 157–176. https://doi.org/10.1002/esp.3633

Vymazal, J. (2013). Emergent plants used in free water surface constructed wetlands: A review. *Ecological Engineering*, *61*, 582–592. https://doi.org/10.1016/j.ecoleng.2013.06.023

Whalen, B. L., Kreeger, D., Bushek, D., & Moody, J. (2012). *Strategic Planning for Living Shorelines in the Delaware Estuary*. 14–19.

Wu, W., Zhang, M., Ozeren, Y., & Wren, D. (2012). Analysis of Vegetation Effect on Waves Using a Vertical 2D RANS Model. *Journal of Coastal Research*, *287*(May), 383–397. https://doi.org/10.2112/jcoastres-d-12-00023.1